UNIVERSITÀ DEGLI STUDI DI PADOVA

DIPARTIMENTO DI INGEGNERIA INDUSTRIALE

CORSO DI LAUREA MAGISTRALE IN INGEGNERIA CHIMICA E DEI PROCESSI INDUSTRIALI

Tesi di Laurea Magistrale in
Ingegneria Chimica e dei Processi Industriali

Design, development and validation of microfluidic platforms for biomedical applications

Relatore: Prof.ssa Elisa Cimetta

Laureanda: GIORGIA BATTAIOTTO

ANNO ACCADEMICO 2017 – 2018

Riassunto

La microfluidica è una scienza che si sta sviluppando negli ultimi decenni e che si propone di studiare i fenomeni alle scale nano e micrometriche, con lo scopo di sfruttare il comportamento dei fluidi che, a queste grandezze, sono governati da forze diverse rispetto alla macroscala. Tra i vari ambiti in cui si sta diffondendo, quelli biologico e biomedico sono di particolare interesse. I dispositivi utilizzati per le colture cellulari hanno lo scopo di migliorare vari e limitanti aspetti relativi alle colture *in vitro*, come i lunghi tempi sperimentali, e l'impossibilità di ricreare fedelmente il complesso ambiente cellulare.

Durante questo lavoro di tesi sono state studiate e ottimizzate due piattaforme microfluidiche, che hanno lo scopo di creare dei gradienti di concentrazione e che verranno in futuro utilizzate per studiare il comportamento degli esosomi (specifiche vescicole cellulari identificate come biomarcatori) nel Neuroblastoma, un aggressivo tumore che si sviluppa in età infantile.

I microbioreattori si studiano preliminarmente tramite simulazioni fluidodinamiche e poi sono prodotti mediante processo di replica da uno stampo. Le piattaforme vengono assemblate poi in una configurazione reversibile o irreversibile, su cui vengono condotti esperimenti di validazione fluidodinamica ed esperimenti biologici.

Il funzionamento della prima piattaforma microfluidica è stato verificato tramite le validazioni fluidodinamiche, mentre non è stato possibile utilizzarla per svolgere esperimenti con campioni biologici, a causa dell'usura di un componente dell'unità di chiusura, che dovrà essere prodotto nuovamente per assicurare il funzionamento del dispositivo.

Per quanto riguarda la seconda piattaforma, lo stampo è stato prodotto tramite l'utilizzo di una microfresatrice. Il comportamento del microbioreattore è stato verificato tramite validazioni fluidodinamiche e biologiche, anche se alcune modifiche, proposte nel corso di questo lavoro di tesi, sono necessarie per ottenere il gradiente di concentrazione desiderato. Anche la compatibilità con l'ambiente cellulare è stata verificata, conducendo esperimenti preliminari di internalizzazione degli esosomi nelle cellule.

Questo lavoro di tesi rappresenta quindi il punto di partenza del progetto di ricerca condotto dalla prof.ssa Elisa Cimetta, che ha lo scopo di comprendere a fondo il ruolo degli esosomi nello sviluppo del Neuroblastoma.

Summary

Microfluidics is a novel science that applies to different fields, and which focus is on the phenomena that happen at the nano- and micro- scales. At these lengths, fluids are governed by different forces with respect to the macroscale. In particular, the devices developed in the biological and biomedical fields are employed principally for the cellular cultures and aim at improving various issues related to the *in vitro* cultures.

During this work of thesis two microfluidic platforms have been studied and optimized. Their objective is the obtainment of concentration gradients, that will be useful to investigate the role of exosomes, cellular vesicles identified as biomarkers, in Neuroblastoma, an aggressive type of tumor that develops during childhood.

The microbioreactors are designed starting from a fluid dynamic simulation. Afterwards, they are produced thanks to a replica molding process, arranged in a reversible or irreversible configuration and employed to conduct fluid dynamics validations and biological experiments.

The performances of the first microfluidic platform have been verified with fluid dynamic validations, but it was not possible to conduct experiments on biological samples. This is due to defects on the clamping unit that will be manufactured again to ensure the performances of the device.

For the second microfluidic platform, its master was produced with a micromiller. The performances of the microbioreactor were verified with fluid dynamic and biological validations; however, some modifications, suggested during this work, are necessary to obtain the desired concentration gradient. The compatibility with the cellular environment was also verified, and preliminary experiments regarding the internalization of exosomes were performed.

This work of thesis represents the starting point of the project led by professor Elisa Cimetta, which aims at studying the role of exosomes in the dissemination of this aggressive disease.

Table of Contents

List of Figures

List of Tables

Introduction

Microfluidics is a science that studies the behavior of fluids at the nano- and micro- scales. Its application to the biomedical and biological fields is useful to improve various issues related to traditional cellular cultures. Thanks to microfluidic devices, it is possible to reduce the experimental times, diminish the quantity of reagents and biological material needed, obtain precise and controllable conditions in the cellular cultures. These features allow to recreate the cellular microenvironment, and to study in a realistic way what happens *in vivo*, and that is not possible to represent in the traditional *in vitro* models.

The microfluidic platforms seem suitable instruments to investigate the role of exosomes in Neuroblastoma, an aggressive type of tumor that develops during childhood. Exosomes are cellular vesicles, crucial during the progression of the most aggressive phenotypes, and that have been identified as biomarkers for the early detection. They are responsible of the communication and the delivery of information between the cells. This is the main field of study of the BIAMET laboratory, where this work of thesis was developed.

The focus of the thesis is the study and the development of two microfluidic platforms, that aim at creating exosomes' concentration gradients to which the Neuroblastoma cells will be subjected. In fact, the creation of these gradients allows to:

- test the effect of exosomes on Neuroblastoma cells;
- exploit the limited quantity of exosomes that can be extracted from cells thanks to the obtainment of high-throughput data;
- mimic what happens *in vivo* thanks to 3D cultures.

Considering these objectives, the two devices aim at creating two different types of concentration gradients: the first platform is characterized by the presence of microwells, in which discrete values of concentration are obtained; the second platform aims at creating a continuous concentration gradient inside a chamber.

The work that regards the first microbioreactor, which master is based on an existing design, consists in a preliminary fluid dynamic simulation, useful to understand its behavior. Afterwards, the platform is produced, arranged in an irreversible or reversible configuration and validated thanks to experiments regarding the fluid dynamics and the biological performances.

As concern the second microfluidic platform, the procedure is analogous: the device is simulated, and the master is produced using a micromiller. The platform is then produced via replica molding, arranged in an irreversible configuration and the performances are verified through fluid dynamic and biological experiments. The production of the master was possible thanks to the collaboration with the TE.SI. laboratory, based in Rovigo.

The thesis is formed by three Chapters.

In the first one, the state of the art about microfluidics and its application to the biological and biomedical fields are presented, focusing on the microfluidic devices. The materials and the techniques employed to produce the master and the platforms are investigated. A specific attention is put on the plasma treatment, a technique widely used in this field. Moreover, a brief description of Neuroblastoma and of the role of exosomes in its dissemination is examined.

In the second Chapter the materials and the methods used for the study and the production of the two microfluidic platforms are described. First, for both the platforms, the design of the master, the mode of operation and the conditions employed in the simulations are presented. Then, the production and assembling techniques (for both the irreversible and reversible configurations), and the validation and biological experiments are described in detail. Also, the procedures employed to daily treat and maintain cells are illustrated, including the methods used to count and estimate the growth rate of cells.

In the third and last Chapter the results are presented and discussed, for both microfluidic devices. The results of the simulations and of the fluid dynamic and biological experiments are shown. The outcomes of these tests, as well as the problems found during the study, are presented. The first platform's performances are verified with fluid dynamic validations, however, because of a problem in the clamping unit, the biological experiments have not been carried out.

The second device is designed, produced and verified both with fluid dynamic and biological validations. However, some modifications on the design are needed to obtain the desired concentration gradient. In order to understand which type of changes are needed, a 3D fluid dynamic simulation is carried out.

Finally, the results of the growth rate estimation are presented, showing an initial trend of growth, followed by a stabilization.

In the Conclusions a brief overview of this thesis is reported, focusing on the results reached, the limitations and the suggestions for the future work.

Chapter 1

State of the Art

In this Chapter, the theories of microfluidics and the main applications to biology and biomedical fields will be investigated, with a specific attention to microfluidic devices, their fabrication methods and the advantages connected to their use. Afterwards, a brief description of Neuroblastoma and of the role of exosomes in the detection of this type of cancer is presented. Finally, the motivation and the aim of the thesis are explained.

1.1 Microfluidics

Microfluidics is a science that studies the behavior of fluids at the nano- and micro- length scale. The usual dimensions of the macroscale devices shrink to the microscale, with lengths ranging from tens to hundreds of micrometers[1]. Therefore, not only the dimensions of the devices, but also the volumes of reagents are dramatically decreased, leading to shorter reaction and residence times, and favoring the possibility of running multiple parallel operations[2]. As a consequence, the experimental times and the overall costs are significantly reduced.

These advantages supported the use of microfluidic devices not only in biology, chemistry and medicine, but also in the fields of control systems and heat management, energy generation and display technology, that are only a few examples of the applications of this science. Other specific applications include protein crystallization, micropumps, sample pre-treatment, separation techniques, and DNA separation, just to name a few[2].

It is now evident that microfluidics is a highly interdisciplinary and versatile science, with advantages that can be exploited and tailored on the specific application.

Along this line, the most relevant feature for the application at the core of this thesis project is the observation that the physical phenomena that typically characterize the macroscale change dramatically at the microscale. The mass transport in the microfluidic devices, for example, is usually dominated by viscous dissipation, while the inertial effects become negligible.

Physical phenomena that are not usually present at the macroscale become predominant, and this can bring different advantages. Considering for example a conduit with a diameter of a

few micrometers, it can be proved that the fluid flow is generally laminar. Therefore, the flow is highly controllable and its conditions are constant over time and diffusion becomes the dominant mechanism of mixing[3]. As a consequence, devices that take advantage of the different diffusion coefficients of the solutes, can be built[2]. Two examples, shown in Figure 1.1, are: a. T sensors, where different fluids are brought together at a T junction to flow alongside down a channel, and solute particles in each stream diffuse into the other; and b. membrane-less filters to separate different solutes from a solution.

Moreover, another fundamental advantage of the microfluidic devices is that they can be

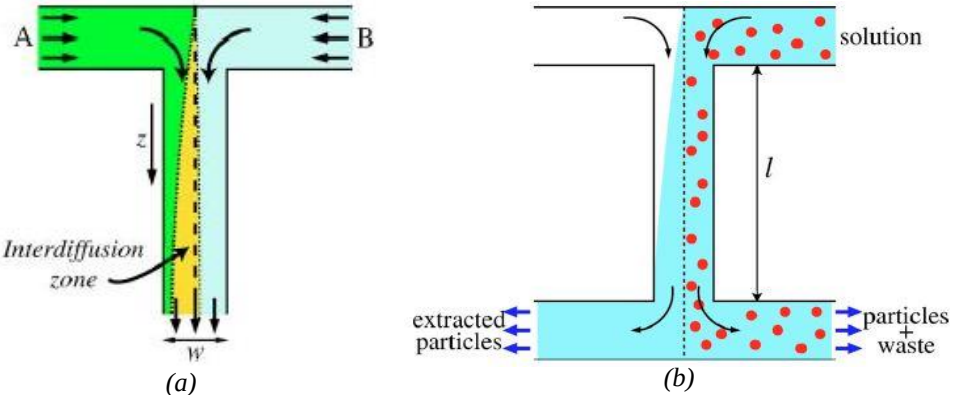

Figure 1.1: *Two microfluidic devices that exploit the different diffusion coefficients of the solute: (a) T-sensors and (b) membrane-less filters. Adapted from [2].*

built in optically transparent materials, allowing the experiment to be visible to the naked eye and to the microscope.

In summary, it can be noticed that experiments at the microscale allow obtaining high precision and high-throughput data: the so called "Lab-on-a-chip" devices are surely a recent and promising field of research.

1.1.1 Dimensionless numbers in microfluidics

A big variety of physical phenomena can happen at the microscale; therefore, it becomes useful to understand the importance of a phenomenon with respect to the others. In order to weight the predominance of different forces and the behavior of fluids in microfluidic devices, different dimensionless numbers can be used. Table 1.1 shows the parameters typically used in such analyses.

Table 1.1*: Dimensionless numbers used in microfluidics. Adapted from[2].*

Acronym	Name	Phenomena compared
Re	Reynolds	Inertial/viscous
Pe	Péclet	Convection/diffusion
Ca	Capillary	Viscous/interfacial
Wi	Weissenberg	Polymer relaxation time/shear rate time
De	Deborah	Polymer relaxation time/flow time
El	Elasticity	Elastic effects/inertial effects
Gr	Grashof	Re for buoyant flow
Ra	Rayleigh	Pe for buoyant flow
Kn	Knudsen	Slip length/macroscopic length

As can be noticed from the table, the use of dimensionless numbers allows to compare two different phenomena or length scales, and therefore, to determine which is predominant. The most commonly used (Re, Pe, Ca) are now explained in detail and calculated with some reference values for a flux of water in a microfluidic platform, as shown in Table 1.2.

Table 1.2: *Typical parameters for a flux of water in a microfluidic device. Adapted from [2].*

Parameter	Value
Velocity	10^{-6}-10^{-4} m/s
Channel radius	10^{-6}-10^{-4} m
Channel length	$5\cdot10^{-3}$-10^{-1} m
Temperature	278 K
Density	1000 kg/m^3
Viscosity	$1\cdot10^{-3}$ Pa·s

The Reynolds number gives an indication of the relative importance between inertial and viscous forces. It's one of the most commonly used dimensionless numbers, both for the macroscale and microscale problems. Considering the incompressible flow of a Newtonian fluid in a pipe, a situation frequently encountered in microfluidics, the Reynolds number can be defined as:

$$\mathrm{Re} \equiv \frac{\rho v D}{\mu} \tag{1.1}$$

where ρ is the density of the fluid, usually expressed in [kg/m^3], v is the average velocity [m/s], D is the pipe diameter [m] and μ is the viscosity of the fluid, usually expressed in [Pa·s]. If the pipe is not tubular, the diameter is calculated as an equivalent diameter, given by the equation (1.2).

$$D_{eq} = \frac{4S}{2P} \tag{1.2}$$

where S is the area available for the passage of the fluid [m^2] and P is the semiperimeter [m]. The Reynolds number expresses the difference of magnitude between the inertial and the viscous forces: in microfluidic devices this value is usually small, therefore the viscous forces overwhelm the inertial ones. It can be demonstrated that, for a tubular pipe, the flow is laminar if Re<2100, and for Reynolds between 2100 and 5000 there is a transition from the laminar to the turbulent flow.

For a representative microfluidic channel characterized by the parameters reported in Table 1.2, calculated values for the Reynolds number range between 10^{-6} and 10. Consequently, in microfluidic devices the flow is laminar: it is highly predictable and it can be described with simpler equations with respect to the turbulent regime. In fact, the turbulent flow is characterized by the presence of eddies and, therefore, by great instability and unpredictability.

For a laminar flow of an incompressible fluid in a pipe, the Navier-Stokes equations, reported in the equation (1.3) in vector notation, can be easily simplified and solved. From the results, it is possible to express the velocity as a function of the radial position r. This result is known as the Hagen Poiseuille equation (1.4).

$$\rho \frac{D\boldsymbol{v}}{Dt} = \frac{\partial \boldsymbol{v}}{\partial t} + (\boldsymbol{v} \cdot \nabla)\boldsymbol{v} = -\nabla p + \mu \nabla^2 \boldsymbol{v} + \rho g \tag{1.3}$$

$$\Rightarrow v = 2V\left(1 - \frac{r^2}{R^2}\right) \tag{1.4}$$

Where $\boldsymbol{v}$ is the vector of the velocity in the three dimensions [m/s], p is the pressure [Pa], $V=Q/A$ is the average velocity [m/s] and R is the radius of the pipe [m].

The resulting parabolic velocity profile is reported in Figure 1.2. It can be noticed that the maximum value of the velocity, corresponding to r=0, is $v_{max}=2V$.

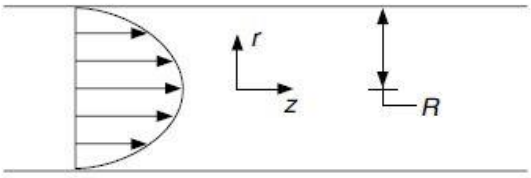

Figure 1.2: *Velocity profile for a laminar flow in a pipe. Adapted from*[4].

Because of these characteristics, it is expected to have small pressure drops along the channel. The pressure drops in a cylindrical pipe can be calculated thanks to the Fanning equation:

$$\Delta P = 2f\frac{L}{D}\rho v^2, \tag{1.5}$$

where f, the friction factor [dimensionless], can be calculated for a laminar flow as:

$$f = \frac{16}{\mathrm{Re}} \tag{1.6}$$

Typical pressure drops can be calculated using values from Table 1.2, and the resulting range is between 50 and 1600 Pa, confirming that pressure drops in these microfluidic channels are extremely small.

So far, we demonstrated that microfluidic devices are characterized by low Reynolds numbers and laminar flows and, therefore, we can infer that transport of solutes happens mainly due to diffusion. The Péclet number explains this behavior. For a cylindrical pipe:

$$\mathrm{Pe} \equiv \frac{vD}{D_i}, \tag{1.7}$$

where v is the velocity inside the pipe [m/s], D is the diameter [m] and D_i is the diffusion coefficient of the species i [m^2/s].

The Péclet number expresses the difference between the convective and the diffusive mass transport: the smaller Pe, the higher the contribution of the diffusion to the mass transport. Using the values in Table 1.2 and the diffusion coefficient of a small protein in water of $4 \cdot 10^{-11} m^2/s$ [2], the Pe number results in a range between 0.05 and 500, demonstrating the key role played by diffusion in the microfluidic devices.

The convective transport is thus usually small when compared to diffusion. Although this feature, on a general perspective, leads to difficulties in mixing, it can be exploited as a great advantage if combined with a careful design of the devices. If, for example, there is a difference of concentration of a species i across the device, the species only moves thanks to diffusion phenomena: this allows obtaining stable concentration gradients inside the microfluidic device. In fact, the conservation equation for the species i can be considered:

$$\frac{\partial c_i}{\partial t} = -\nabla(c_i v) - \nabla(J_i) + R_i, \tag{1.8}$$

where the term on the left-hand side represents the variation of the concentration of i with time, the first on the right-hand side represents the convective flux, the second term is the diffusive flux and the third represents the production or consumption of the species during a chemical reaction. Considering the usual conditions present in a microfluidic device, that include the predominance of diffusion with respect to the convection, the absence of a reaction and the achievement of the stationary state, the equation (1.8) can be simplified as:

$$0 = -\nabla(J_i) \tag{1.9}$$

This translates in the evidence that the diffusive flux is constant, assuring constant conditions across the device.

The diffusive flux [mol/m^2s] can be described by Fick's law:

$$J_i = -D_i \nabla c_i , \tag{1.10}$$

where D_i is the diffusion coefficient of i in the medium [m^2/s] and ∇c_i is the gradient of concentration of the species i [mol/m^3].
The diffusion coefficient of a generic particle can be calculated thanks to the Einstein-Smoluchowski equation:

$$D_i = \eta k_B T , \tag{1.11}$$

where η is the mobility of the particle [kg/s], k_B is the Boltzmann constant [J/K] and T is the temperature [K]. In the particular case of a spherical particle in a viscous fluid, equation (1.11) becomes the Stokes-Einstein equation:

$$D_i = \frac{k_B T}{6\pi\mu r} , \tag{1.12}$$

where r is the radius of the particle [m].

Although we will only use miscible fluids in our microfluidic devices, we will briefly discuss the behavior of immiscible fluids characterized by a surface tension γ, that affects the dynamics of the system[2]. Surface tension can be a fundamental aspect to be considered in these systems. For example, microfluidic devices, and T junctions, in particular, can be used to create controllable droplet emulsions, by injecting water into an oil stream: thanks to the surface tension, the interfacial area between the two liquid phases is reduced to the minimum value forming spherical droplets. By an analysis of the stresses at the interphase, the viscous and interfacial stresses can be balanced to obtain the radius of the droplets:

$$R \sim \frac{\gamma}{\eta v} h = \frac{h}{Ca} , \tag{1.13}$$

where the capillary number [dimensionless] is defined as:

$$Ca = \frac{\mu v}{\gamma} \tag{1.14}$$

The capillary number expresses the competition between the interfacial and the viscous stresses. It is useful to estimate the possibility of producing monodisperse droplets. In the microscale, the interfacial stress has a more dominant role with respect to the macroscale, and this characteristic has been exploited, for example, to conduct protein and cell sorting, perform nanoreactions for protein crystallization and passively drive fluids through microchannels[5].

1.1.2 Microfluidics in biology

One of the most important aims of the biological field is the complete understanding of the cellular mechanisms, by studying the intra- and inter- cellular interactions that contribute to trigger and coordinate cellular events[6]. However, the complexity of the biological systems makes this goal a tough task. Standard *in vitro* experiments are not able to represent in a comprehensive way the complex *in vivo* milieu that characterizes the cellular environment. This limitation is imputable to a multiplicity of aspects; among the most important ones we cite: the presence of different cell types, the extracellular matrix and the intricate network of molecular and physical factors that activate different signal pathways and regulate cells' functions and fate[7]. Also the lack of spatial proximity, and organelle compartmentalization can create big problems and lead to potential false positives[6]. In general, standard *in vitro* models lack in a precise control of culture conditions and are limited by the big volumes that are needed. Moreover, due to the intricacy of the biological systems, high-throughput experiments are preferred to obtain a quantity of data adequate to describe the entire system. In light of the listed issues, it can be observed that microfluidic devices seem useful instruments to solve them, in particular thanks to the following characteristics:

- the small volumes involved, that allow to use restrained and precise amounts of reagents and of cells. The doses provided to the cells can be measured in a very accurate way with respect to the reagents in the microfluidic experiments;
- the possibility to insert the cells in a precise number, for a specific volume or area of the device. The cells, if required, can also be arranged in a specific position to obtain high-precision experiments;
- the small dimensions and distances that are travelled by the fluids, comparable with the cells' dimensions;
- the laminar flow in the microchannels, that allows to establish precise conditions and concentration gradients, and to control the position of the molecules in the microfluidic device;
- the high-throughput of the experiment;
- the possibility of controlling chemically and physically the microenvironment by the use of in chip membrane valves[8];
- the possibility of organizing the cells into three-dimensional geometries in matrices like hydrogels, making the cultures of cells in these structures resembling those in tissues[8];
- the possibility of using optically transparent materials allows the live observation with the microscope.

Thanks to these advantages, in the last decades there has been a growing interest in the application of microfluidics to the biological and biomedical fields.

Another positive aspect of microfluidics is the possibility of performing live cell experimentations: techniques like fluorescent imaging can be used within these devices, thanks to the highly specific control or perturbation of the cellular microenvironment[6]. The precise spatial and temporal control of the devices can lead to high-resolution study of the phenomena happening, also in stable long-term cultures[9].

It can be understood how engineering knowledge can be mixed and implemented with biological problems, to obtain promising experiments and studies.

An example of the difference between the micro and the macroscale in the detection of proteins from a single HeLa (cancer) cell can be observed in Figure 1.3.

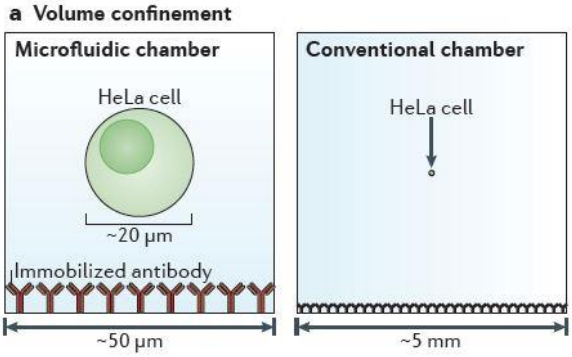

	Microfluidic	Conventional
Chamber volume	~10^{-10} l	~10^{-4} l
Dilution factor from a HeLa cell	~10^{-3}	~10^{-9}
Protein concentration for median abundance protein from a HeLa cell	~1 nM (~10^{-4} g l^{-1})	~1 fM (~10^{-10} g l^{-1})
Diffusion time	5 seconds	13 hours
Reaction time related to protein abundance	1 hour	10^6 hours

Figure 1.3*: Detection of proteins from a single HeLa cell. The difference between the microfluidic and the conventional devices can be observed, with a particular attention to the reaction time. Adapted from [7].*

From the table in the Figure 1.3, the differences of magnitude between a microfluidic and a conventional biological experiment can be observed: in particular, the diffusion time and the reaction time differ the most, providing a significant reduction in the experimental time. Nevertheless, even if this approach seems extremely convenient and revolutionary, it still presents several drawbacks, especially when working at lower end of the microscale[9]:

- the loss of sample, caused by the high area to volume ratio, that allows to dissipate heat in an effective way, but determine also losses by surface adsorption. In these cases, a surface treatment may be needed to avoid big losses;
- the loss of sample, caused by the conventional micropipettes employed, that usually deliver microliter volumes, instead of the nanoliter volumes analyzed in microfluidic devices. A non-negligible part of sample will not be analyzed in the device;
- microchannels may be clogged by debris or bubbles, and this problem can make the experiment fail;
- incompatibility with rapid processing of large sample volumes: large volumes (~1mL) may require long times (~1000 minutes) to pass through a microfluidic device. In these cases, a mesofluidic or macrofluidic approach may be more useful;
- loss of standards and controls: it may result difficult, or even impossible, to compare the results of the experiments with published and confirmed studies, because of the

lack of accepted standards and controls. The new studies and researches can be slowed down by this limitation;

- specialized requirements: special instrumentation, expertise in engineering design and non-conventional data interpretation strategies may be required in the studies, in particular during the first steps of the device design.

1.1.2.1 Cell cultures in microfluidic devices

Traditional cell culture techniques, consisting in the use of cell culture dishes, have remained almost unvaried since the first decades of the XX century. Only small improvements have been achieved in the use of robotic systems to eliminate the time-consuming pipetting steps[8]. Because of the purpose of the biological experiments (i.e. the analysis of single cells instead of bulk cultures to obtain more accurate results), traditional dishes and micropipettes are in the last decades being substituted by microfluidic devices, whose various advantages were described in paragraph §1.1.2.

Macroscopic cell cultures typically comprise 10^4-10^7 cells, large numbers that might even out and mask some of the local and important heterogeneity within a cell population. Microfluidic cell cultures use only a few hundred cells, or even a single cell, making it possible to underline any perturbation or difference between individual cells[10]. In Table 1.3 the improvements that can be exploited in the passage from macrofluidic to microfluidic cell cultures are shown.

Table 1.3: *Basic requirements for cell culture, and improvements when microfluidic methods are used. Adapted from[8].*

Requirements	Conventional cell culture	Microfluidic cell culture
Control of temperature and gasses	Large fluid volumes prevent fast changes	Small volumes allow dynamic control
Addition of nutrients and removal of metabolites	Infrequent, manual exchange of large volumes	Precisely measured, continuous or transient
Stimulation with drugs/proteins and simultaneous imaging	Usually not feasible	Feasible
Parallelization of cellular assay	Not feasible	High capability for parallelization
Automation of cell culture	Bulky, expensive fluid-handling robots must be used	High capability for automation in compact, inexpensive format
Single-cell manipulation and analysis	Manually involved, inaccurate, low-throughput	Accurate and high-throughput

As it can be observed, control of fluids, more accurate imaging, parallelization and automation of cell cultures are feasible tasks which can be achieved thanks to an appropriate design of the microfluidic platform. When microfluidic platforms are properly designed to mimic the cell's environment, cell cultures inside them represent a valid alternative to the macroscopic methods to study the complex cellular environment.

The potential applications of microfluidic devices for cell cultures are numerous, however it's important to take into consideration not only the advantages but also the limitations during the design of the new platforms: the medium turnover is usually faster and needs to be assessed for each cell type and device; the growth rates have to be re-evaluated when the cells are cultured in microfluidic platforms[10].

1.2 Microfluidic devices for biological applications

Microfluidic devices are designed by taking into consideration not only the physics and the phenomena that are present at the microscale, but also the final application of the platform, since all geometrical constraints are also dictated by the number of cells and their 2D vs 3D organization. A single platform typically consists of a series of microchannels arranged in such a way to obtain the desired fluxes and performances. Moreover, the devices can be complemented with a big variety of additional elements, such as pumps, valves and mixers.

Numerous fabrication materials can be used for biological applications, like silicon-based organic polymers (the most common is Polydimethylsiloxane -PDMS-), glass, or metals; each is chosen with respect to the specific application.

Focusing on the devices for the biological field, the most used materials is PDMS, a silicon rubber, mainly thanks to its high compatibility with the cellular environment. Its characteristics will be explained in detail in the following paragraphs.

With regards to fabrication methods, currently used techniques include micromachining, soft lithography, embossing, *in situ* construction, injection molding and laser ablation[3]. Each technique has different advantages and disadvantages, and the most suitable one depends on the specific function.

First, the microfluidic devices can be divided into monolayer and multilayer platforms, with respect to the number of functional layers they are composed of:

- Monolayer platforms are composed by a single layer of polymer that is usually attached to a glass slide or to another polymer, to obtain hydrodynamic seal. Their design is quite simple with respect to the multilayer ones; they are among the most used microfluidic devices.
- Multilayer platforms are constituted by at least two layers, attached to each other and to a support, to obtain more complex systems, with different features with respect to the monolayer ones. Their design is more complicated, since each individual layer is studied to obtain specific elements, like valves or pumps. However, these platforms allow to use automatized systems and to obtain more complex structures.

Usually the production of microfluidic devices starts with the fabrication of a master, employed to replicate the platform thanks to a process called replica molding. The material

used in this process is usually PDMS. Also processes in which the device is directly moulded exist.

1.2.1 Design and production of the master

The master is usually designed in a 2D and 3D-CAD environment and produced with different techniques. Between the most important, soft lithography, micromilling and stereolithography can be examined[3,11].

1.2.1.1 Soft lithography

This is a fast and cheap technique that does not require specialized skills. It consists in the patterning of surfaces via stamping and the following fabrication of microchannels using molding and embossing. The first step is the generation of a photoresist master on a crystalline silicon wafer carrying the features of the desired platform, device or design in general (typically the negative replica). Photoresist masters are used to mold an elastomeric material, usually PDMS, produced by mixing an elastomer and a curing agent.

Figure 1.4 reports an overview of the process of soft lithography. Briefly, a silicon wafer is cleaned and dried (Figure 1.4*a*) to allow the deposition of a photoresist (photosensitive epoxy resin) with a specific thickness (Figure 1.4*b*). A photomask, a film with the desired design printed, is placed over the photoresist (Figure 1.4*c*). Successively the base is exposed to an UV light and the mask is removed (Figure 1.4*d*). The UV light selectively polymerizes the photosensitive resin, and the rigid master is obtained after a chemical treatment that removes the unpolymerized residues. Afterwards, the master can be employed to produce the platform via the replica molding process.

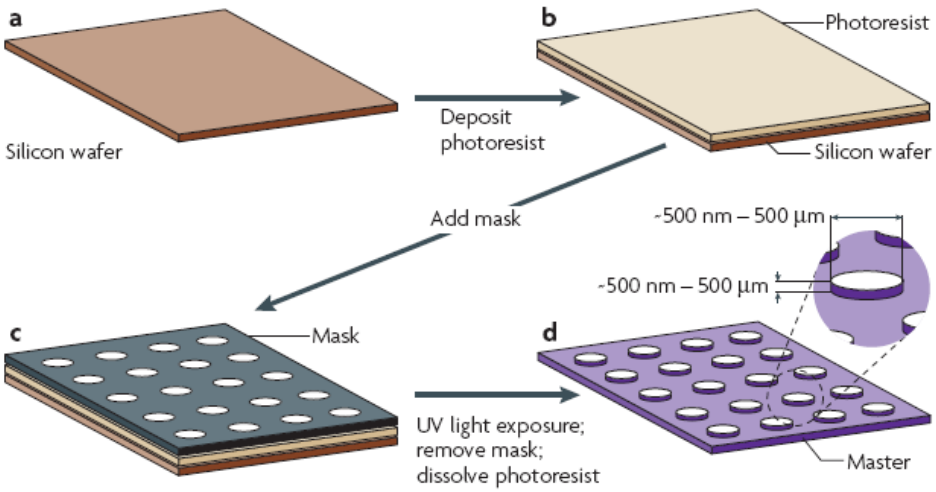

Figure 1.4: *Fabrication of the rigid master with soft lithography:(b) deposition of the photoresist on the silicon wafer; (c) deposition of the mask; (d) exposure to UV light and removal of the mask. Adapted from [10].*

Within the soft lithography technique, PDMS itself can be used as a soft mold for an additional process of replica molding and thus allowing to use a wider range of materials, like agarose or agar. The initial pattern is imprinted on the PDMS surface as in the traditional process, then this PDMS mold is used to pour and polymerize a different liquid polymer (such as agarose or agar), that is then carefully separated from the mold like in the general process in Figure 1.4.
Different other soft lithography techniques, like capillary molding, microcontact printing and microtransfer molding are used; the choice depends on the material used and on the design of the microfluidic device.

1.2.1.2 Micromilling

This technique is used to produce rigid masters on whom a polymer, usually PDMS, is poured and baked at high temperatures to obtain its reticulation. Thanks to the process of replica molding an infinite number of PDMS devices can be produced. Micromilling allows to obtain precise structures, with dimensions in the order of hundreds of microns. Different tools are used in the micromilling machine to mill an initial block, usually made of a metallic (for example Aluminium) or a plastic material. One of the main issues of the application of milling to microfluidic devices is the optimization of the working parameters: the cutting forces that are generated during the production can create deflections and defects, which entity is comparable with the dimensions of the device. The cutting forces should thus be finely controlled thanks to the choice of the cutting parameters.

1.2.1.3 Stereolithography rapid prototyping

The standard stereolithography rapid prototyping technique consists in the use of a tank, in which a liquid resin is poured. Then a UV light is used to polymerize some layers of the resin, obtaining highly detailed objects.

1.2.2 Production of microfluidic platforms

Microfluidic platforms are produced mainly in two ways:

- with the replica molding process, starting from an existing master and using a polymer (usually PDMS) to replicate the device;
- through the direct production of the device, with different techniques, such as silicon micromachining and micromolding.

1.2.2.1 PDMS

The most widely used material in the production of microfluidic devices for the biological applications is polydimethylsiloxane, known as PDMS. Its low shrinkage rate and the ability to replicate microscale features make it suitable for these applications.

PDMS is a silicon-based organic polymer, it is optically clear, inert, non-toxic and non-flammable. Apart from microfluidic applications, it is used as a food additive, in shampoos and as an anti-foaming agent in beverages or lubricating oils[12]. It is build up by a sequence of the monomer [$SiO(CH_3)_2$]; its chemical structure is reported in Figure 1.5.

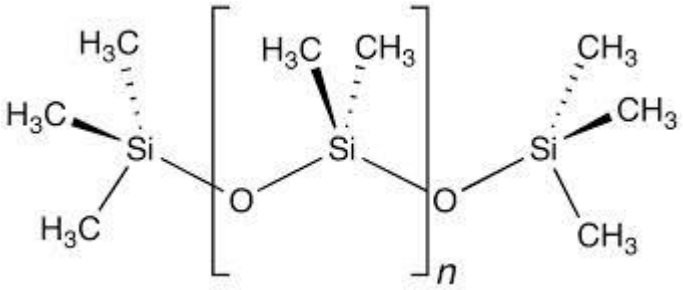

Figure 1.5: *PDMS structure*[12].

The main characteristics of the cured polymer are[13,12]:

- Biocompatibility;
- Transparency at optical frequencies (240nm-1100nm), that allows the observation of the content of the microchannels visually or thanks to a microscope;
- Low autoflorescence;
- Gas-permeability, that allows O_2, CO_2 and N_2 to permeate across the material and reach the cell culture;
- Non-permeability to water;
- Hydrophobicity;
- Low-cost;
- High-resolution.

These properties make PDMS a suitable material to produce microfluidic devices for cell cultures. However, different issues can be found in the application of PDMS to microscale cell culture systems[8,12]:

- PDMS is hydrophobic and porous: it can absorb hydrophobic molecules like lipids from the culture media. Therefore, regular replacements of the media are needed. To reduce this phenomenon, a pretreatment of the devices may be necessary;

- The permeability to gases and fluids can result in a rapid evaporation of the culture media. The device can be placed in a high-humidity environment, or some on chip media reservoirs may be useful;
- PDMS that is not completely cured is toxic to the cells. Attention should be taken during the curing step, with respect to the required curing period. Usually, chips are also autoclaved to increase the cell's compatibility;
- Cells don't usually attach to PDMS: proteins like fibronectin, or mixtures like laminin or Matrigel can be used as coating, to favour the cells' attachment;
- PDMS is sensible to the exposure to some chemicals, like hydrofluoric acid, sulfuric acid, and potassium hydroxide.

PDMS is typically supplied as a two-part liquid component kit, a pre-polymer base and a cross-linking curing agent. They are mixed together in a certain proportion (usually 10:1), the bubbles formed during the mixing are removed with a vacuum desiccator and then the mixture, poured on a rigid master, is cured either at room or at higher temperatures. The final mechanical characteristics depend on the temperature and time of the curing step, in addition to the chosen proportion between the base and the curing agent. Taking as an example the PDMS Sylgard® 184 (Dow corning), the recommended curing duration with respect to temperature is reported in Table 1.4.

Table 1.4: *Recommended curing duration for PDMS Sylgard® 184. Adapted from [14].*

Temperature [°C]	Recommended curing duration
25	48 h
100	35 min
125	20 min
150	10 min

The mechanical properties can be studied for the different curing durations, and the graphs in Figure 1.6 show the relationship between the curing temperature and the most significative mechanical characteristics: the tensile stress and the Young's modulus.

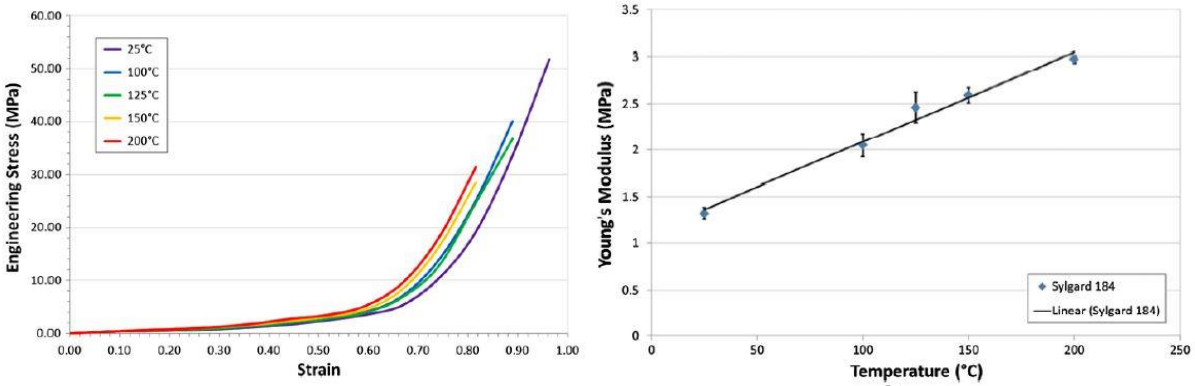

(a) *(b)*

Figure 1.6 *PDMS Sylgard® 184's mechanical properties. (a) tensile stress versus strain at different curing temperatures; (b) Young's Modulus trend with the curing temperature. Adapted from [13].*

The tensile stress increases with a linear behaviour up to strain values of 40%, and then with a non-linear behaviour until failure: this is typical of a viscoelastic material. The tensile stress values increase at higher temperatures, but the failure value decreases as the temperature grows. As concerns the Young modulus, it linearly increases with the curing temperature. Therefore, by using higher curing temperatures, the final cured PDMS will result less stiff, but failure happens at smaller values of the strain. During the design of specific elements, like valves, these behaviours must be considered to obtain the desired performances. To summarize, the main characteristics of PDMS are shown in Table 1.5.

Table 1.5: *Properties of PDMS prepared with the kit Sylgard® 184 (Dow Corning). Adapted from [15].*

Property	Value
Colour	Colourless
Density	965 kg/m^3
Viscosity	3.5 Pa·s
Pot life (at 25°C)	90 min
Young's Modulus (curing temperature of 65°C)	1.71 MPa
Melting point/Boiling point	N/A (it vetrifies)

The pot life is the amount of time for which the mixture of the pre-polymer base and the curing agent remains stable at room temperature. After this period, the mixture starts to harden.

Although not technically challenging, the PDMS devices' fabrication process is quite labour demanding, since it usually consists in the initial molding of the polymer with a rigid master, followed by the inlet punching (of the size of the future connection tubes), and finally by a chemically bonding step (plasma treatment) to seal the channels. This procedure is difficult to be automated, since it varies with respect to the design, therefore it's not suitable for commercialization and large-scale applications. The application of PDMS devices is suitable for the laboratory scale.

1.2.2.2 Replica molding

This process is in common with different techniques, in which a master is used to produce microfluidic devices. A polymer, usually PDMS, is poured on the master and reticulated at high temperatures for a defined time. Finally, PDMS can be easily removed from the master to obtain the microfluidic layer. Figure 1.7 shows the steps of replica molding. After the curing of PDMS, the layer is removed from the master.

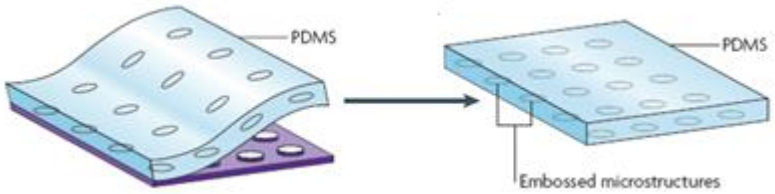

Figure 1.7: *Replica molding of PDMS: (a) molding of the PDMS layer; (b) removal of PDMS from the master. Adapted from [10].*

After the obtainment of the PDMS layer, the microchannels are usually sealed to a glass slide, or with another layer of PDMS, through a plasma treatment that allows the creation of permanent covalent bonds between the two layers.

1.2.2.3 Silicon micromachining

Micromachining is widely used in microelectromechanical systems (MEMS), and it is one of the first techniques that have been applied to microfluidics. However, the typically used crystalline silicon is not an ideal material for microfluidic devices, since it is opaque, expensive, the component integrations are difficult and the surface characteristics are not suitable for biological operations. Moreover, the production techniques themselves are expensive and require specialized skills. Therefore, this technique is preferably used for chemical applications that require strong solvents, high temperatures, and chemically stable surfaces.

1.2.2.4 Micromolding

Injection molding is one of the techniques used for the low-cost fabrication of microfluidic devices. A thermoplastic polymer is heated above its glass transition temperature, and then it is injected into a cavity that contains the master. The cavity is at a lower temperature with respect to the plastic, and therefore a rapid cooling and the hardening of the polymer occur. The master can be produced in several ways, such as through micromachining, electroplating, or silicon micromachining. This approach is cheap and quite fast; however, the main limitations involve the available materials and the resolution.

1.2.3 Plasma treatment

The plasma treatment is used to create chemical bonds (covalent), to seal the microchannels of a PDMS microfluidic platform to a glass slide or to another piece of PDMS in order to form a perfect hydraulic seal.

The plasma is a state of matter where gas molecules have lost electrons, for example because of a high frequency electromagnetic field. Plasma consists of electrons, ions and neutral atoms or molecules. The plasma electrons are at much higher temperature than the neutral gas species (10^4 K), although the plasma gas itself is at near ambient temperature. Its density is around 10^{10} cm^{-3} [16]. The plasma can be created both with an inert atmosphere or with air: at low pressures, the combined effect of the electric field acceleration of electrons and the elastic scattering of the electrons with neutral atoms or field lines leads to the heating of electrons. When they gain a certain amount of excess kinetic energy, the electron-neutral collisions lead to further ionization, releasing additional free electrons[17].

When a surface is exposed to the air plasma, the following phenomena occur[16]:

- Ablation of the surface contaminants, such as oils, mold releases that are characterized by the presence of weak C-H bonds, because of the electrons and the ions bombardment;
- Activation of the surface, creating chemical functional groups on the surface, thanks to the plasma gases, such as oxygen, hydrogen, nitrogen and ammonia that dissociate and react with the surface. The polymers' surface activation consists in the substitution of the surface groups with groups from the plasma gas that are reactive carbonyl, carboxyl and hydroxyl groups. This activation leads also to the change of the surface characteristics of the polymer: wetting (the surface becomes hydrophilic) and adhesion are increased.

In particular, during the plasma treatment of PDMS and glass, the plasma reactive molecules create silicon atoms with one missing electron on the surfaces[18]. These silicon bonds combine with the hydrogen atoms creating silanol (SiOH) groups both on the PDMS and on the glass slide's surfaces, making them hydrophilic. Afterwards, when the two surfaces are put into contact, these bonds recombine to form a covalent connection Si-O-Si between the glass and the PDMS. The device is sealed and can resist to pressures up to 5 bar[18]. The hydrophilicity of the surfaces lasts approximately 1 hour. Figure 1.8 shows the described process.

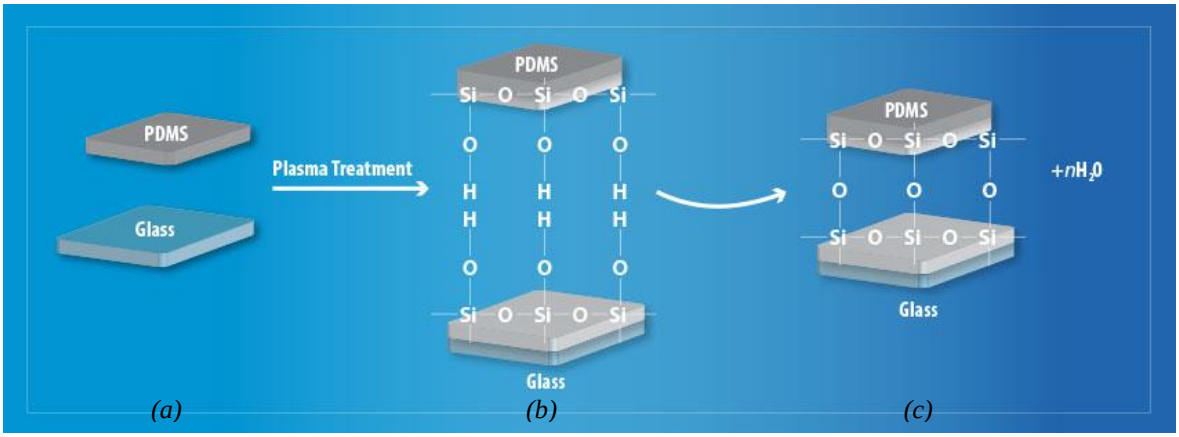

Figure 1.8: *Use of plasma treatment to: (b) activate PDMS and glass' surfaces and (c) create bonding*[18].

The main advantages of the plasma treatment are[16]:

- the plasma affects only the surface, it does not modify the bulk properties of the material. Moreover, it does not leave any organic residue or contaminant and it can clean rough and porous surfaces. It happens at near-ambient temperature, minimizing the risk of damage to heat-sensitive materials;
- it can be used for cleaning, activation and general alteration of surface characteristics with a wide variety of materials;
- it is highly efficient, with short processing times, no drying stage and a small amount of energy is consumed. There is no need for any solvent: the costs are reduced and the compatibility of the PDMS with the cellular environment is maintained;
- it is user and environmentally safe: again the temperature is near-ambient, and there is a little or no direct worker exposure.

The main drawback in the use of plasma treatment to seal microfluidic devices for cell cultures is the need to use the plasma before the cells are inserted in the platform. In fact, the plasma, energetic and reactive, can damage the cells. Usually the device is punched to create an inlet for the cells and then sealed. Afterwards the cells are put inside the platform with a micropipette.

1.3 Neuroblastoma

Neuroblastoma is an embryonal tumor of the sympathetic nervous system, arising during fetal or early post-natal life from sympathetic cells derived from the neural crest. It is the most common malignant tumor in infants: in the United States the incidence is 1 case per 100000 children[19]. Moreover, it represents about 8% of all malignancies diagnosed in pediatric patients, and it causes the 15% of the pediatric cancer deaths[19].

Neuroblastoma is an extremely aggressive and heterogeneous disease: tumors can regress or mature spontaneously, even without therapy, or display an aggressive phenotype, poorly responsive to therapy and subjected to relapse. However, different factors can be identified as responsible for this heterogeneity, to predict the clinical behavior of the disease, such as the age and stage of diagnosis or specific molecular abnormalities[19].

Within this serious situation, the early diagnosis and the understanding of cancer progression and response to therapy become primary issues.

1.3.1 The role of exosomes in cancer detection

Exosomes are extracellular vesicles, with dimensions of 40-100nm, secreted by various cells in our bodies, and identified in most bodily fluids such as urine, amniotic fluid, blood, and saliva. They contain proteins, lipids, mRNAs and microRNAs, in a proportion that depends on the physiological and pathological condition and on the cell of origin. Exosomes have been identified as carriers of cellular contents, playing an essential role in intracellular communication, not only in normal physiological processes, but also in pathological processes of many diseases, including cancer[20]. In fact, it has been found that cancer cells secrete at least 10-fold more exosomes than normal cells[20]. Therefore, cancer-derived exosomes can be used as diagnostic biomarkers for the early detection of the tumour since they carry information about alterations in the cell of origin. In particular, exosomes provide a stable source of miRNA, an established marker for cancer:

To understand the role of exosomes as biomarkers, pure exosomes samples are required: different methods are employed to isolate exosomes, like ultracentrifugation (UC) and ExoQuick precipitation[21].

1.4 Motivation and aim of the thesis

As described in this first Chapter, microfluidics is a promising science and microfluidic platforms can be used to achieve specific conditions in a cell culture. These devices seem suitable for the study of Neuroblastoma and the role of exosomes in its dissemination: the engineering knowledge can be coupled with the biomedical expertise, to obtain a deeper comprehension of this aggressive disease. In particular, microfluidic devices can be used to create concentration gradients and stable conditions of the fluid, to conduct high-throughput and highly controllable experiments.

An appropriate design of the microfluidic platforms and the study of their behaviour is necessary to obtain a profitable application of the devices to the problem described.

Within the study of the exosomes in Neuroblastoma dissemination, the advantages of the use of microfluidic devices are:

- The possibility to generate exosomes gradients, in order to test their local and long-range effects;
- The high-throughput data, useful to take advantage of the small exosome material that can be obtained from the tumour cells;
- The possibility to test gradients on 3D cell cultures, capable of represent the *in vivo* situation.

The work behind this thesis, based on the initial part of the project led by professor Elisa Cimetta, consists in the study of two types of microfluidic platforms, called microbioreactors (μBRs). During this work, Neuroblastoma cells were not examined within the devices, as the biological section of the team is still characterizing them. To perform all our development, optimization, and validation experiments and to assess the biological compatibility of the microbioreactors, we used another type of cells: HEK-293. In the following steps of the study, the devices will be used to analyse the exosomes secreted by Neuroblastoma tumour cells: this project provides an important opportunity to advance the understanding of the role of these vesicles in the cancer dissemination, task not completely achieved in the studies conducted so far.
The two platforms were studied, improved and finally tested to understand the fluid behavior and dynamics. Afterwards, the cellular behavior inside the reactor was assessed, by performing some biological experiments on the HEK-293 cells.

Chapter 2

Materials and methods

This Chapter deals with the design, the fabrication methods and the procedures followed during the production and the testing of the two microfluidic platforms. Afterwards, a brief description of the biological protocols is reported, including the methods used to daily treat and maintain the HEK-293 cells.

2.1 First microfluidic platform

2.1.1 Design and production of the master

The first microfluidic platform studied and tested is based on an existing design, developed with a 3D-CAD software. The 2D design of the platform and the 3D-CAD design of the master are shown in Figure 2.1.

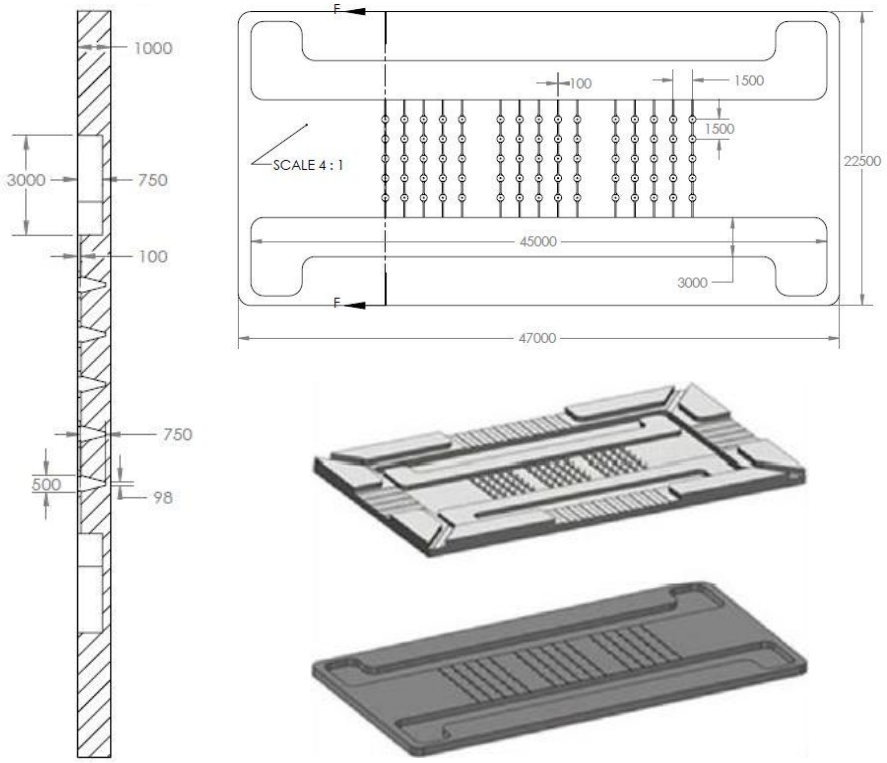

Figure 2.1: *2D and 3D-CAD design of the first microfluidic platform proposed. Adapted from*[1].

The device is formed by two lateral channels (750 x 3000µm height x width) that are used to provide fluids to the central microchannels. These latter have a width of 100µm and connect different microwells in a row. Each microwell is conical: the upper diameter is 500µm, and the lower 98µm. They create a matrix, where each row is independent from the others and connected to the lateral channels.
The overall dimensions of the microbioreactor used during the work of thesis are reported in Figure 2.1, while the number of microwells per row is increased to nine. As a consequence, the space between each well's center is reduced from 1500 to 900µm.
The master available was produced using a standard stereolithography rapid prototyping technique[7], described in paragraph §1.2.1.3. The master is used to obtain PDMS devices via the procedure of replica molding. A picture of the rigid master is shown in Figure 2.2.

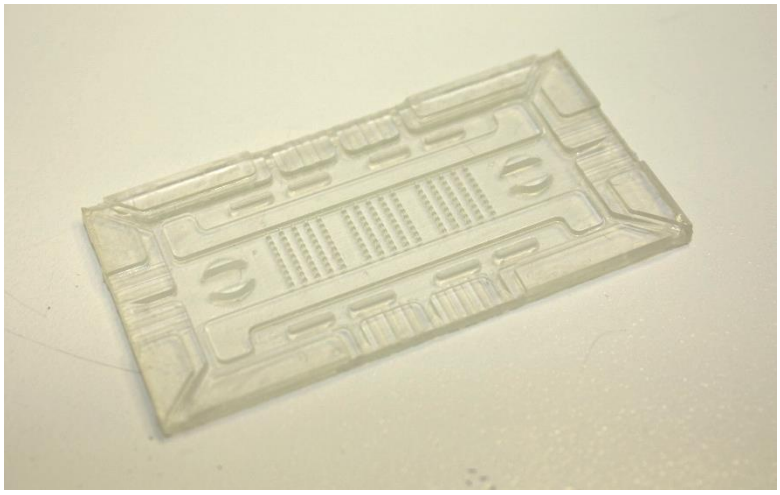

Figure 2.2: *Rigid master of the first microfluidic platform.*

2.1.2 Operating principles

When this microfluidic platform operates, two different fluids flow along the lateral channels. The four enlargements of the channels, placed in the four corners, are employed as inlets and outlets. The fluids are provided in such a way to establish a steady state condition inside the platform: the inlet and outlet flow rates are equal and do not change with time. Considering the dimensions of the lateral channels to calculate their section (Figure 2.1) and assuming a flow rate of 100µL/min, the Reynolds number in the two channels can be determined, using the equivalent diameter and the physical parameters of water in Table 1.2.

$$D_{eq} = \frac{4S}{2P} = 1.2 \cdot 10^{-3} m \tag{2.1}$$

$$\mathrm{Re} = \frac{\rho v D_{eq}}{\mu} = 0.89 \tag{2.2}$$

The value of the Reynolds number demonstrates that the flow inside the lateral channels is laminar, leading to a predictable behavior of the microfluidic platform and to the possibility of creating the conditions to establish constant concentration gradients.
In fact, since the dimensions of the central channels are really small if compared to the lateral ones (diameter of 100µm), the velocity is extremely reduced at their entrance: Pe is small and the convective flux of the species *i* within the channels is dominated by the diffusive flux, that plays a key role in this device. Therefore, by providing two fluids at different concentrations of a certain species, or two different tracers, a concentration gradient inside the microchannels is created. A fluid-dynamic simulation is performed to predict the behavior inside the platform.
The final use of the device consists in culturing cells inside the microwells, and exposing them to exosomes' concentration gradients, provided by one lateral channel, to obtain high-throughput data.

2.1.3 COMSOL Multiphysics® simulation

The COMSOL Multiphysics® modelling software is used to simulate the fluid dynamics of the microbioreactor, and to understand quantitatively the entity of the concentration gradient inside the microwells. The results of the simulation are compared with the experimental data, to validate the proper operations of the platform. COMSOL Multiphysics® is organized in modules, that are selected to add a specific physics interface to the system. Our first approach was based on a 2D model of the platform. The physics that are added to this simulation are: *a.* the laminar flow of a single-phase incompressible fluid, to describe fluid motion inside the channels, and *b.* the transport of a diluted species, to simulate the convective/diffusive behavior of a generic species *i* inside the platform. The fluid inside the microbioreactor is assumed to be water, since its physical properties are comparable to the ones of the solutions used during the experiments.

2.1.3.1 Laminar flow

The laminar flow of a single-phase fluid is described by the Navier-Stokes equations (conservation of mass, momentum and energy), that are solved considering that the fluid is Newtonian, the density is constant (if the temperature is almost constant) and that the no-slip condition applies to the walls. The problem is analyzed at the steady state, and the parameters that are inserted to solve the laminar flow problem are:

- temperature;
- inlet medium velocity, that is changed to simulate different inlet flow rates;
- outlet pressure;

The whole platform is interested by the laminar flow.

2.1.3.2 Transport of Diluted Species

This module allows the study of the evolution of the behavior of chemical species transported by diffusion and convection[22]. The species are assumed as diluted: their concentration is small if compared to that of the solvent. Therefore, the mixture properties such as density and viscosity are assumed as those of the solvent. As explained in paragraph §1.1.1, Fick's law governs the diffusion of the solute, and the mass balance of the species is given by equation (1.8). While the diffusive term is always included in this module, the convective term is active by default but can be excluded by the user. The velocity term is calculated by coupling this physics interface with the laminar flow.
In the problem treated, the convective term is kept active. The parameters that must be defined in this interface are:

- the diffusion coefficient, that is changed to simulate the different types of solutes that can be flown through the lateral channels;
- the initial concentration *c* (at the inlets) of the species.

The characteristics of the species, except for the diffusion coefficient, are not needed since the solution is assumed to be extremely diluted. Therefore, the properties of the solute do not affect the solvent's ones.

2.1.4 Production of the microfluidic platform

The microfluidic platform is produced with PDMS Sylgard® 184 (Dow Corning), that is provided as a two-part kit (DOWSIL™ 184 Silicone Elastomer kit): a silicone elastomer base and a curing agent. This kit is used to produce microbioreactors, thanks to the replica molding process, which steps are:

1. Weighing of the base and curing agent in a proportion of 10 parts of base:1 part of curing agent, inside a disposable plastic container;
2. Energetic mixing of the base and the curing agent in order to create a homogeneous mixture. During this step, a large quantity of bubbles is formed inside the mixture;
3. Removal of the bubbles thanks to a desiccator (Figure 2.3), connected to a vacuum pump: the plastic container with the mixture is placed inside the desiccator chamber,

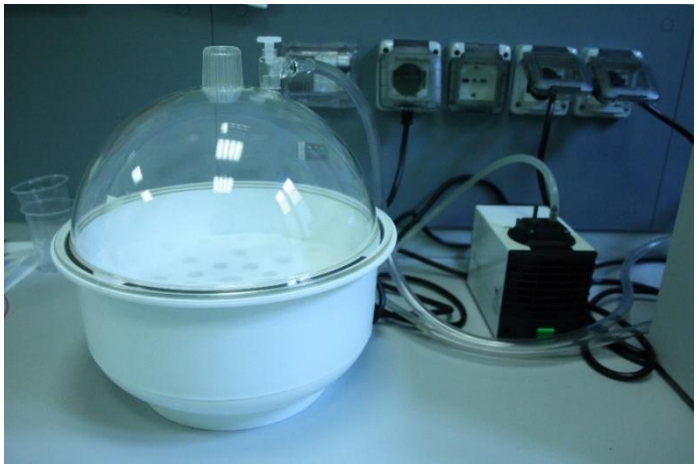

Figure 2.3: *Desiccator connected to the vacuum pump used in the BIAMET laboratory.*

the pump is switched on to create vacuum inside the chamber and thus allowing the bubbles emerge and expand. After some minutes, the pump is switched off and the valve of the desiccator is opened to gently return to atmospheric pressure. This step makes the bubbles on the surface of the mixture blow up. The procedure is repeated different times (usually 4 or 5) to remove all bubbles;

4. Pouring of the PDMS on the rigid master, and possible removal of additional bubbles that can create during the pouring step, with the same procedure of step 3;
5. Curing of the PDMS on the master at 65°C for 75min, inside an oven. This temperature was set based on the provided values listed in Table 1.4 and optimizing them for the specific case;
6. Removal of the cured layer from the rigid master, using a scalpel to ease this operation.

Finally, the platform's sides are cut to remove the lateral parts, present only for an easier removal from the master. Once the microfluidic platform has been cured and removed from the master, it can be employed in an irreversible or reversible configuration.

2.1.5 Irreversible configuration

The irreversible configuration consists in the use of the plasma treatment to form the hydraulic seal of the microfluidic platform to a supporting material. The microbioreactor in this configuration is used to perform the fluid dynamic validations to understand the behavior of fluids.

First, the inlets and the outlets of the fluids are created with a biopsy punch (diameter of 1.5mm). Then, the microbioreactor is sealed to a glass slide or to another piece of PDMS, with the following procedure:

1. cleaning of the device and of the glass (or PDMS) base with scotch tape, to remove dust or any residue from the surfaces;

2. insertion of the two pieces, with the surfaces that must be activated upwards, inside the Plasma Cleaner (PDC-002-CE by Harrick Plasma, Figure 2.4*a*) and closing of the small door, keeping the valve closed (vertical position);
3. starting of the vacuum pump to create vacuum inside the Plasma Cleaner;
4. after approximately 4 minutes, the plasma is switched on and, after its appearance, the valve is slightly opened to allow the entrance of some air. The color of plasma should be an intense pink (Figure 2.4*b*), meaning that an adequate quantity of oxygen is present inside the chamber. If the color tends to violet or blue, it means that there is a lack of oxygen, and the valve should be gradually opened (turning it counter clockwise). The plasma is maintained for 1 minute;
5. after 1 minute, the plasma is switched off. Then the vacuum pump is switched off and the valve is slowly opened to return to atmospheric pressure.

(a) *(b)*

Figure 2.4*: (a) Plasma Cleaner by Harrick Plasma used in BIAMET laboratory and (b) the color of plasma when an adequate quantity of oxygen is present in the chamber.*

Then the door is opened, and the two layers are removed paying attention to not touching the activated surfaces. Afterwards, they are put into contact and they attach, thanks to the formation of chemical bonds, as explained in paragraph §1.2.3.

Finally, the microfluidic platform is put in the oven for at least 10 minutes at 65°C, to promote the formation of the covalent bonds.

The irreversible configuration can be used with some tracers (colored or fluorescent), to ensure the correct operation and the formation of the chemical gradient inside the microchannels. In fact, since the whole platform is optically clear, the lateral channels and the microwells can be observed visually as well as with the microscope.

The use of the plasma treatment ensures a perfect seal of the platform; however, this configuration cannot be exploited for the biological experiments. In fact, the cells cannot be inserted neither before the plasma treatment, because of its high energy that can damage the culture, nor after the plasma treatment, since the punching of each microwell is not possible.

2.1.6 Reversible configuration

Since the irreversible configuration does not allow for an easy insertion of the cells inside the microwells, a reversible configuration must be used for the biological experiments. We thus used a clamping unit (Figure 2.5) that, from bottom to top, is formed by[7]:

- an aluminum base;
- a glass slide;
- the microbioreactor with the open wells facing upwards;
- a polycarbonate (PC) manifold, perforated in the positions corresponding to the inlets and outlets of the fluids;
- a clamping plate.

Two slide latches are used to tighten the PC manifold against the microbioreactor, ensuring the hydraulic sealing.

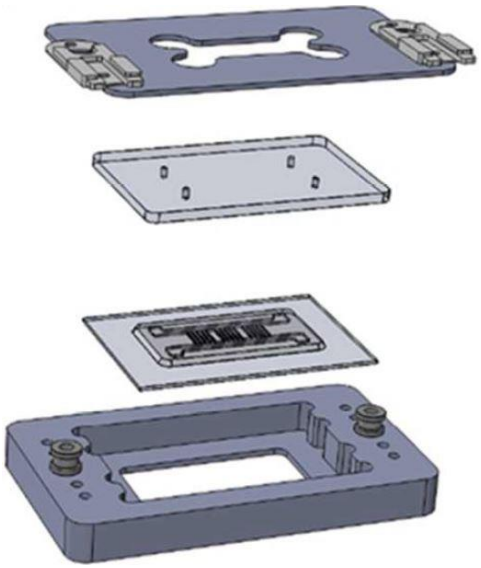

Figure 2.5: *Clamping unit employed in the reversible configuration of the first microfluidic platform. Adopted from[1].*

Thanks to the reversible configuration, the cells can be inserted in the microwells, and then the device can be closed and sealed. After an experiment, the clamping unit can be opened, and, if needed, the cells can be removed and analyzed.
This configuration also allows the observation of the microbioreactor with the microscope and visually, since the central part of the clamping unit is perforated.
The assembled unit is prepared by the following steps:

- the microbioreactor, placed in the center of the glass slide, is inserted in the Aluminum base;

- a certain amount of liquid (water in the validation experiments or fibronectin and then cells in their culture media in the biological experiments) is placed over the microwells. Then the device is put in the desiccator, where the vacuum allows to remove the air present in the microwells;
- the PC manifold is placed on the microbioreactor, avoiding including air between the two layers;
- the clamping plate is positioned, and the two latches are closed, to assure the sealing of the platform.

This configuration can be employed for validation experiments with colored and fluorescent tracers and for biological experiments, to test the compatibility with the cellular environment.

2.1.7 Validation experiments

Both the irreversible and the reversible configurations are used to perform validation experiments, employing colored tracers (food coloring) and fluorescent tracers to compare the behavior of the fluid with the fluid dynamic simulation. The food coloring solution is simply prepared by mixing it with water, in a proportion suitable to obtain an intense color. The fluorescent tracers are fluorescein isothiocyanate-dextrans (SIGMA-ALDRICH®), polymers of anhydroglucose, available in three different average molecular weights: 65000-85000, 250000 and 500000Da. Their maximum excitation is at a wavelength of 490nm, and the maximum emission is at 520nm. The fluorescence increases with pH and is optimal at a value of 8 or above[23]. The average diffusion coefficient changes with respect to the molecular weight, and therefore, the three dextrans simulate three solutes of different dimensions. The isothiocyanate-dextran solution is prepared by diluting it in phosphate buffered saline (PBS) or water in a proportion 0.0005g/10mL. The culture media is not used as a solvent for the fluorescent tracers, since it contains phenol red that can interfere with the fluorescence acquisitions.

A syringe pump is used to infuse and withdraw the solutions to and from the microbioreactors. The pump PHD Ultra (Harvard Apparatus), in Figure 2.6, is supplied with a double mechanism that allows using pairs of syringes to simultaneously infuse and withdraw the fluids at the same flow rate.

The pump is formed by two elements: a central body (on the right in the image) with a

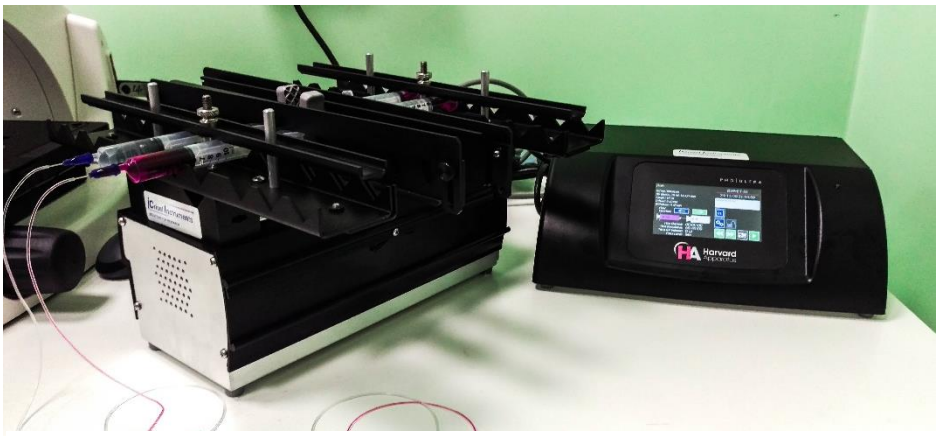

Figure 2.6*: Pump PHD Ultra by Harvard Apparatus employed in BIAMET laboratory.*

display that allows to set up the pump, connected to a mechanical multi-rack remote unit (on the left), on which up to 10 syringes per side can be placed.
To carry out an experiment, four 10mL syringes (NYPRO) are prepared: a 21G steel dispensing tip (DRIFTON) is inserted inside a microtube (inner diameter of 0.5mm, outer diameter of 1.5mm, TYGON® TUBING), and then connected to the syringe.
Two of the four syringes, one filled with the food coloring or with dextran solution and the other one filled with water, are placed on the infuse side of the pump, while two empty syringes are placed on the withdraw side. The type of syringe, the volumetric flow rates and the target volume are manually set on the display. The volumetric flow rates are usually set between 50 and 150 µL/min.
The procedures employed for the two configurations are now described in detail.

2.1.7.1 Irreversible configuration

The microbioreactor, arranged in the irreversible configuration, is used immediately after the plasma treatment, in order to exploit the increased hydrophilic nature of the surfaces. The procedure followed in the installation of the device is:

- the µBR is placed inside a small container filled with water, and a micropipette is used to fill the lateral and the micro channels. The use of the device right after the plasma treatment allows the internal surfaces to get completely wet, without the need of using the desiccator;
- the pump is started and once water has completely filled the tubing, the infuse syringes, and then the withdraw syringes, are connected to the ports (made with the biopsy punch) thanks to the microtubes;
- after approximately 2/3 minutes the concentration gradient forms and reaches the steady state. It is not immediate, since the movement of the species inside the microchannels is led by diffusive flux.

Figure 2.7*: Fluorescence microscope used in BIAMET laboratory.*

Finally, images of the gradient are taken: during the experiments with food coloring, bright field pictures are enough to obtain a qualitative and semi-quantitative result, while during the experiments with dextrans, a fluorescence microscope is used to acquire data. The fluorescence microscope used in BIAMET laboratory (Invitrogen EVOS^{TM} FL Cell Imaging System by ThermoFischer Scientific), shown in Figure 2.7, is provided with a monochrome camera, used for both transmitted light and fluorescence signals. The different EVOS Light Cubes installed (DAPI, GFP, RFP) allow using different fluorescence wavelengths. The GFP Cube is used with the fluorescent tracers. Using a 10x magnification, different images of a row are taken and saved; afterwards, they are combined to obtain a picture of the entire row of interest.

The images are stitched with Paint, and then the software ImageJ is employed to obtain semi-quantitative information. The image is loaded, and then changed to an 8-bit type, to obtain a black and white picture. Using a circle, 11 Regions of Interest (ROIs) are identified (the nine microwells and the two lateral channels), and the medium light intensity is detected (commands Analyze and Measure). Since the absolute value of emission is not known, the eleven intensities are normalized with respect to the highest absolute value, to obtain a scale comparable with the results of the COMSOL Multhyphysics® simulation.

2.1.7.2 Reversible configuration

The clamping unit is prepared with the procedure described in paragraph §2.1.6. Differently from the irreversible configuration, it is necessary to remove the air present inside the microwells using the vacuum desiccator and remove the air bubbles formed with the aid of a micropipette.

After the closing of the clamping unit, the pump is started and the microtubes are inserted in

the PC manifold's holes, with a procedure analogous to the irreversible configuration's one. After approximately 2/3 minutes, the system reaches the steady and then pictures are collected with the same procedure of the case of the irreversible configuration.

2.1.8 Biological experiments

Some biological tests are performed in order to assess the biological compatibility of the microbioreactor. Only the reversible configuration can be employed during these experiments: as explained, the irreversible one is not suitable, since the plasma treatment is aggressive and can damage the biological content. Moreover, the design of the platform does not allow the inserting of cells after the sealing of the microchannels.

For the biological experiments, all the material needed (glass slides, µBRs, microtubes, clamping unit) must be sterilized in the available autoclave (Europa B Evo, Arco Scientifica), and the steps of the procedure are conducted inside the biological safety cabinet (MSC-Advantage, Thermofisher Scientific).

The procedure followed during the closing of the clamping unit is the one described in paragraph §2.1.6, but the first steps are partially different and need to be explained in detail. In fact, the central part of the µBR, placed on the glass slide and put inside a Petri dish to maintain the sterility, is initially coated with fibronectin (FN, a protein that favors the attachment of cells to the PDMS surface), prepared in solution with $PBS^{=}$ (phosphate buffered saline without ions), in a proportion 1:4. About 300µL of solution are placed over the microchannels. The covered Petri dish is placed in the desiccator, where the vacuum helps the removal of air from the microwells, and the consequent filling with the FN solution. The air bubbles are then removed with the aid of a micropipette. The µBR is then placed in the incubator (HERACELL^{TM} VIOS by Thermofischer Scientific) for 1h.

The FN solution is then removed and the cells in their culture media, usually 250-500cells/mm^2, are added. Another step in the desiccator may be needed. After some hours the cells deposit inside the microwells and attach to the PDMS surface: the excess culture media is removed and replaced with fresh media. The platform is then left overnight in the incubator.

At this point, the clamping unit can be closed following the usual procedure, and the experiment can be started. To ensure the sterility of the materials, the clamping unit is prepared inside the biological safety cabinet, as well as the syringes. The syringe pump is placed near the incubator, and the clamping unit is left inside the incubator during the entire experiment.

The tracers used during the biological tests are different from the ones employed during the validations. In fact, fluorescent tracers that highlight the presence of cells are:

- Hoechst stain, a blue fluorescent dye used to stain DNA, excited by UV light at 350nm and with a maximum emission at 461nm. It is prepared using PBS as solvent, in a proportion 1:5000 (2µL of dye in 10mL of PBS). This solution must be protected by light and, if stored at 2-6°C, it remains stable up to 6 months;
- Calcein-AM (SIGMA-ALDRICH), a reagent staining the cytoplasm in cells, with a maximum excitement at 496nm and emission at 516nm. The Calcein-AM supplied by the producer (1mg, that corresponds to 1µmol) is used to prepare a 10mM stock solution, by diluting it in 100µL of dimethyl sulfoxide (DMSO). In order to obtain a 10µM working solution, 10µL of stock solution must be diluted in 10mL of PBS. Therefore, 10 aliquots of stock solution are prepared and stored at -20°C.

The syringes are prepared and the microtubes are inserted in the PC manifold's holes. After a few hours, necessary to let the tracers absorb in the cells, images are taken with the microscope, using the DAPI Cube for the Hoechst dye and the GFP Cube for the Calcein-AM. Therefore, the concentration gradient can be verified in both the directions, and the cell viability is observed.

2.2 Second microfluidic platform

2.2.1 Design and production of the master

The master of the second platform was developed and produced in collaboration with the TE.SI. laboratory, based in Rovigo. The 2D-CAD designs of the platform and of the master are shown in Figure 2.8.

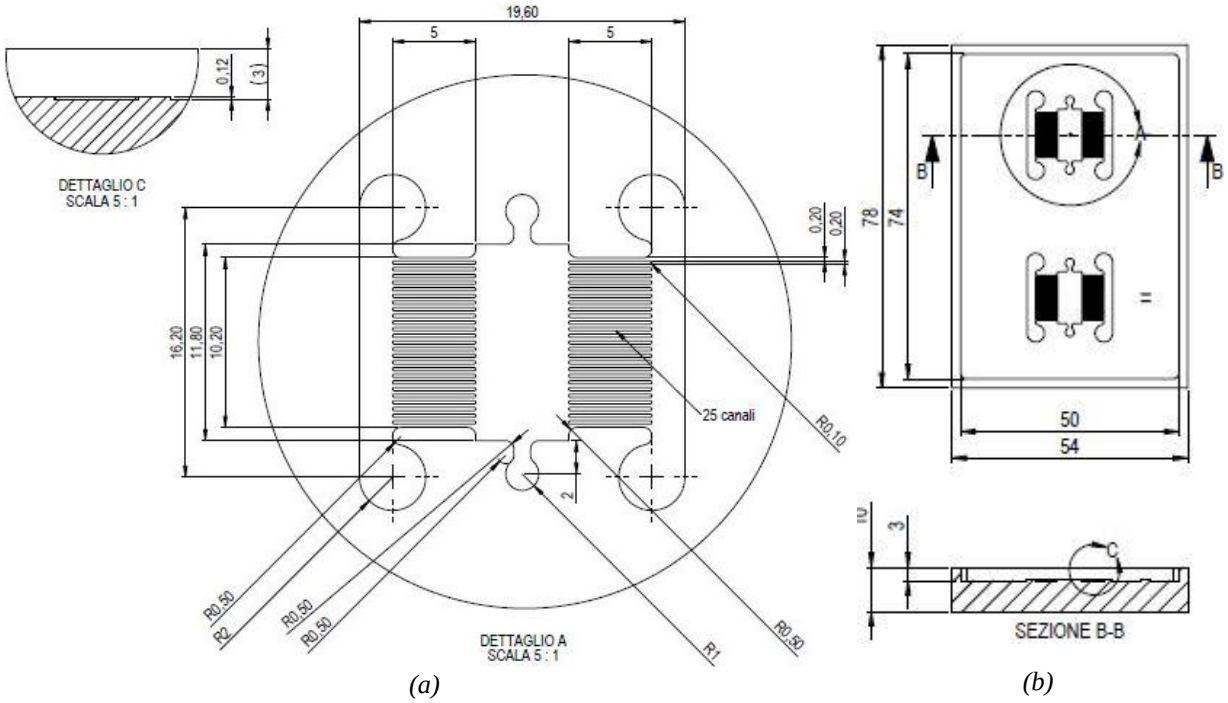

Figure 2.8: *2D-CAD design of the platform (a) and of the entire master (b) of the second platform. Lengths in mm.*

The platform is composed by: a. two lateral channels that, similarly to the first platform, are used to flow the two fluids at different concentrations; b. two series of microchannels (rectangular section, 120 x 200µm) and c. a central chamber, where the cells are seeded. The chamber is equipped of two seeding ports, useful to inject the cells inside the microbioreactor. As can be observed from Figure 2.8*b*, two platforms are present on the same master.

The master was produced in the TE.SI. laboratory with a standard micromilling technique. The master was created with the miller Kugler MICROMASTER® 5X, a high precision machining center, specially designed and optimized for micromachining and microstructuring, supplied with 5 simultaneous axes of motion[24]. As explained in paragraph §1.2.1.3, the choice of the working parameters and of the tools is fundamental to obtain a highly precise result.

Starting from the 3D-CAD design of the master, tools of different dimensions are selected, and the miller is prepared:

- an Aluminum block is fixed on a support;
- the tool is settled and rotated for 10 minutes, to increase its temperature and stabilize its dimensions;
- the zero of the machine is set up thanks to an automated procedure;
- the velocity is set up to 31831 rpm for the outer surface and to 150000 rpm for the platforms;
- the machine is started, and the block is milled.

The tools used for this procedure were a 3mm tool for the outer surfaces, a 2mm tool for the lateral channels and the central chambers and a 0.2mm tool for the microchannels. The tools must be replaced at the first signs of wear to obtain a precise milling of the entire master.
After the milling, the master is immersed in ethanol and cleaned in an ultrasound bath.
We then conducted some tests on the master to estimate the precision of the milling procedure. In particular, the measures of interest are the height of the different elements of the master and the roughness of the surfaces. Variable values of heights or high values of roughness may bring to difficulties in the attachment of the microbioreactor to the glass slide with the plasma treatment. The measurements were done using a 3D optical profiler (Sensofar® S Neox), with the possibility of employing three modes[25]:

- Confocal Scanning, a technique that utilizes an aperture at the confocal plane of the objective, used to capture 3D and 2D images of the object;
- Optical Interferometry, that exploits the path difference between light reflected in the two arms of the interferometer to yield spatial interference pattern, that contains information on the surface topology of the sample;
- Focus Variation, that scans the entire sample to obtain continuous images, varying continuously the focus and building up the image.

As concerns the heights' measurements, the Focus Variation mode is employed, with a 20x objective:

- different areas of interest are selected;
- on each area, the focus was manually changed to set the upper and the lower planes, between which values the analysis is carried out by the profiler;
- the analysis is started, and the heights between the two planes are studied.

On a different area, the roughness can be measured with a similar procedure, but using the confocal mode, instead of the focus variation.
A picture of the produced master is shown in Figure 2.9.

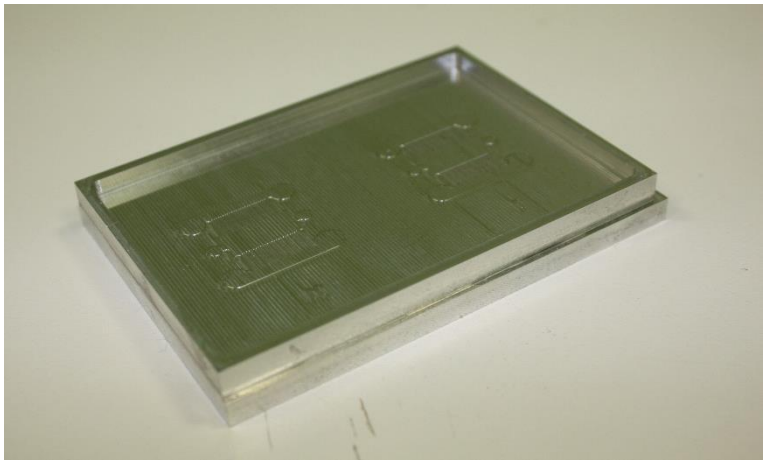

Figure 2.9: *Master of the second microfluidic platform.*

2.2.2 Operating principles

The operating principles of this microfluidic platform are quite similar to those of the first device. In fact, two fluids are provided to the microbioreactor. They enter from one side of the two lateral channels and they are removed from the other side, assuring the achievement of the steady state condition. The two lateral channels have rectangular section (120 x 2000μm), which determines the establishment of a laminar flow. In fact, considering a typical inlet flow rate used in this device of 5μL/min ($8.33 \cdot 10^{-11}$ m^3/s), the Reynolds number in the lateral channels can be calculated, estimating the equivalent diameter and taking into consideration the parameters in Table 1.2:

$$D_{eq} = \frac{4S}{2P} = 2.26 \cdot 10^{-4} m \tag{2.3}$$

$$\mathrm{Re} = \frac{\rho v D_{eq}}{\mu} = 7.8 \cdot 10^{-2} \tag{2.4}$$

The flow is laminar, since the Reynolds number is extremely small.
The general objective of the use of this platform is to obtain a concentration gradient inside the central channel. However, the dimensions of the microchannels of the mold we produced are not suitable for this application. In fact, they have the same height of the lateral channels (and of the central chamber), and a width of 200μm. These dimensions do not allow the predominance of the diffusion flux on the convective one: this problem will be investigated and the possibilities to solve it will be presented in the next chapter. However, the platform is employed to conduct some biological experiments, in which the cells are seeded in the

central chamber and two fluids at different concentrations are provided in the lateral channels. The final objective is to use the platform to obtain exosomes gradients within the central chamber.

2.2.3 COMSOL Multiphysics® simulation

The COMSOL Multiphysics® modeling software is used to simulate the fluid dynamics of the second microfluidic platform. The results of the simulation are compared with the experiments, to validate the performance of the device. In this case we performed two simulations:

- a 2D simulation to understand and validate the operations of the platform;
- a 3D simulation to understand how the platform can be modified to obtain the overcoming of the diffusive flux on the convective flux in the central chamber.

The interfaces used are the laminar flow, since the flow is laminar in the whole platform, and the transport of diluted species, since the solutions used in the experiments are extremely diluted.

2.2.3.1 Laminar flow

The hypothesis and the conditions set in the laminar flow interface are the same defined in the paragraph §2.1.3.1. The entire platform is interested by the laminar flow.

2.2.3.2 Transport of Diluted Species

Like in the first platform's case, described in paragraph §2.1.3.2, both diffusion and convection are active in this interface, and the velocity term is calculated by coupling it with the laminar flow.
The parameters defined are the diffusion coefficient of the species and the initial concentration.

2.2.4 Production of the microfluidic platform

The microfluidic platform is produced with a method analogous to the one employed for the first platform, as described in paragraph §2.1.4. In the process of replica molding the PDMS is prepared, poured on the master and then cured for 75 min.
After curing, the PDMS layer is removed, the two platforms are separated and cut with the

dimensions of a glass slide. Afterwards, the two microbioreactors are assembled thanks to the plasma treatment, obtaining an irreversibly sealed device.

2.2.5 Irreversible configuration

This microfluidic platform is used only in an irreversible configuration. After the cutting of the PDMS layer, the inlets and the outlets of the fluids are created with a biopsy punch with a diameter of 1.5mm, whereas a punch with a diameter of 1mm is used for the seeding ports (the cores are stored). Finally, the punched layer is attached to a glass slide with the plasma treatment, with the same procedure described in paragraph §2.1.5. This irreversible configuration can be employed both for qualitative experiments, using colored or fluorescent tracers, and for biological experiments. These latter are possible thanks to the two seeding ports: they allow to easily seed the cells in the central chamber after the plasma treatment. The stored cores are now used to plug the seeding ports, before connecting the device to the pump.

2.2.6 Validation experiments

The performance of the second microfluidic platform can be validated and compared with the COMSOL Multiphysics® simulation, by performing some validation experiments. Food coloring and fluorescein isothiocyanate dextran can be employed as tracers for this aim.
When the microbioreactor is prepared for a validation experiment, it is not necessary to punch the seeding doors, since cells will not be inserted in the platform. After the plasma treatment, the device is completely filled with water with the aid of a micropipette, and then the experiment can be set up.
The syringes and the pump are prepared with the procedure described in paragraph §2.1.7. Then, the pump is set up and started and the microtubes are connected to the platform, exploiting the four ports created with the 1.5mm punch. The volumetric flow rates are usually set between 5 and 20µL/min.
After approximately 2/3 minutes, when the functioning is stable, some pictures are taken in the case of the food coloring tracer, and the microscope is used in the case of the fluorescent tracers.

2.2.7 Biological experiments

Some biological tests are performed in order to assess the biological compatibility of the microbioreactor. As explained, the irreversible configuration is suitable for these experiments, since the seeding doors allow the insertion of cells after the plasma treatment, without damaging them.

During the biological experiments, all the material used is sterilized in the autoclave, and the steps of the procedure are conducted inside the biological safety cabinet.
After the preparation of the platform, procedure described in paragraph §2.2.5, an autoclave treatment ensures sterilization of the device and the cores. The µBR is placed in a Petri dish, inside the safety cabinet. Then, 13µL of fibronectin solution (diluted with $PBS^{=}$ in a proportion 1:4) are carefully injected in the central chamber from a seeding port, using a micropipette. After 1h, the same volume of cells in their culture media is seeded in the central chamber; this allows the removal of FN. The cells' density used is typically between 500-1500cells/mm^2.
After a few hours, the cells start adhering to the bottom surface. At this point, some fresh culture media is added in the lateral channels and in the microchannels. Finally, 200-300µL of culture media are placed over all the holes of the platform, to ensure availability of nutrients and ideal survival environment for the cells during static culture. The platform is left overnight (or for a maximum of two days) in the incubator. Before starting the experiments, the two seeding ports are plugged using the autoclaved cores. The pump is prepared with the same procedure of paragraph §2.1.8, using Hoechst stain and Calcein-AM as tracers in the two syringes.
The microtubes are inserted in the lateral channels ports; after at least 2 hours some pictures are acquired with the microscope. In these experiments, the performance of the platform can be observed, together with its biological compatibility. Figure 2.10 shows the arrangement during the biological experiments, where the microbioreactor is connected to the pump and placed inside the incubator.

Figure 2.10: *Experimental configuration during a biological experiment, where two µBRs, placed in the incubator, are connected to the syringe pump.*

2.3 Biological protocols

2.3.1 HEK-293

The HEK-293 cells employed during this work of thesis and provided by ATCC, are human embryonic kidney cells, grown in tissue culture. They have been widely used in biology research, because of their reliable growth and propensity for transfection.

2.3.2 Cellular splitting

The procedure of cellular splitting is a process of subculturing, consisting in the periodic separation of the cell population, in our case seeded in a $75cm^2$ flask. The aim is to avoid the overcrowding of cells that attach to the flask's bottom surface and to increase their number. A specific value of confluence (the filling percentage of the flask bottom surface) must not be exceeded, since cells would not be able to grow anymore and would detach from the surface. The -293 cells, for example, have a maximum confluence of 90%. Figure 2.11 shows cells that have almost reached the maximum confluence.

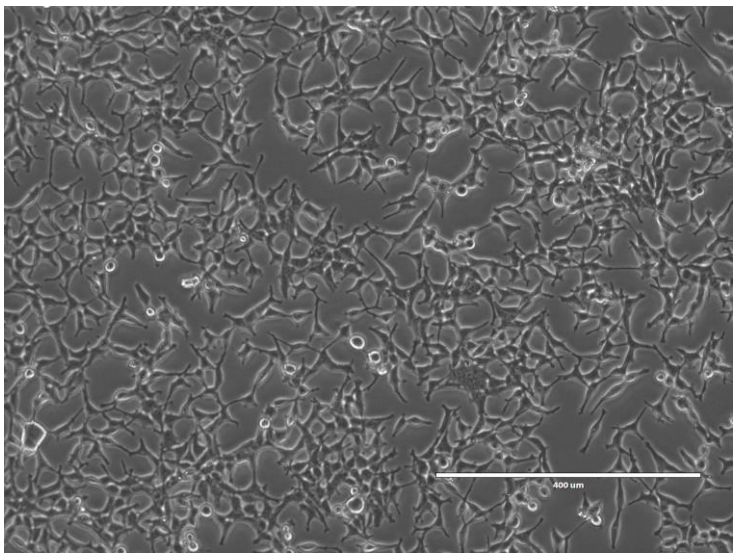

Figure 2.11: *HEK-293 cells seeded in the $75cm^2$ flask.*

The culture media in which cells are bathed varies with respect to the type of cells treated and allows their growth, providing them nutrients. In the case of HEK-293, it is prepared starting from the base medium, called DMEM (Dulbecco's Modified Eagle Media by Thermofisher Scientific). It does not contain any proteins, lipids or growth factors, so it is completed by creating a solution containing $10\%_{v/v}$ of fetal bovine serum (FBS), $1\%_{v/v}$ of Glutamine (an amino acid) and $1\%_{v/v}$ of Penstrep (an antibiotic). These additional elements allow the supplying of nutrients and growth factors and assure the sterility of the cellular

culture. The mixture is filtered (with the Vacuum Driven Disposable Filtration System, Millipore) and stored at 4°C.
With regards to cellular splitting, this procedure is completely executed inside the safety cabinet, to ensure sterility and avoid any contamination of cells. First, culture media and Trypsin/EDTA solution (Biochrom GmbH) are warmed in a 37°C waterbath (Bagnomaria Serie Pura, Julabo, Sacco srl). Then, the old flask is taken from the incubator, placed in the safety cabinet, and the protocol can be started:

- the old medium (8-9 mL) is removed by aspiration with a serological pipet, and approximately 4 mL are stored and kept in a 15 mL Falcon tube. The rest is discharged;
- the flask bottom surface is gently rinsed with 5-7 mL of PBS at room temperature, to remove any trace of culture media, that contains trypsin inhibitors. Then PBS is aspirated and discarded;
- 1.5 mL of Trypsin are added on the cell layer and the flask is placed in the incubator for 5-7 min. The detachment of cells can be observed by gently hitting the flask;
- the 4 mL of old medium are inserted in the flask, to inhibit the action of Trypsin. By gentle pipetting, the cells are aspirated from the bottom surface and placed in the Falcon tube;
- the cells are counted and an appropriate aliquot of cell suspension is added to a new 75 cm^2 flask, with 8-9 mL of fresh culture media. An inoculum of $2 \cdot 10^3$ to $6 \cdot 10^3$ cells/mm^2 is recommended.

If some residues are present in the old flask, an additional step can be carried out after counting the cells and before adding the inoculum inside the new flask. The Falcon tube containing the cells is centrifuged at 950 rpm and 25°C for 3 minutes and setting the soft deceleration. This induces the sedimentation of the cells that form a dense pellet, while the residues remain in the supernatant. The liquid is aspired and the cells are resuspended in an appropriate quantity of new culture media.
The cellular splitting is usually done every 3-4 days. However, the medium renewal may be necessary every 2-3 days. The medium must be replaced when its color tends to change from an intense red to yellow. It means that its pH has changed, because of the depletion of nutrients and growth factors and accumulation of waste products by the cells.

2.3.3 Cellular counting

The cellular counting procedure is necessary whenever the number of cells must be known, for example during splitting or during the seeding of the microbioreactors in the biological experiments. The Bürker chamber (Figure 2.12) is the instrument employed: it is formed by

a rectangular microscope slide with a rectangular indentation that creates a chamber. This latter is engraved with a laser-etched grid of perpendicular lines. The area enclosed by the lines is known, as well as the volume of the chamber. Therefore, it is possible to count the number of cells present in a specific volume of fluid, and so the total number of cells.

The Bürker chamber is formed by two 3 x 3mm cells, with a depth of 0.1mm. Each cell is

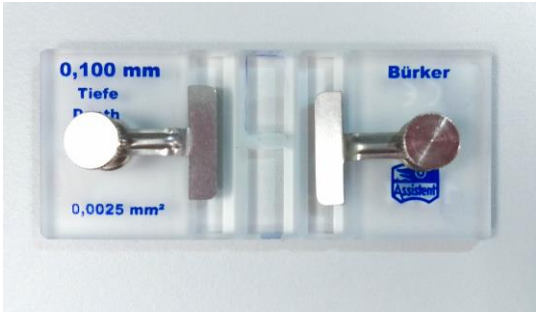

Figure 2.12: *Bürker chamber.*

divided in 9 squares (1mm side), each one divided in 16 squares (0.2mm side).
The chamber is prepared by placing a glass slide of the right dimensions over the chamber and fixing it with the two lateral latches, and then this procedure is followed:

- the cell suspension is diluted (usually 10 times) with some fresh culture media and pipetted in order to avoid sedimentation and clustering of cells;
- 10µL of cell suspension are collected with a micropipette and positioned on one side of the Bürker chamber, forming a bubble. Then 10µL of Trypan Blue (Invitrogen), a cell stain that colors only dead cells, are mixed with the cells by pipetting. Viable cells do not take up this dye, since their membrane is impermeable, but dead cells' membrane is permeable and therefore become blue;
- 10µL of the mixture are inserted between the chamber and the glass slide by capillarity;
- the chamber is observed at the microscope with a 10x enlargement. At least 3 squares are considered: the number of live cells is counted for each square, and then the arithmetic mean is calculated. In Figure 2.13 the difference between live cells (green circles), dead cells (red circles) and residues (blue square) in a square is highlighted.

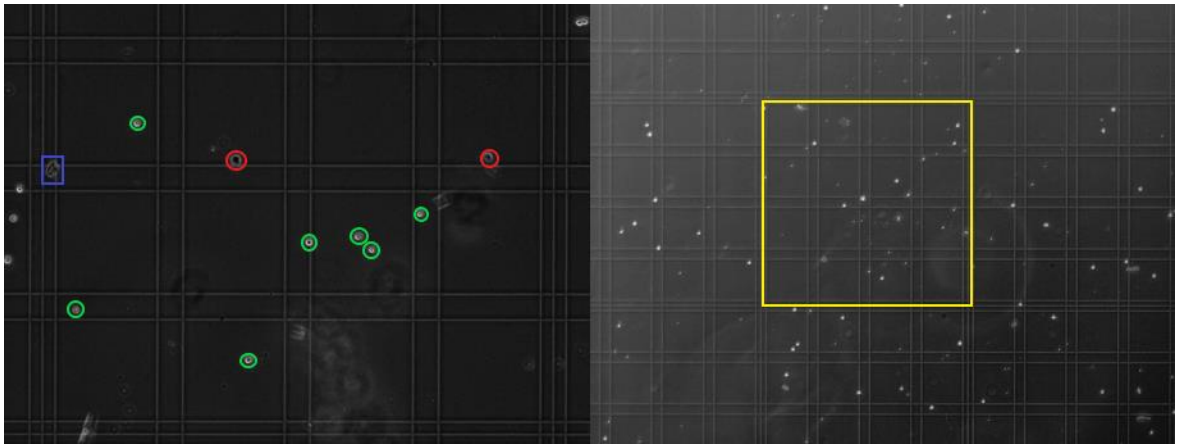

Figure 2.13: *Enlargement of one square of the Bürker chamber: on the left, the green circles highlight live cells, the red circles highlight dead cells and the blue square is positioned on one residue.*

Finally, knowing the mean number of cells per square (N_{mean}), the concentration of cells can be calculated as follows:

$$N\left(\frac{cells}{mL}\right) = N_{mean}\left(\frac{cells}{square}\right)\cdot 10\cdot 10000 \qquad (2.5)$$

where 10 is the dilution factor and 10000 is a coefficient used in this calculation, that includes information about the geometry and volume of the chamber (number of squares per mL). The number of cells per mL is obtained, and this value can be multiplied for the total volume to obtain the total number of cells.

2.3.4 Growth rate estimation of HEK-293

The growth rate of the cells is an important parameter, useful to quantify the cell splitting procedure. In fact, the interval between two cell splitting can be easily calculated, knowing the initial number of cells and the maximum number that cannot be exceeded, to avoid the overcrowding of the flask surface.

The estimation of the growth rate is performed using a 6-well culture plate (SIGMA-ALDRICH®). On the first day, the same inoculum of cells is placed in each well. Then, on the following days, the cells are counted with the procedure reported in paragraph §2.3.3, using a different well for each day.

Since the initial number of cells is known, the percentage growth rate can be calculated each day as:

$$GR\% = \frac{N_{tot} - N_0}{N_0}\cdot 100\% \qquad (2.6)$$

where N_{tot} is the number of cells counted and N_0 is the initial number of cells.
Therefore, knowing the initial number of cells and the percentage growth rate, the number of days needed to obtain a final population can be calculated.

Chapter 3

Results

This Chapter describes the results of the simulations and the experiments conducted on the two microbioreactors. The performances and the biological compatibility are tested and verified, to understand how to best use the two platforms in the future studies.

3.1 First microfluidic platform

3.1.1 Design and production of the master

Since the master is based on an existing design and was already available in the lab, it is not studied or subjected to any additional quality test.

3.1.2 COMSOL Multiphysics® simulation

The COMSOL Multiphysics® simulation is useful to understand if the device works as hypothesized and studied with the dimensionless numbers. It is expected to have laminar flow inside the whole microfluidic platform, and to find a concentration gradient of a defined species *i* within the rows, because of the dominating effect of the diffusive flux on the convective one.

The simulation is performed in a 2D geometry, in which the microwells are assumed to have the maximum diameter of the top opening (500µm). Moreover, the lateral channels are designed with a rectangular section, without the existing four enlargements used to ease the insertion of the microtubes. After the creation of the geometry, three meshes are built and used to evaluate three case studies, in which the results of the previous case (except for the first) are set as the initial values. The element size is chosen as normal for the first mesh, fine for the second and extra fine for the third. Figure 3.1 shows an image of the built geometry.

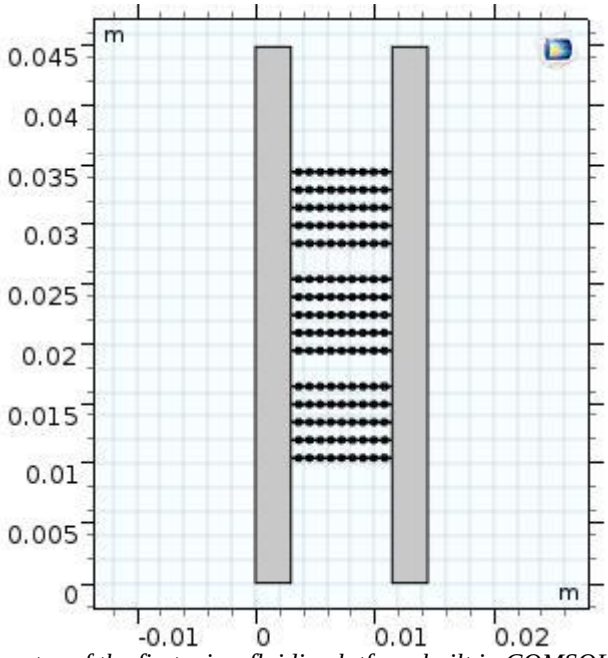

Figure 3.1*: Geometry of the first microfluidic platform built in COMSOL Multiphysics®.*

First, the laminar flow is set on the entire platform, to understand the behavior of the fluid and validate the calculations of the Reynolds number, previously presented in paragraph §2.1.2. Then, the Transport of Diluted Species interface is added, to simulate the trend of the concentration of the chemical species and evaluate the magnitude of the diffusive and convective fluxes in the microchannels and microwells.

3.1.2.1 Laminar flow

As explained in paragraph §2.1.3.1, the laminar flow is set on the entire platform to solve the Navier-Stokes equations for the single-phase fluid at the steady state. The fluid is assumed to enter the two upper sides of the lateral channels, and exit via the two lower sides. The inlet velocity is calculated from typical inlet flow rates and diving them for the available cross section ($2.25 \cdot 10^{-6}$ m^2) of the channel. This is an approximation, since the fluid, in the real device, enters perpendicularly with respect to the channel. However, by performing a 2D simulation of the initial part of the channel, it can be demonstrated that the laminar flow is fully developed before reaching the central part of the device. Table 3.1 shows the flow rates, and the corresponding average velocities, modeled in the simulations.

Table 3.1: *Values of flow rates and corresponding average velocities used in the COMSOL Multiphysics® simulation of the first microfluidic platform.*

Case	Flow rate [µL/min]	Flow rate [m^3/s]	Velocity [m/s]
1	50	$8.33 \cdot 10^{-10}$	$3.7 \cdot 10^{-4}$
2	100	$1.67 \cdot 10^{-9}$	$7.42 \cdot 10^{-4}$
3	150	$2.5 \cdot 10^{-9}$	$1.11 \cdot 10^{-3}$

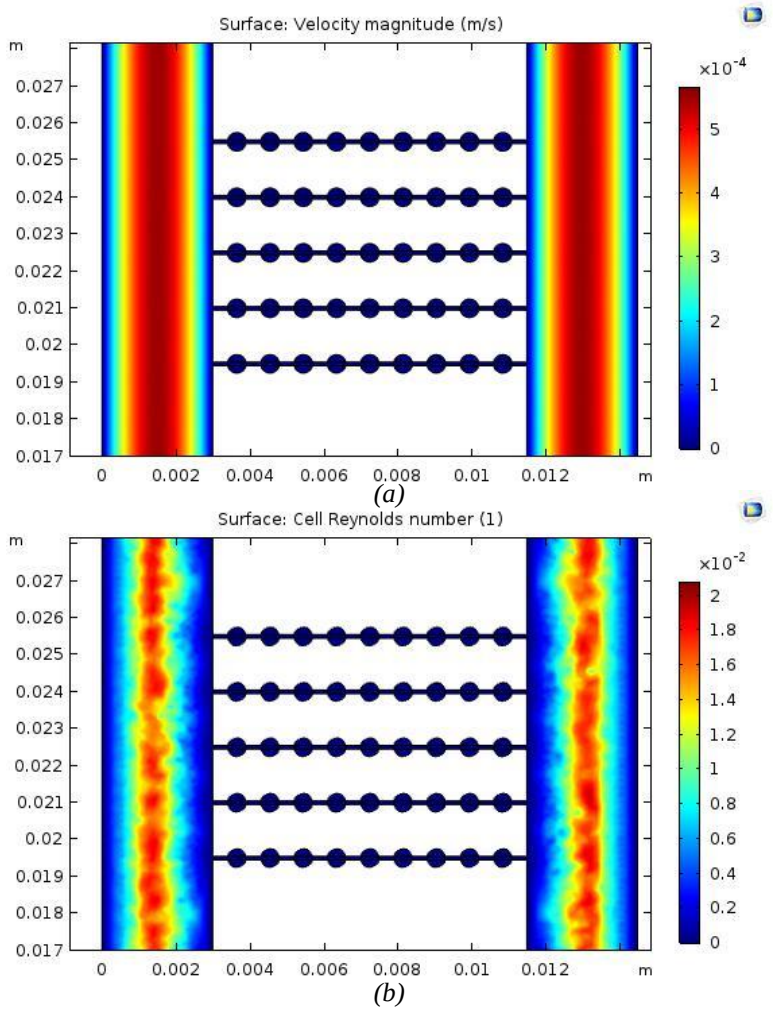

Figure 3.2*: Results of the COMSOL simulation for case 1: (a) velocity magnitude and (b) cell Reynolds number.*

As concern the outlets of the fluids, a condition on the pressure is set, in which the relative pressure is assumed to be zero. The temperature is set as the ambient one (293.15K).
Figure 3.2 shows the surface plots of the absolute velocity and of the cell Reynolds number of an enlargement of the central part of the platform, for the first case of Table 3.1. The other two cases have quite similar results and thus the same conclusions can be deduced; these results are reported in the Appendix for sake of completion (Figures A.1, A.2).

Figure 3.2*a* shows the velocity trend inside the platform; it can be observed that the velocity in the lateral channels follows our predictions and has a parabolic profile, indicative of a laminar flow. In fact, the value is maximum in the center of the channel ($\sim 5.5 \cdot 10^{-4}$ m/s) and tends to zero approaching the walls. This behavior is confirmed by Figure 3.2*b*, displaying the trend of the cell Reynolds number: its maximum value is approximately $2 \cdot 10^{-2}$, confirming the establishment of the laminar flow.
With regards to the rows and microwells, the velocity (and Reynolds number) tends to zero: this is the desired behavior to obtain a negligible convective flux of species *i* if compared to

the diffusive flux. However, the velocity is not zero in the microchannels, but has a maximum value of approximately $2 \cdot 10^{-9}$m/s, five orders of magnitude smaller than the inlet velocity. Therefore, the Péclet number can be calculated as:

$$Pe = \frac{vD}{D_i} = 3.26 \cdot 10^{-2} \tag{3.1}$$

where D is the diameter of the microchannels and D_i is the diffusion coefficient of the species of interest, exosomes. Pe is smaller than one: this confirms the dominant effect of diffusive flux over the convective one.

Moreover, when translating the findings of the 2D modeling to the actual device, it can be noticed that the velocity in the microchannels is surely smaller in the real device, since the channels have a smaller diameter than the height of the lateral channels and they are positioned in the upper part. Here, the presence of the wall determines a reduction of the velocity. Therefore, from now on, the velocity inside the microchannels will be set as equal to zero, to neglect the presence of the convective flux of the species. This is a first approximation, and a 3D simulation would be needed to know the exact velocity inside the microchannels. This must be considered when comparing these results with the experimental data.

3.1.2.2 Transport of Diluted Species

The addition of the Transport of Diluted Species interface, as explained in paragraph §2.1.3.2, does not require the properties of the species *i*, except for the diffusion coefficient. The species that are taken into consideration are the exosomes and the three fluorescent tracers available. The diffusion coefficient of exosomes in water is calculated with the Stokes-Einstein equation (equation 1.12), and considering an average diameter of exosomes of 70nm ($7 \cdot 10^{-8}$ m):

$$D_{exosome} = \frac{k_B T}{6\pi\mu r} = \frac{1.38 \cdot 10^{-23} \cdot 293.15}{6\pi \cdot 10^{-3} \cdot 3.5 \cdot 10^{-8}} = 6.14 \cdot 10^{-12} \frac{m^2}{s} \tag{3.2}$$

In order to calculate the diffusion coefficient of the three fluorescent tracers in water, it is necessary to calculate their radius. The producer of dextrans, SIGMA-ALDRICH, provides information about the trend of the average Stokes radius of the particles (considered as spherical) with respect to the molecular weight, as reported in Table 3.2.

Table 3.2: *Stokes radius of the fluorescent isothiocyanate dextran with respect to the molecular weight*[1].

Molecular weight [Da]	Stokes radius [Å]
4000	14
10000	23
20000	33
40000	45
70000	60
150000	85

Starting from these data, we used Excel to calculate a regression curve, and the Stokes radii of the available tracers. Figure 3.3 shows the extrapolated curve.

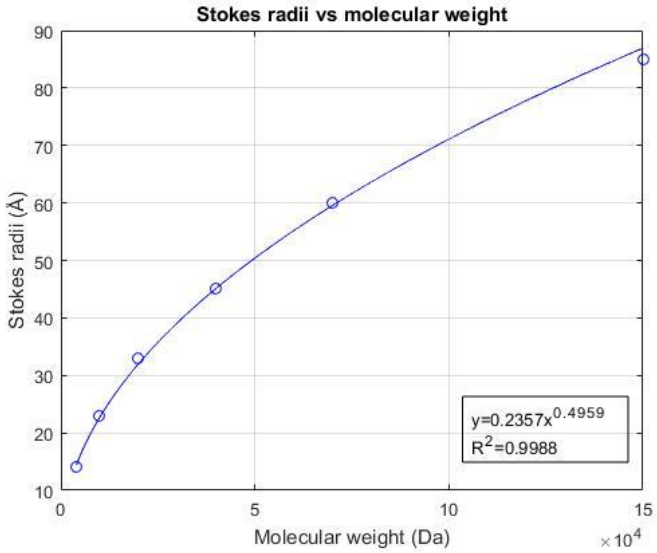

Figure 3.3: *Regression curve of the Stokes radii of the isothiocyanate-dextrans with respect to the molecular weight.*

Therefore, the three radii can be extrapolated from the curve and the diffusion coefficient can be calculated with the Stokes-Einstein equation, using the same properties employed in the equation 3.1. All the values calculated are reported in Table 3.3.

Table 3.3: *Calculation of the Stokes radii and of the diffusion coefficients of the three fluorescent isothiocyanate-dextrans available, starting from the regression curve.*

Molecular weight [kDa]	Stokes radius [Å]	Diffusion coeff. in water [m^2/s]
75	62	$3.48 \cdot 10^{-11}$
250	112	$1.92 \cdot 10^{-11}$
500	158	$1.36 \cdot 10^{-11}$

It can be observed that the three fluorescent isothiocyanate dextrans have diffusion coefficients with the same order of magnitude. Therefore, it is expected to have similar results from the simulations. The exosomes' diffusion coefficient is one order of magnitude smaller with respect to the tracers' one, because of the bigger dimensions. The simulations

are useful to understand if this difference leads to any discrepancy in the behavior of the species inside the device.

The second information needed is the initial concentration *c* of the species at the inlets. At one inlet (usually the left-hand one) the concentration is set at an arbitrary value, while at the other one the concentration is set as equal to zero. The final graphs are created by normalizing the concentration, dividing it for the initial value, to obtain a dimensionless scale (from zero to one), easily comparable with the quantitative results of the experimental validations. We ran several simulations in COMSOL: our variables were the three velocities in Table 3.1, and the four diffusion coefficients, with the goal of observing potential differences. As explained in the previous paragraph, since the height of the microchannels with respect to the lateral channel is not inserted as a data in the 2D simulation, and considered the big difference between the velocity in the lateral channels and in the microchannels, the latter is set as equal to zero. Therefore, even when setting a different velocity at the inlets, the results are the same for the three cases. So, it becomes more important to observe the difference between the four species, to underline any difference in the diffusion within the microchannels.

The following graphs show the concentration of the species in the central part of the device, with the same flow rate of 50µL/min (case 1).

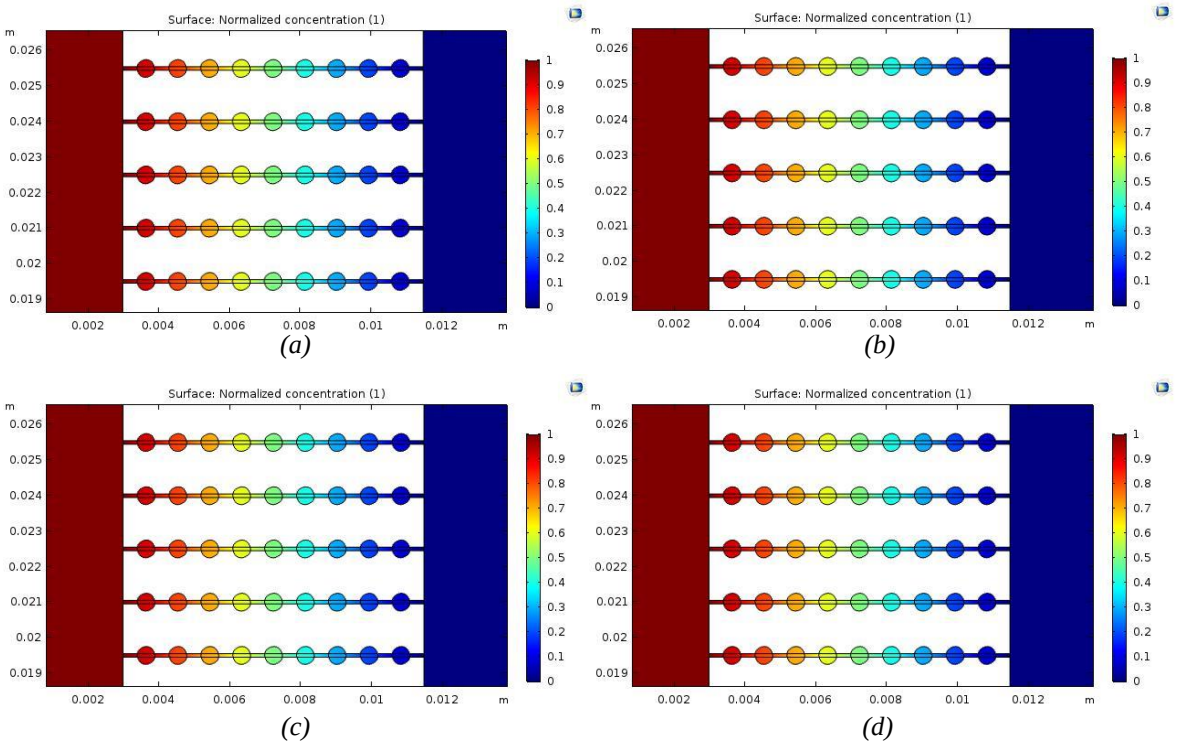

Figure 3.4*: Trends of the concentration profiles of the species in the microchannels of the central part of the microbioreactor. The species considered are: (a) exosomes, (b) dextran with MW=75kDa, (c) dextran with MW=250kDa, (d) dextran with MW=500kDa.*

The trend is the same in the four cases, and the diffusion coefficient does not affect the result of the simulation. This is due to the fact that this is a stationary simulation, where only the steady state results are presented. The species with higher diffusion coefficients (smaller dimensions) reach the steady state faster. Moreover, if modelling the device considering the presence of a small amount of convective flux, here neglected by setting the velocity as equal to zero, the result may be slightly different. A 3D simulation would thus be necessary to obtain a precise result.
The trend of concentration in the microchannels is the desired one: the normalized concentration goes from 1 to zero following a linear trend. Each microwell is characterized by a discrete value of concentration.
This simulation confirms the hypothesis of paragraph §2.1.2: the diffusive flux overwhelms the convective one, allowing to create a concentration gradient. The values of the concentration in the rows are exported to a data file in order to compare them with the results of the validation experiments.

3.1.3 Production of the microfluidic platform

The microfluidic platform is produced with the procedure reported in paragraph §2.1.4. However, during the operation of the device, it was noticed that it was not possible to obtain the perfect sealing of the microchannels both in the irreversible and the reversible configurations. This problem was caused by a defect in the master: the lateral sides (external with respect to the lateral channels) have two small protrusions, that determine two indentations in the final PDMS layer. This defect did not allow proper sealing following the plasma treatment, since the two surfaces (glass-PDMS or PDMS-PDMS) did not come into perfect contact. Moreover, hydraulic sealing with the clamping unit becomes difficult since the layer is not perfectly horizontal.
To solve this problem, it is necessary to fill the indentations with some uncured PDMS, place the layer between two glass slides to maintain the shape and cure it in the oven. Afterwards, the excess PDMS is removed with the help of a scalpel.

3.1.4 Irreversible configuration

The irreversible configuration of the first microfluidic platform is created with the procedure reported in paragraph §2.1.5, using a plasma treatment to seal the microchannels. Figure 3.5*a* shows the final device, where the holes created with the biopsy punch can be observed.

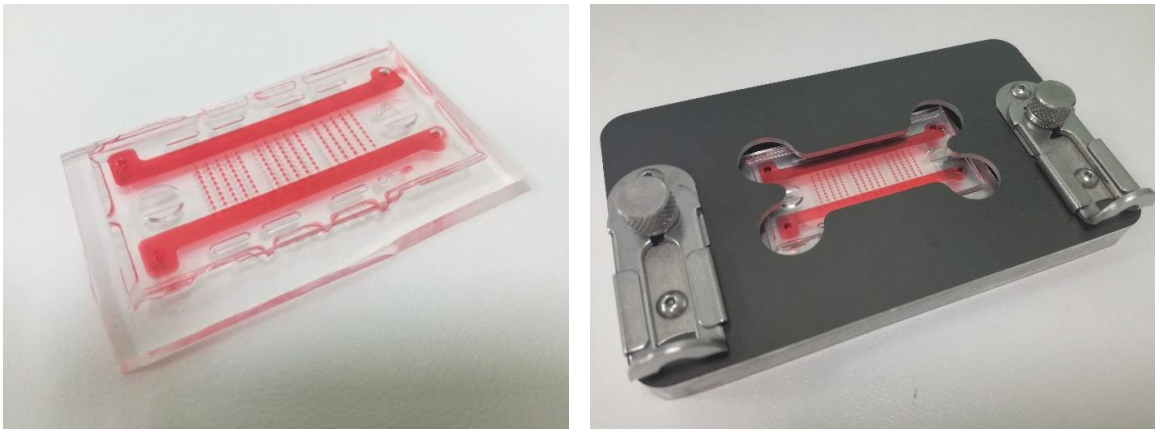

(a) *(b)*

Figure 3.5: *First microfluidic platform in the two configurations: (a) irreversible configuration and (b) reversible configuration. Both the devices are filled with food coloring.*

3.1.5 Reversible configuration

The reversible configuration is produced as described in paragraph §2.1.6. The clamping unit prepared is shown in Figure 3.5*b*.

3.1.6 Validation experiments

In order to obtain qualitative and quantitative data about the performances of the microfluidic device, validation experiments are conducted on both the irreversible and reversible configurations, as described in paragraph §2.1.7. Food coloring and fluorescent isothiocyanate-dextrans are prepared and used in these experiments. We typically used the fluorescent tracer with the highest molecular weight in order to obtain results comparable to and representative of the behavior of exosomes inside the µBR. However, some tests with the lower molecular weight tracers have also been carried out, and the results confirm that there are no relevant differences.
The syringe pump is set up by placing the four syringes both on the infuse and withdraw sides. It is advisable to fill the two syringes on the withdraw side with a small quantity of water (approximately 1mL), to ease the withdrawal operation.
The flow rates are set on the pump display:

- initially at a high value (150µL/min) to favor the rapid establishment of the steady state;
- then diminished, usually to 50 or 100µL/min, and some minutes are waited to observe if the stability is maintained.

Some pictures are then taken to observe the result of the validation qualitatively and quantitatively.

3.1.6.1 Irreversible configuration

The microbioreactor is prepared for the validation experiments with the procedure in paragraph §2.1.7.1. The device is usually used immediately after the plasma treatment to exploit the increased hydrophilicity of the surfaces. However, if this is not the case and the microbioreactor is prepared for later use, it is advisable to use the desiccator to remove the bubbles present in the microwells: the µBR is filled and placed in a small container with water and some vacuum cycles are performed.
First, the food coloring is used to obtain qualitative information about the performances of the device. The syringes are prepared and placed on the pump, which is started and then the microtubes are inserted in the holes of the platform. After approximately 2/3 minutes the device reaches the steady state, and the situation is shown in Figure 3.6.

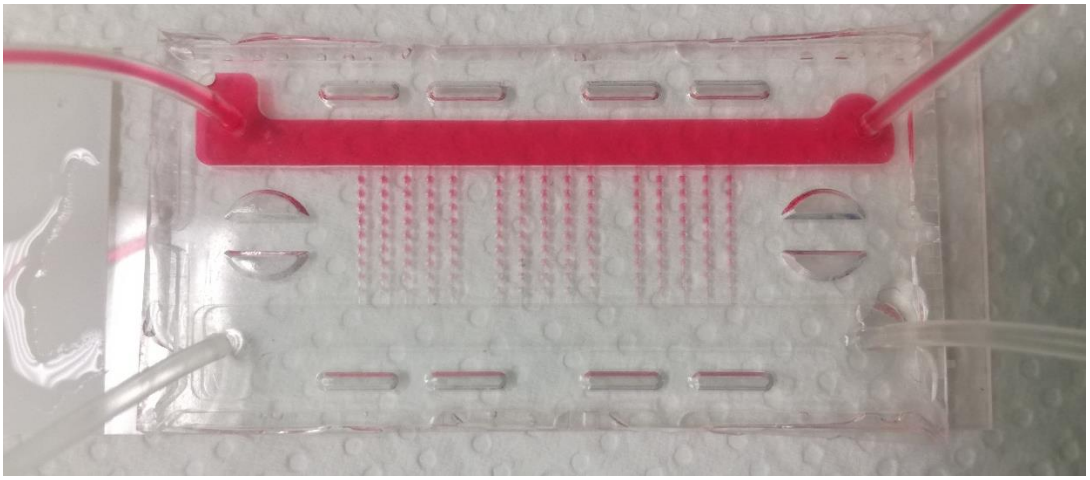

Figure 3.6: *Result of the validation experiment with food coloring on the irreversible configuration of the first microfluidic platform. The concentration gradient can be visually observed.*

Based on the image in Figure 3.6, the fluids enter the left-hand side and exit via the right-hand side. The upper channel is connected with the syringe containing the food coloring solution, while the lower is filled with water. The microchannels are characterized by the presence of a concentration gradient, as it can be observed from the picture. Visually, the color tends to lighten from an intense pink to transparent, meaning that the concentration of food coloring in water is decreasing.
This experiment shows the desired result, i.e. the formation of a concentration gradient across the microwells that is equal in all the independent rows of microchannels. However, this is only a qualitative information.
The next step is the use of fluorescent isothiocyanate-dextrans to obtain quantitative data, thanks to the fluorescence microscope. All the data reported refer to the dextran with the highest molecular weight (500kDa), that has the nearest diffusion coefficient with respect to the exosomes. During these experiments, the pump is prepared and started with the same

method used in the previous case. However, now it is necessary to wrap the syringe containing the fluorescent tracer and, if possible, the microbioreactor with aluminum foil to protect them from light. Since fluorescent dextrans are light sensible, this procedure is necessary to ensure the stability of the solution.

During these experiments, the µBR is placed and kept on the microscope stage, to avoid an excessive movement that can create turbulences inside the platform. So, images can be taken with the fluorescence microscope (GFP Cube), combined and analyzed with ImageJ. Figure 3.7 shows an image of an entire row.

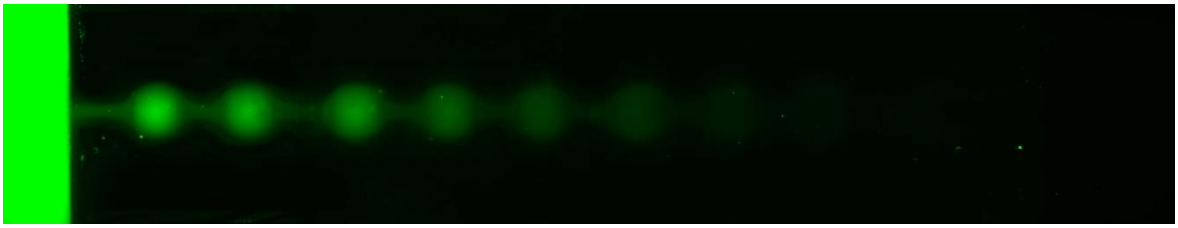

Figure 3.7: *Result of the validation experiment with high MW fluorescent isothiocyanate-dextran on the irreversible configuration of the first microfluidic platform. The concentration gradient can be observed.*

The presence of the concentration gradient can be easily observed. Moreover, it is possible to load the image in ImageJ and measure the light intensity in the lateral channels and in the microwells. Values are normalized to a 0 to 1 scale with respect to the highest intensity value. The results can be compared with normalized concentration values of the COMSOL Multiphysics® simulation. It is not expected to have a perfect correspondence, since in the simulation the convective flux is manually set to zero. However, this procedure is useful to obtain a quantitative comparison with the simulation. The following graph shows the difference between theoretical and experimental values.

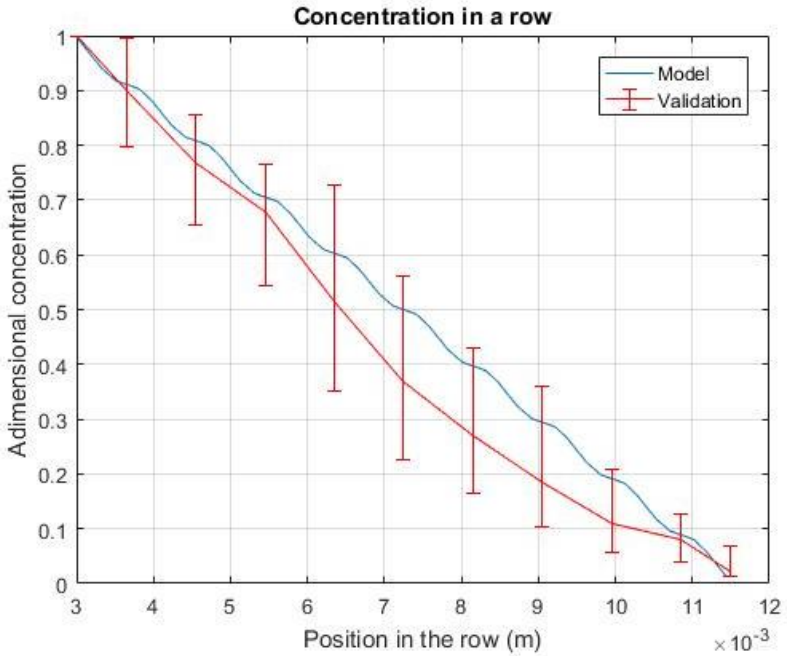

Figure 3.8: *Difference between the normalized concentration values exported from COMSOL Multiphysics® and the experimental values, obtained from different experiments with dextrans.*

The experimental data in good agreement with the theoretical values, exported from the simulation. The measurement error (standard deviation on 16 data points), tends to increase in the central microwells. This can be explained considering that the measurement of the light intensity with ImageJ is not an extremely precise method, and an error is expected from this type of measure.
It can be stated that the performances of the microfluidic platform arranged in the irreversible configuration are validated, since it shows the desired and expected trend of concentration. However, this configuration can be employed only for the validations, for the impossibility of inserting the cells before the closing of the device.

3.1.6.2 Reversible configuration

The clamping unit is prepared with the procedure described in paragraph §2.1.7.2. Then, the pump is started and the microtubes are inserted in the PC manifold's holes. After some minutes, the behavior of the fluid is not the desired one. In fact, as can be observed in Figure 3.9*a*, the concentration gradient of food coloring does not appear, because of the absence of a perfect hydraulic sealing. There is the formation of a thin layer of liquid over the microchannels.

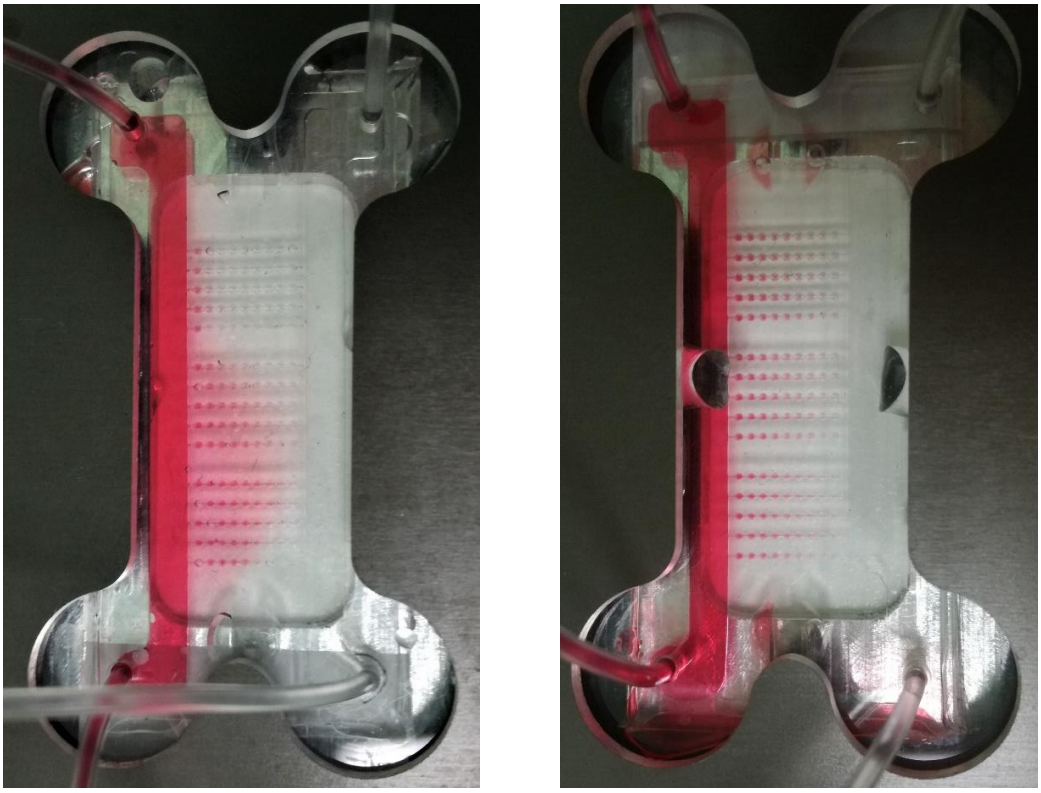

(a) *(b)*

Figure 3.9: *Results of the validation experiment with food colouring on the reversible configuration of the first microfluidic platform: (a) failed experiment because of deformations on the clamping plate and (b) addition of two PDMS cores to apply a uniform pressure and creation of the concentration gradient.*

This problem is probably caused by a deformation of the clamping plate on the top of the unit, that has not been used for different years and does not allow to close and apply the same pressure on the whole PC manifold.
This problem can be solved by adding two PDMS cores (diameter of 3mm) under the central part of the clamping plate to create a uniform pressure on the PC manifold and seal the channels, as it can be observed in Figure 3.9*b*.
However, this solution is not permanent, and the procedure is not easy to be reproduced in the same way during each attempt of the experiment.
To solve this problem, different trials have been done to ensure the application of a uniform pressure, such as the placing of an additional PC layer under the glass slide, or the addition of two PDMS parallelepipeds under the two extremities of the PC manifold. Unfortunately, these solutions were not suitable to obtain the desired functioning.
To conclude, the performances of the platform is qualitatively verified also with the reversible configuration, but the clamping unit need to be refabricated to obtain the perfect sealing of the device.
This malfunction can be observed in the validation experiments with the fluorescent tracers. In fact, the formation of a thin layer of liquid between the microbioreactor and the PC manifold is highlighted in the microscope images (Figure 3.10).

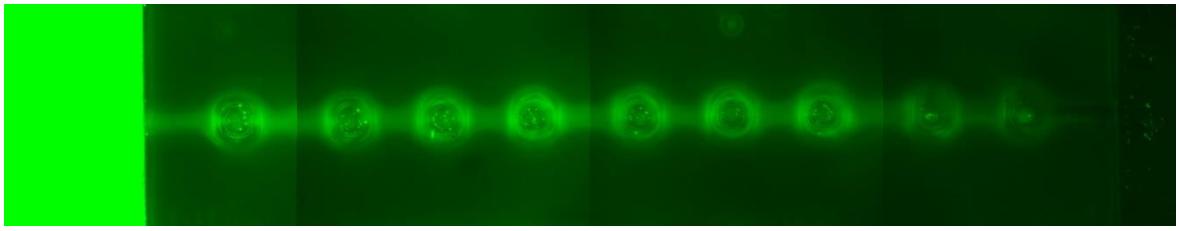

Figure 3.10: *Result of the validation experiment with high MW fluorescent isothiocyanate-dextran on the reversible configuration of the first microfluidic platform. The presence of a layer of liquid between the microchannels and the PC manifold can be observed.*

In conclusion, the clamping unit ensures the functioning of the platform but does not allow the sealing of the microchannels. A new clamping plate is needed, to ensure a uniform pressure applied and the correct performance of the platform.

3.1.7 Biological experiments

The reversible configuration, as explained, is the only one suitable for the biological experiments since it allows the insertion of cells without their damage. However, because of the problems found in the closing and use of the clamping unit, it was not possible to perform biological experiments.
Some experiments were started, and the capability of cells to attach to the PDMS surface was observed. It was found that the optimal amount of time needed to FN to have an effect

on the PDMS' surface is 1h, after which it can be removed, and the cells can be seeded. After only a few hours, cells start to fall inside the microwells and to attach to any free surface. The situation after this amount of time can be observed in Figure 3.11.
From the figure it can be noticed that the cells are present both inside the microwell and on the PDMS surface, where they are starting to attach. Therefore, the device is suitable for the cells' viability. As concern the cells that are on the surface, they will be removed or killed during the closing of the clamping unit.

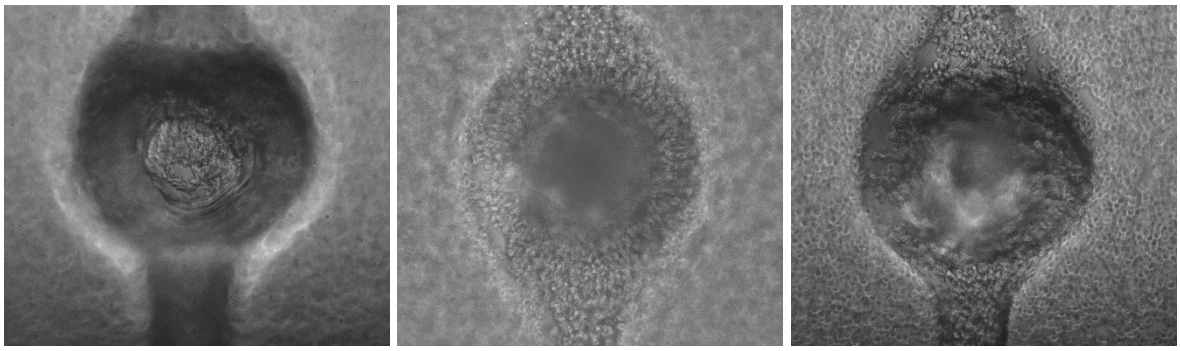

Figure 3.11: *Pictures of a microwell filled with cells. From the left to the right, the focus is changed to observe different planes: the bottom of the microwell, an intermediate height and the upper surface.*

The main task about the reversible configuration is, therefore, the manufacturing of a new clamping device. It may be produced with the micromilling technique, starting from an Aluminum block, to obtain a new and rigid device. Moreover, since the main problem is represented by the deformation of the clamping plate, while the Aluminum base is still rigid and stable, only this element need to be produced. The suggestion is to produce a thicker layer, to avoid its deformation.

3.2 Second microfluidic platform

3.2.1 Design and production of the master

The master used for the validations and the biological experiments is the one shown in Figure 2.8. However, this is not the first design of the platform, since the central chamber and the microchannels were initially larger, as shown in the 2D-CAD design of the first prototype in Figure 3.12.

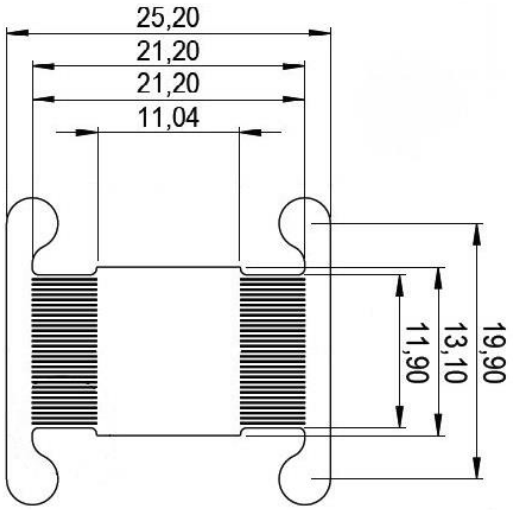

Figure 3.12: *First design of the second microfluidic platform. Lengths in mm.*

The seeding ports are not present, since they have been introduced with the second design. The height of all the elements is 60µm, half of the new platform's, and the width of the microchannels is 300µm.

The main issue with this first device was observed during plasma treatment. In fact, the PDMS over the central chamber collapsed in the mid part and attached to the underlying glass slide. This was most likely due to its dimensions, as the chamber is wide and has no supporting elements guaranteeing structural integrity. Consequently, it was decided to reduce the chamber width and double its height. At the same time, the width of the microchannels was reduced from 300 to 200µm, and the two seeding ports, useful to inject the cells after the plasma treatment, were introduced. This led to the final design, shown in Figure 2.8.

As explained in paragraph §2.2.1, the master of the second microfluidic platform is produced with a micromiller, and some tests are performed to understand the quality of the master produced. The 3D optical profiler can provide information about the heights and the rugosity of the master.

The heights of specific areas of interest are studied with the Focus Variation mode. The areas are identified in Figure 3.13.

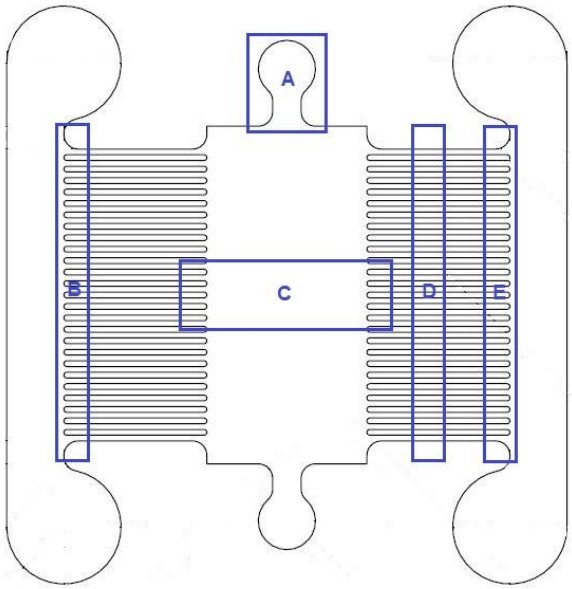

Figure 3.13: *Areas of interest of the second microfluidic platform studied with the profiler to find the values of heights.*

The profiler analysis shows the high level of precision reached with the milling procedure, since there are negligible differences in the heights of the microchannels. As an example, the results for the area C are reported in Figure 3.14.

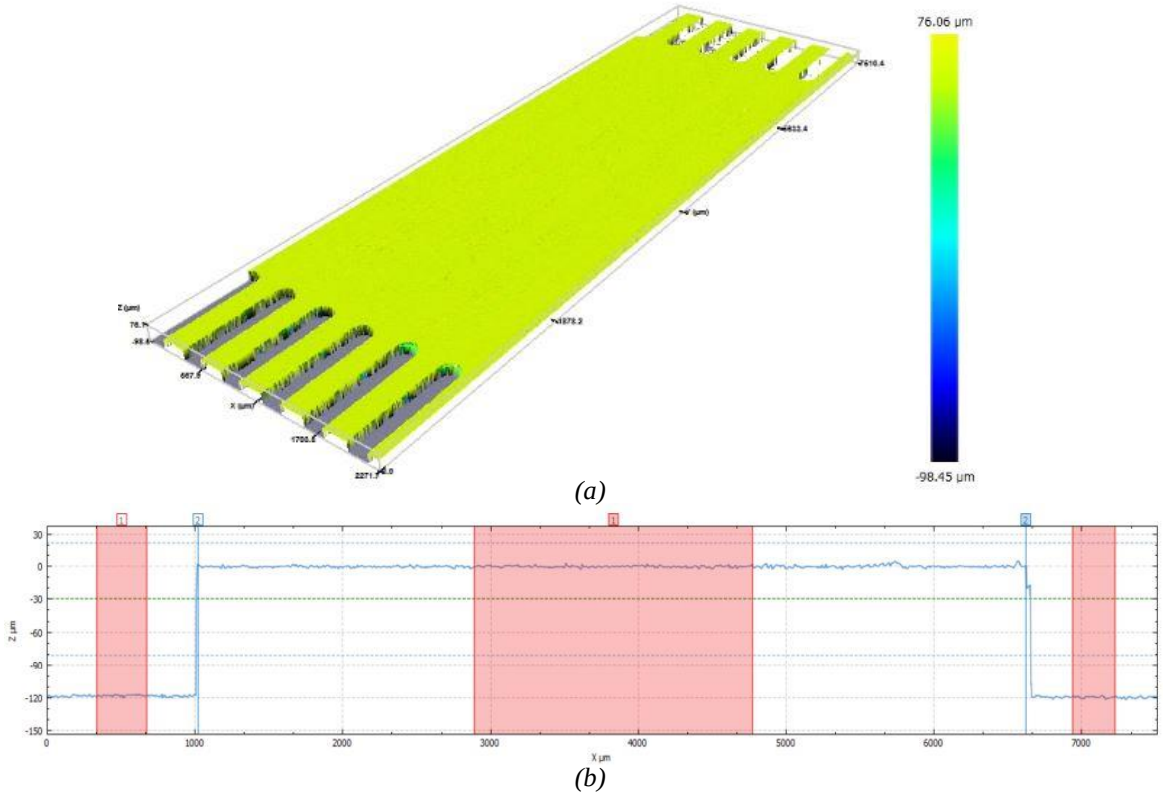

Figure 3.14: *Results of the profiler analysis on area C: (a) representation of the values of heights and (b) quantitative information about the heights.*

Figure 3.14*b* gives information about the width and the height of the chamber, reported in Table 3.4. The miller produced a precise object, with negligible differences in the heights. So, it is expected to obtain a precise mold of the master, a PDMS layer that will easily attach to the glass slide's surface with the plasma treatment. To verify this hypothesis, we also studied a PDMS layer molded on the master with the profiler, confirming the expected results. Considering the same area C the values of interest are reported in Table 3.4.

Table 3.4: *Results of the profiler analysis on the area C, both for the Aluminum master and the PDMS layer, compared with the values set in the design.*

	Width of the chamber [µm]	**Height of the chamber [µm]**	**Absolute rugosity [nm]**
Design value	5600	120	-
Aluminum master	5599.9	118.68	92.873
PDMS layer	5578	118.07	225.3

Another important parameter to be considered in the quality of attachment with plasma treatment is the rugosity, which needs to be as small as possible to have a smooth surface. The rugosity is studied with the profiler in Optical mode, considering as the area of interest the central part of the chamber, without the microchannels. The absolute rugosity of both the master and the PDMS are reported in the table: a value under 100nm represents a completely smooth surface. Therefore, the master has a perfectly smooth surface, but also the rugosity of the PDMS layer can be considered a satisfactory value.

From these results, it can be said that micromilling is a suitable technique to produce masters for microfluidic devices, considering also the fact that the removal of the cured PDMS layer is easy and does not leave any residue.

The only limitation of this technique involves the tools used in the micromilling of the mold; the head mills must be substituted often, as soon as they show signs of wear, thus increasing the costs and the times; moreover, there are minimum dimensions of the tools that limit the lengths of the elements of the device.

3.2.2 COMSOL Multiphysics® simulation

The COMSOL Multiphysics® simulation is again used to understand the mode of operation of the device, and to suggest potential modifications in order to obtain the desired performances. For this reason, both a 2D and a 3D simulation have been performed.

In the 2D simulation the lateral channels are drawn as rectangles and the seeding ports are not added to the geometry since they do not contribute to the fluid dynamics of the device. The modeled design is shown in Figure 3.15. This section is a representative model of the whole device since the height is constant for all the elements.

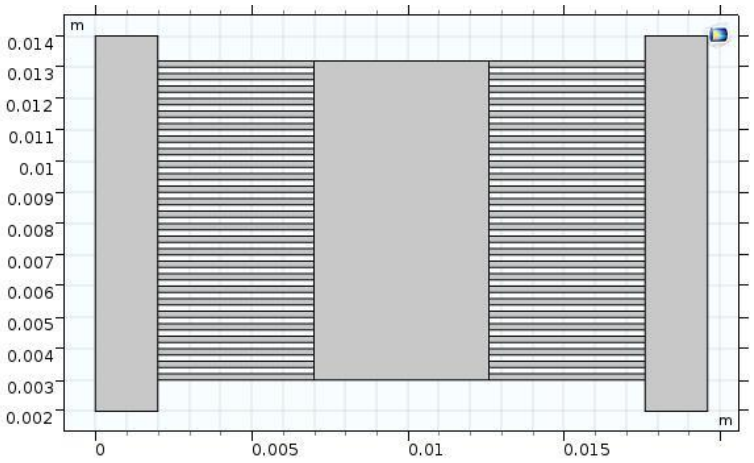

Figure 3.15: *Geometry of the second microfluidic platform built in COMSOL Multiphysics®.*

Similarly to the first device's simulation, three meshes are built and used to conduct three studies; in each study (except for the first) the initial values are given by the results of the previous case. The element size is normal for the first mesh, finer for the second and extra fine for the third.

The laminar flow interface is added in the whole platform to study the fluid behavior; then the transport of diluted species is used to understand the trend of the concentration of the species.

3.2.2.1 Laminar flow

The laminar flow is set on the entire platform to solve the Navier-Stokes equations for the single-phase fluid at the steady state. Like in the previous case, the fluid is assumed to enter the two upper sides of the lateral channels, while it exits via the two lower sides. Knowing the inlet flow rates typically set during the experiments, the inlet average velocity is calculated dividing them for the section of the channel ($2.4 \cdot 10^{-7}$ m^2). Table 3.5 shows the flow rates, and the corresponding average velocities, employed in the simulations.

Table 3.5: *Values of flow rates and corresponding average velocities used in the COMSOL simulation of the second microfluidic platform.*

Case	Flow rate [µL/min]	Flow rate [m^3/s]	Velocity [m/s]
1	5	$8.33 \cdot 10^{-11}$	$3.47 \cdot 10^{-4}$
2	10	$1.67 \cdot 10^{-10}$	$6.96 \cdot 10^{-4}$
3	20	$3.33 \cdot 10^{-10}$	$1.39 \cdot 10^{-3}$

The velocities have the same orders of magnitude of the first microfluidic platform (Table 3.1). In correspondence to the outlets of the fluids, the relative pressure is set as equal to zero. The temperature is 293.15K.

The surface velocity and the cell Reynolds number for the first case are shown in the

following figures. All other cases have a similar behavior, and the resulting trends of the velocity and of Reynold number are reported in the Appendix (Figures A.3, A.4).

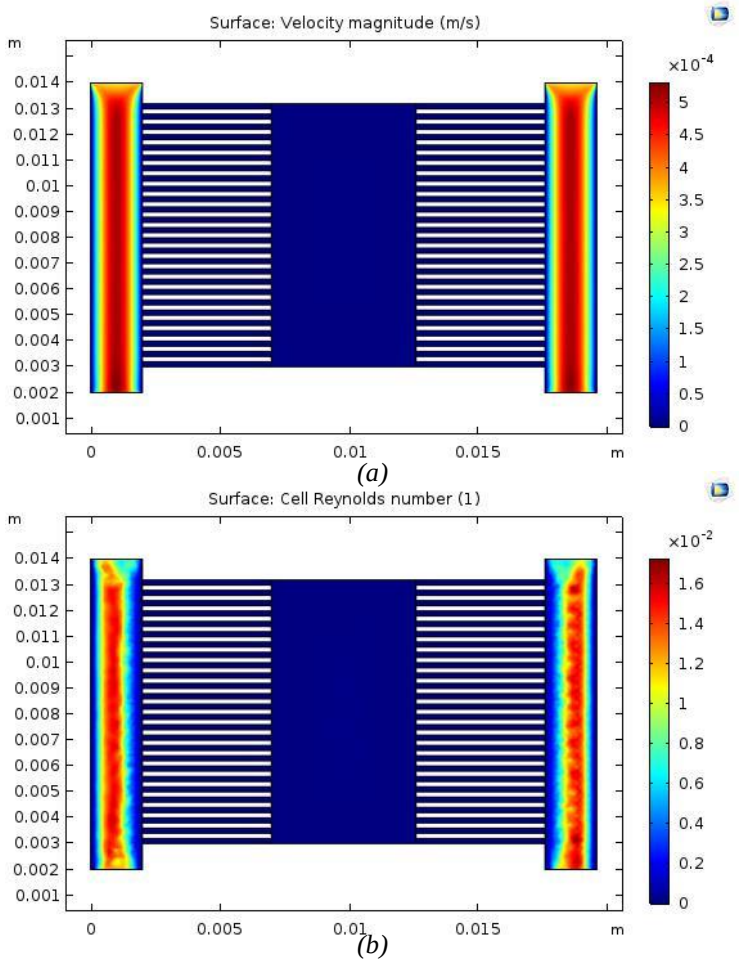

Figure 3.16: *Results of the COMSOL Multiphysics® simulation of the second microfluidic platform for case 1: (a) velocity magnitude and (b) cell Reynolds number.*

The flux is laminar and the trend is constant, as confirmed by the value of the cell Reynolds number, which has an order of magnitude of 10^{-2}.

As concern the microchannels, from the figures it may seem that the velocity is almost zero. However, by plotting the velocity vectors in the whole device, it can be noticed that there is a certain flux in the microchannels. The fluid enters the central chamber from the first half of the microchannels and exits via the second half, as shown in Figure 3.17. Moreover, to understand the velocity magnitude, the velocity profile at the end of the microchannels (in correspondence to the entrance of the central chamber) is plotted, obtaining the result in Figure 3.18.

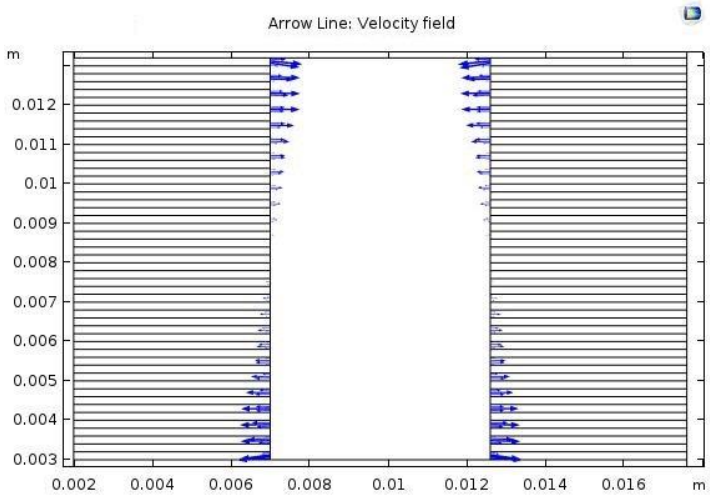

Figure 3.17: *Arrows representing the velocity trend at the end of the microchannels of the second microfluidic platform.*

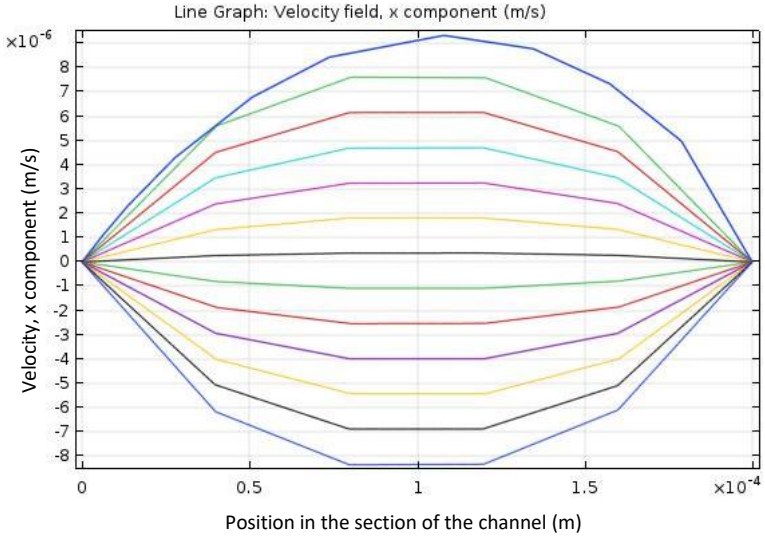

Figure 3.18: *x component of the velocity profile at the end of half of the microchannels of the second microfluidic platform.*

The different curves show the x component of the velocity profile at the outlet section of some microchannels (only half of them is reported for an easier comprehension). The curves on the upper section (above 0) represent the microchannels near the inlet of the fluid, while the lower ones represent the microchannels near the outlet. It can be observed that the velocity has an order of magnitude of 10^{-6} m/s, while it was 10^{-4}m/s in the lateral channels. In case 3, the order of magnitude reaches a value of 10^{-5}. Considering an average velocity of 10^{-6} m/s, the Péclet number in the microchannels can be calculated as:

$$D_{eq} = \frac{4S}{2P} = 1.5 \cdot 10^{-4} m \tag{3.3}$$

$$Pe = \frac{vD_{eq}}{D_i} = 24.4 \tag{3.4}$$

where D_{eq} is the equivalent diameter of the microchannels and D_i is the diffusion coefficient of exosomes. Pe is higher than one: it is thus expected to find a non-negligible convective flux with respect to the diffusive one. This hypothesis will be verified by adding the Transport of Diluted Species interface. Therefore, it is not possible and justifiable to neglect the convection in the microchannels and in the central chamber by setting the velocity as equal to zero.

3.2.2.2 Transport of Diluted Species

In this interface, the only parameter that is needed is the diffusion coefficient of the species: the exosomes and the three fluorescent isothiocyanate-dextrans are considered as solutes. The respective diffusion coefficients are the same of the first simulation: the value in equation 3.1 for exosomes, and the coefficients in Table 3.3 for the tracers. Afterwards, the initial value of concentration is added to proceed with the simulation: this value can be set arbitrarily at one inlet, usually the left-hand one, and is set as equal to zero at the other one. In the final graphs the concentration is normalized to obtain a general result, comparable, if needed, with the validation experiments.
Differently from the first microfluidic platform's simulation, the velocity in the microchannels is not set as equal to zero since its value is not negligible and the calculation of Pe shows the presence of the convective flux. Consequently, the trend of the concentration inside the device is expected to be slightly different if the inlet velocity is changed in the three cases of Table 3.5. In Figure 3.19 the trend of concentration when the velocity is increased is reported, considering the exosomes as solute.
In all the cases reported, the flux of exosomes is characterized by the predominance of the convective flux in the whole platform: only in the center of the chamber, where the two fluxes meet, there is a diffusive layer that increases in width towards the bottom of the chamber because of the mixing of the two fluids. These results are determined by the behavior of the two fluids inside the device: they enter in the central chamber from the first half of the microchannels and exit through the second half. Moreover, the last microchannels are characterized by a different concentration of exosomes, because of mixing. The same trend can be observed when the dextrans are employed, in the Appendix (Figures A.5, A.6, A.7).

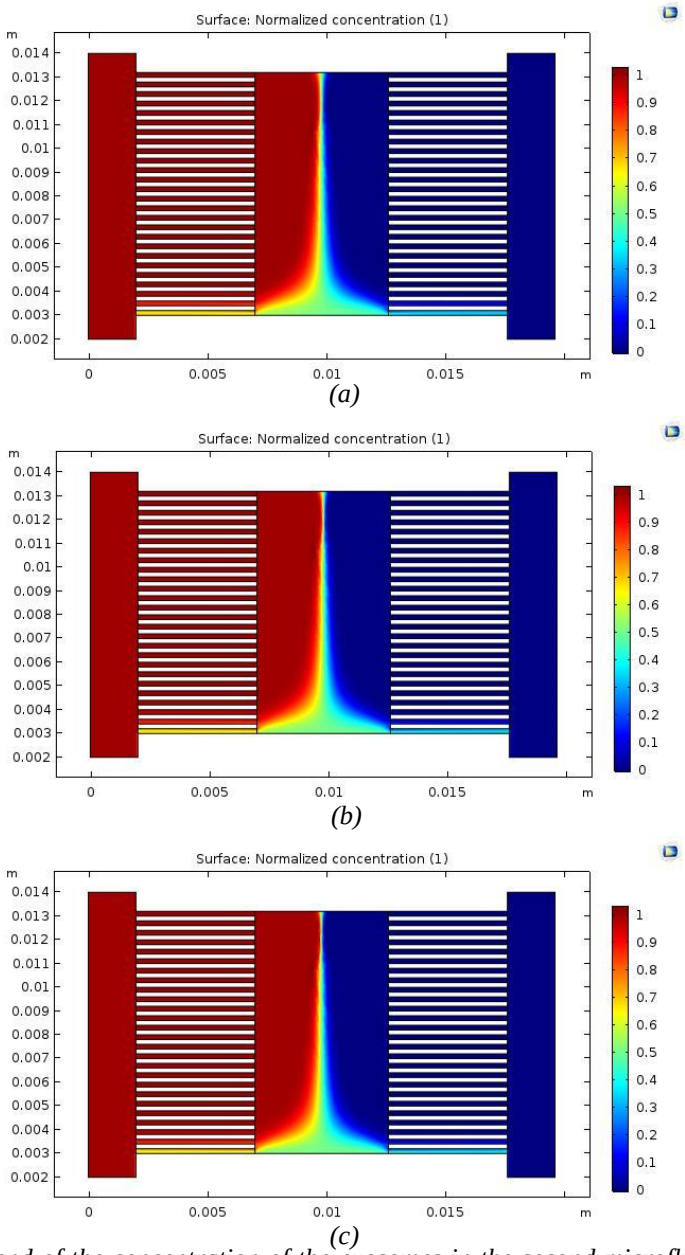

Figure 3.19*: Trend of the concentration of the exosomes in the second microfluidic platform, at three different velocities: (a) case 1, (b) case 2, (c) case 3.*

However, any significant difference can be visually observed between the three cases, demonstrating that, also by slightly changing the velocity, the convective flux always overcomes the diffusive one and that these velocities are too close to determine a big difference in the result. In the simulation, the trend of concentration starts changing if the velocity is changed of over one order of magnitude.

Even if the performance of the platform is not the desired and final ones, this device can be employed for other types of experiments, where two fluids at different concentrations (or two tracers) are used to obtain an “on-off” system.

3.2.2.3 Further studies and 3D simulation

The platform can now be further studied to obtain a final design, suitable to achieve the concentration gradient inside the central chamber. The focus is on the dimensions and on the shape of the microchannels, to obtain a value of Pe smaller than one. A 3D simulation is now advantageous to understand how the microbioreactor should be modified.
First, it is needed to understand which parameters must be considered and eventually modified to change the Péclet number in the microchannels. Its value, that expresses the amplitude of the convective flux with respect to the diffusive, depends on: a. the diffusion coefficient of the species *i*, that is constant for each species if the temperature is constant; b. the velocity of fluid inside the channel, c. the equivalent diameter of the channel. Therefore, it can be stated that the parameters that should be studied are:

- the aspect ratio (length/height of the channel)
- the geometry of the microchannels (shape and dimensions)

The velocity depends on both aspects.
Moreover, the limitations on the master's production technique must be considered: the minimum width of the microchannels is 150µm, and the height can vary in a range between 10 and 450µm. These limitations are imposed by the dimensions of the tools of the micromiller and by their wear during the milling of the Aluminum block.
The first case evaluated consists in keeping the microchannels' shape constant (rectangular section) and varying the dimensions. Two of the three dimensions are fixed, while the height is varied to observe the trend of the Péclet number:

- L=5000µm
- w=150µm
- h=10-450µm

where *L* is the length of the microchannel, *w* is the width and *h* is the height. Since the height of the other elements of the platform is kept constant (120µm), this is the maximum height of the microchannels.
Some preliminary calculations can be performed to understand the trend of the Péclet number if the height is changed. These calculations are made assuming that the velocity is constant and fixed at a value of 10^{-6} m/s, which is an approximation, since the velocity itself depends on the height of the microchannels. The trend of Pe is shown in Figure 3.20.
Pe decreases as the height of the channel is reduced, reaching a value near to one with the smallest dimensions. However, this is only a first calculation to understand the trend of this important parameter. In fact, the velocity is expected to increase as the section becomes smaller, but also the contribution of the wall is not considered.

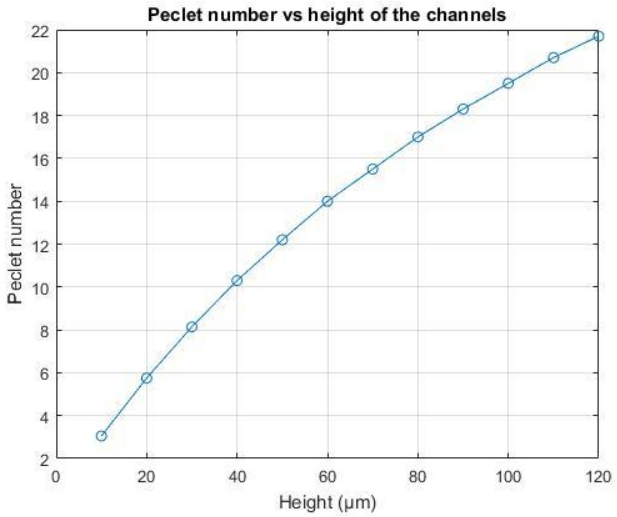

Figure 3.20: *Trend of Péclet number vs height of the microchannel, fixing the width at 150µm, the length at 5000µm and the velocity at 10^{-6}m/s.*

Therefore, it becomes important to understand the velocity field in a 3D simulation, and, in particular, the contribution of the wall to the fluid behavior and the transport of the chemical species. This contribution cannot be investigated in a 2D simulation but becomes important at this point of the analysis.

The 3D simulation is performed using the COMSOL Multiphysics® software, and employing the same interfaces and parameters (velocities, diffusion coefficients) of the 2D simulation. In this case, however, the entire geometry is built, taking into consideration the design in Figure 2.8. The lateral channels are built like two parallelepipeds, and the seeding ports are not added, in order to simplify the simulation and decrease the computational effort.

The convergence of this simulation is not easy, mainly due to: a. the difficulty of the software to find a stationary solution without any initial value, also with the coarsest mesh; b. the coupling of two different interfaces, where competing phenomena happen at different scales and orders of magnitude.

The first problem is solved by performing an initial transient study and using these results as initial values for the stationary simulation. Afterwards, a stationary simulation with an extremely coarse mesh is performed, and its solution is employed as initial value for the following simulation with a normal mesh. The second problem is solved by solving both the interfaces at the same time. It would be less computationally heavy to solve the laminar flow interface first, and then use these results to solve the second interface, but it is not possible to find a solution. All the results shown refer to the case 1 in Table 3.5.

The solution that is found is in accordance with the 2D simulation, however, in this case, the velocity inside the microchannels result one order of magnitude higher than the previous simulation, leading to a reference value of the Péclet number of 244. Moreover, the presence of the wall determines a different trend of the velocity. In fact, because of the no-slip condition, the velocity decreases towards the wall unless the zero is reached. This behavior

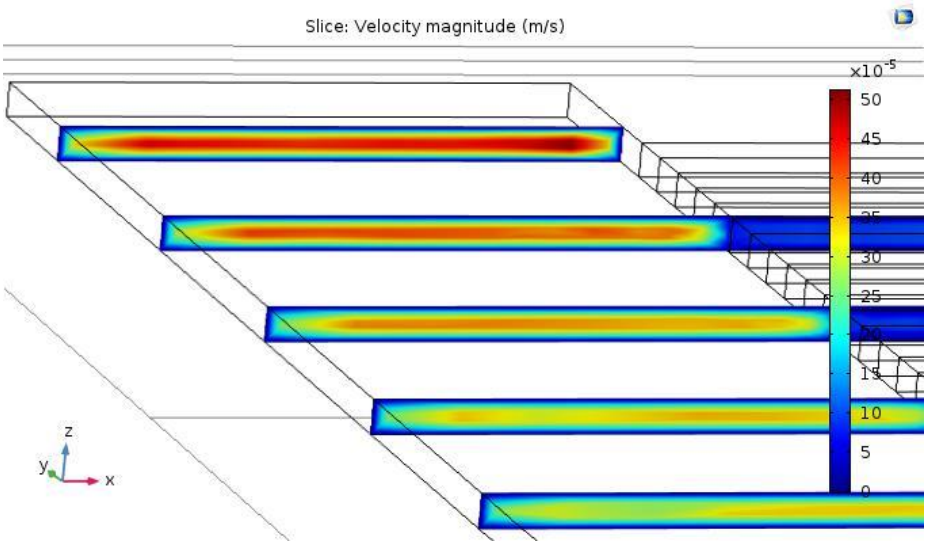

Figure 3.21: *Slices of velocity magnitude in the xz plane for case 1. The reduction of velocity towards the walls can be observed.*

can be observed in Figure 3.21, where different slices of the velocity magnitude in the xz plane are shown, and can be exploited to obtain the desired performances of the platform. The idea is to reduce the height of the microchannels and to keep them in the upper part of the platform, so that the reduction of velocity determined by the presence of the wall causes a decrease in the Péclet number (determined also by the reduction of the equivalent diameter). The resulting trend of concentration is almost the same of the previous simulation.

However, an interesting result that can be observed is the concentration of exosomes in the central chamber in the z axis, shown in Figure 3.22. The central part of the upper side of the chamber is shown, where the thin diffusive layer is highlighted.

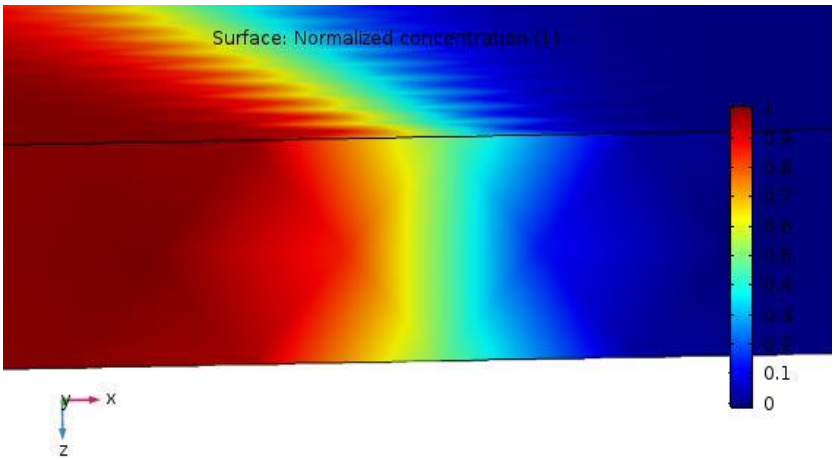

Figure 3.22: *Concentration of exosomes in case 1, considering the central part of the upper side of the central chamber (z axis).*

The concentration of exosomes is almost the same in the whole thickness, demonstrating that the presence of walls does not determine concentration gradients in the z axis. Therefore, during the biological experiments, the cells, even if placed on different planes, will be subjected to the same value of exosomes' concentration.

The next step is the simulation of the platform, where the dimensions of the microchannels are changed, in order to obtain a smaller Péclet number. As explained, the width and the length are set as 150 and 5000 µm, respectively, while the height is changed.

First, a simulation in which the height is set as 10µm is performed. However, this simulation has serious convergence problems, due to the big difference between the dimensions of the microchannels and of the lateral channels, where the mesh elements resulted much bigger. It is not possible to create the coarsest meshes, therefore it is not possible to carry out an initial and less computationally heavy simulation. At least the normal mesh must be built, bringing to difficulties in the convergence. Moreover, the transient simulation also encounters the same problems.

Therefore, we decided to simulate only one lateral channel and the relative microchannels, using only the Laminar Flow interface, and to employ the exported data of velocity to calculate the Péclet number. The ends of the microchannels are set as outlets, where the relative outlet pressure is determined from the 3D simulation of the actual device as 1.2Pa. The results of the velocity trend inside the platform show that the velocity magnitude at the end of the microchannels is higher for the first channels, and then tends to diminish, with an order of magnitude that goes from 10^{-6} to 10^{-7} m/s. Table 3.6 shows the average velocity at the exit of the first, an intermediate and the last microchannels, for the typical inlet flowrate of 5µL/min. The last channels, as exemplified from the value of velocity of the microchannel n.26, have an opposite trend of velocity, in accordance with the previous simulations. This is another behavior that should be modified: the objective is to have the same trend of velocity in all the microchannels.

This result is obviously not highly representative of the entire platform since the fluid is assumed to exit via the microchannels. However, an estimation of the Péclet number can be done, finding a range between 2.38 and 8.78. So, potentially, the diffusive flux of exosomes could overcome the convective one. The pressure drops along the microchannels can be calculated with the Fanning equation (equation 1.5), finding the results in the table.

Table 3.6: *Data of the velocity (and following calculation) at the end of the microchannels exported from a COMSOL® Multiphysics simulation, considering only the lateral channel and the microchannels of the second microfluidic platform.*

Microchannel	Average outlet velocity [m/s]	Péclet number	Pressure drops [Pa]
1	$2.88 \cdot 10^{-6}$	8.78	1.31
13	$7.79 \cdot 10^{-7}$	2.38	$3.54 \cdot 10^{-1}$
26	$-1.49 \cdot 10^{-6}$	4.56	$6.80 \cdot 10^{-1}$

Now, it can be useful to understand how the trend of the fluid inside the microchannels would change if their shape is modified. Two short radial elbows of 45° and three elbows of 90° are added in each microchannel, and the velocity is calculated fixing the pressure drops as the ones of the linear channels. These pressure drops are now given by the addition of the distributed pressure drops (along the channel) and the concentrated pressure drops in the elbows. Using the method of the equivalent diameters, an equivalent length is calculated, that corresponds to these additional pressure drops. The entire procedure is reported in the Appendix A.3. From the Fanning equation, and explicating the friction factor, we can derive equation A.5, and calculate the average velocity, if the five elbows are added in the microchannels. From these velocities, also the Péclet number is calculated, finding the results in Table 3.7.

Table 3.7: *Estimation of the average velocity and of Péclet number in the microchannels, when adding two 45° and three 90° elbows.*

Microchannel	Average outlet velocity [m/s]	Péclet number
1	$1.71 \cdot 10^{-6}$	5.22
13	$4.63 \cdot 10^{-7}$	1.41
26	$-8.89 \cdot 10^{-7}$	2.72

The velocity halves, determining the same behaviour in the Péclet number. So, this configuration brings to a higher diffusive flux with respect to the linear channels, but this reduction of the Péclet number is not enough to justify such a complication in the geometry of the master.

To conclude, the suggestion is to produce a new master, where the lateral channels and the central chamber have the same dimensions, while the microchannels' dimensions are reduced to 150 x 10 x 5000 μm.

3.2.3 Production of the microfluidic platform

The microfluidic platform is produced as described in paragraph §2.2.4. No problem is encountered during this operation; moreover, the removal of the PDMS layer from the master is easy, and leaves no residues. Therefore, micromilling is a suitable technique to obtain a master for microfluidic applications since Aluminum does not negatively interact with PDMS.

3.2.4 Irreversible configuration

The procedure in paragraph §2.2.4 allows to build the final microbioreactor, shown in Figure 3.23 filled with food coloring to ease visualization of its geometry.

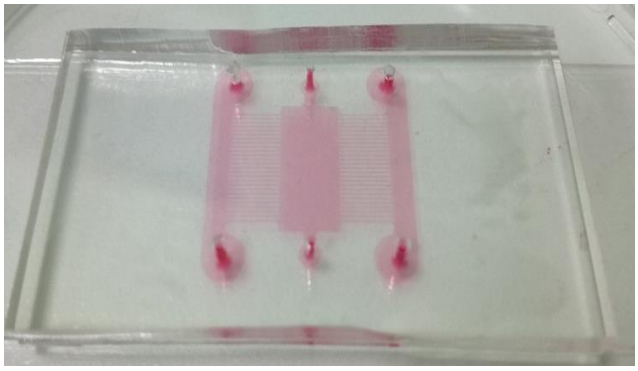

Figure 3.23: *Second microfluidic platform, filled with food colouring to better visualize its shape.*

3.2.5 Validation experiments

The performances of the second microfluidic platform are validated and compared with the COMSOL Multiphysics® simulation, using mainly food coloring. The fluorescent tracers, because of the expected performances of the device, are not employed. In fact, since only a thin diffusive layer is expected, the quantitative information is not required.
The food coloring solution is loaded in the syringe and the pump is prepared. The infuse and withdraw velocities are initially set at 15 or 20µL/min and after 2/3 minutes they are set at 5µL/min, to maintain the steady state. The result is shown in Figure 3.24.
Comparing the image with the COMSOL Multiphysics® simulation, it can be noticed that the behavior of the fluid is the expected: the central chamber is divided in two parts: on the left only the food coloring solution is present, and on the right only water. In the center of the chamber, the diffusive layer can be observed. Moreover, the mixing of the two fluids in the bottom of the chamber is evident, and causes some diluted food coloring solution to exit from the right outlet.

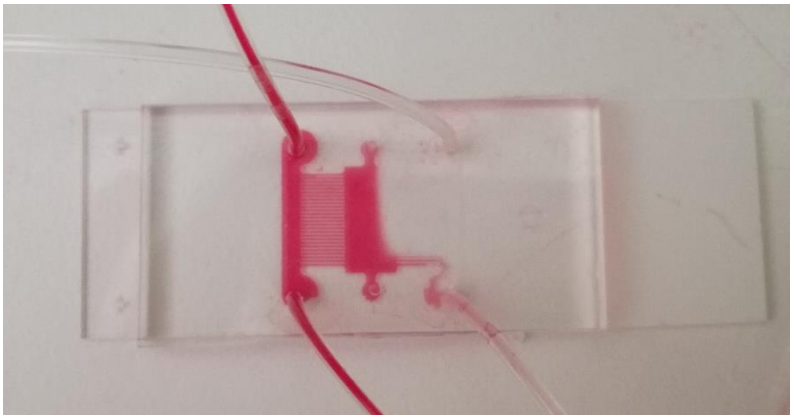

Figure 3.24: *Result of the validation experiment with food coloring on the irreversible configuration of the second microfluidic platform. It can be noticed that the behavior is completely in accordance with the COMSOL Multiphysics® simulation.*

At this point of the study, the qualitative analysis conducted with the food coloring is enough to validate the performances of the platform, so no fluorescent tracers were used. When the final master will be produced, the fluorescent tracers will be more useful and a quantitative and precise analysis will be performed.

3.2.6 Biological experiments

The microbioreactor produced is used to perform some biological tests, in order to define a procedure for the injection of cells and to observe the cell viability. The device is prepared for the biological experiment as described in paragraph §2.2.7. The day after the cell seeding (or two days after), the condition of cells in the central chamber should be similar to Figure 3.25, where cells are attached to the surface, alive and not clustering. This is the ideal situation to perform an experiment. At this point, the test can be started, connecting the platform to the syringe pump. The two infuse syringes are filled with Calcein-AM and Hoechst dye, to highlight the presence of the cell population.
At least 2 hours are waited to obtain an effect of the two tracers on the cells. Then, the fluorescent microscope is used to observe the cells inside the chamber, and in particular, in the central part where the presence of the diffusive layer can be analyzed. Two images of the same area shown in Figure 3.25 are here taken as fluorescence acquisitions, as presented in Figure 3.26.

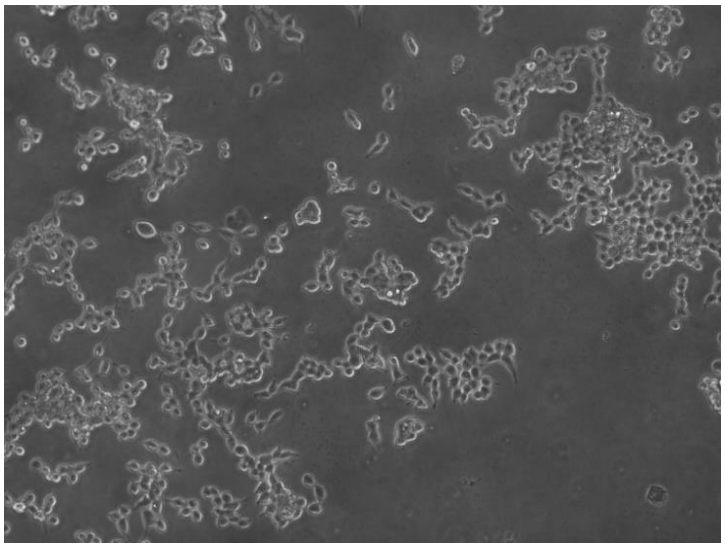

Figure 3.25: *Bottom surface of the central chamber of the second microfluidic platform one day after the seeding of cells.*

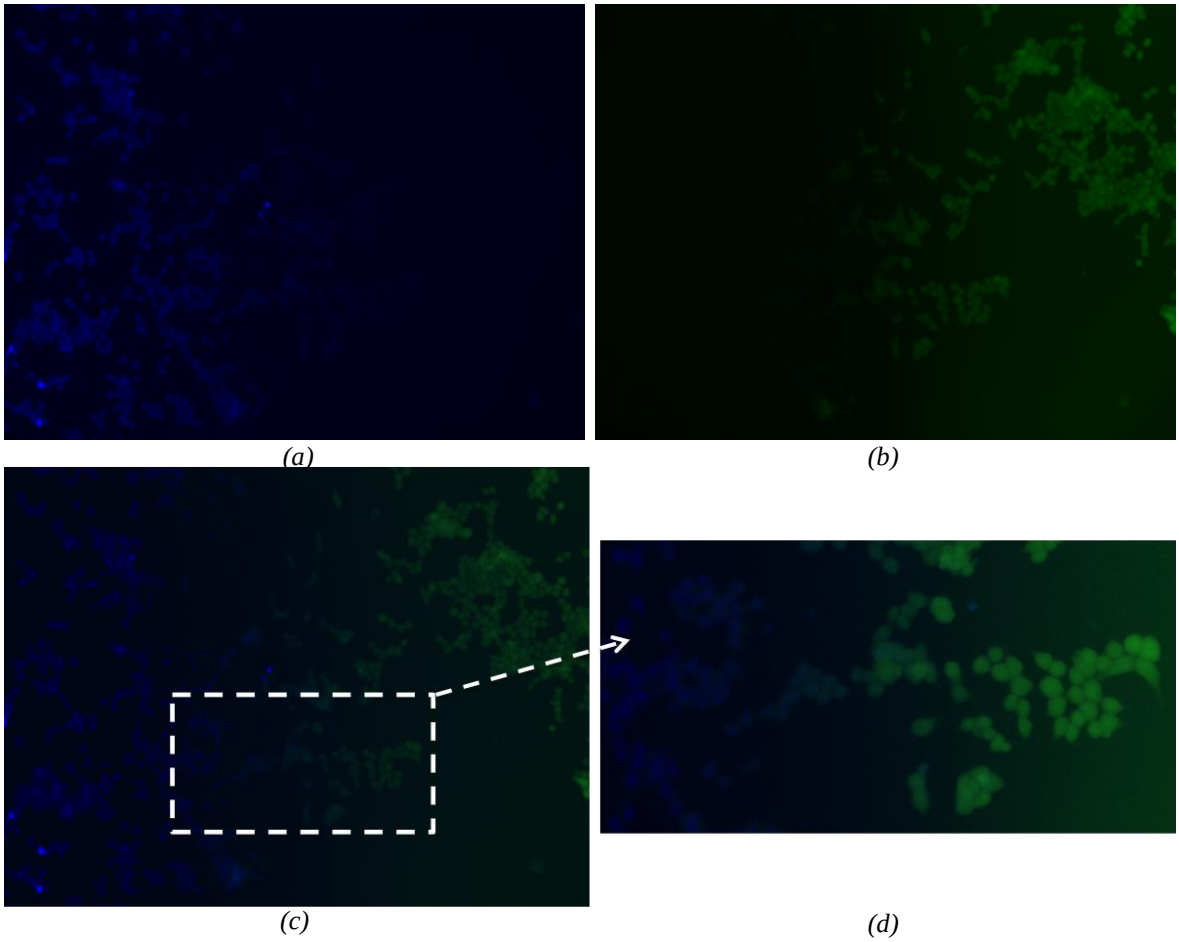

Figure 3.26: *Fluorescence acquisitions of the central part of the second microfluidic platform during a biological experiment. (a) The cells on the left are fluxed with Hoechst stain, that highlights the cells' nuclei, (b) while on the right they are subjected to a flux of Calcein-AM, that highlights the cytoplasm. (c) Overlay of the two images and (d) enlargement of the lower central part of the chamber, where the diffusion layer can be observed.*

Figure 3.26*a* shows a fluorescence acquisition of the central part of the chamber with the DAPI Cube, where the Hoechst dye highlights the nuclei of all cells. Figure 3.26*b*, taken with the GFP Cube, shows the cells' cytoplasm highlighted by Calcein-AM. Only metabolically active, alive cells express Calcein-AM. An overlay of the two images is shown in Figure3.26*c*. The enlargement of this image (Figure3.26*d*) underlines the presence of the diffusive layer.

The performances of the platform are thus confirmed by the results of this experiment. In fact, the central part of the chamber is divided by a thin diffusive layer. In the left-hand side the cells' nuclei can be observed as blue spots, as in the right-hand side the whole cell is highlighted by the green stain. Also the suitability of the device for the cells' living is confirmed.

The device, therefore, can be employed to study the behavior of cells, when they are subjected to a constant flux of a solution containing exosomes.

3.2.6.1 Biological experiment with exosomes

Since the operation of the second platform is validated (even if it is not the final one) and the viability of cells is confirmed, an experiment using exosomes can be carried out. At this point of the project, an efficient way to extract exosomes from Neuroblastoma cells has been found. These cells (SKNAS and SKNDZ Neuroblastoma cells) secreted exosomes after being cultured in normoxic condition for 48h, in hypoxia for 48h and after 48h of reoxygenation. The correct isolation of exosomes is confirmed by Scanning Electron Microscopy: Figure 3.27 shows the exosomes in two different dilutions.

The images are analyzed and exosomes size falls within the expected diameter range of 50-100nm, for both the SKNAS and SKNDZ cells. The graphs in Figure 3.28 show the distributions of the dimensions of exosomes: the first cell line has a peak of dimension of 59nm and an average of 68nm, while the second cell line has the peak at 62nm and shows an average dimension of 86nm.

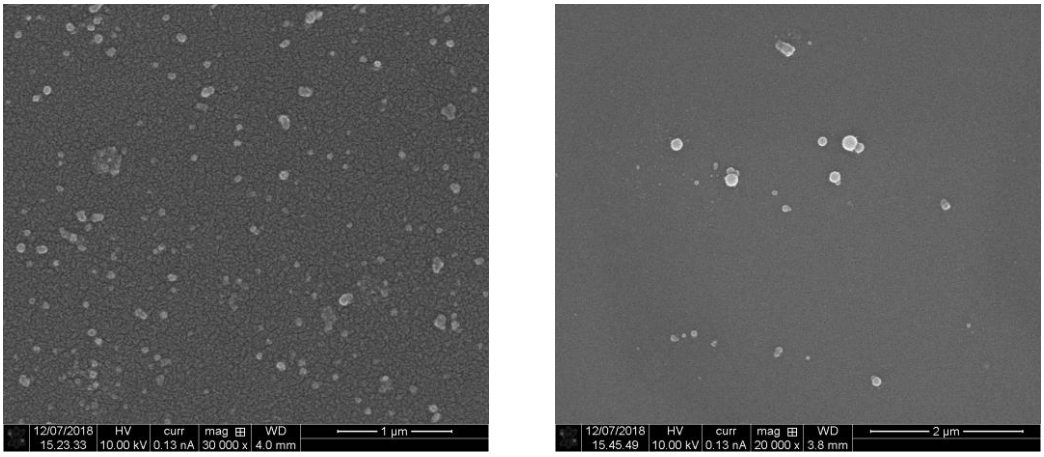

(a) *(b)*

Figure 3.27: *Scanning Electron Microscopy used to observe the exosomes isolated from Neuroblastoma cells. The two images show different dilutions: (a) dilution 1:100 and (b) dilution 1:1000.*

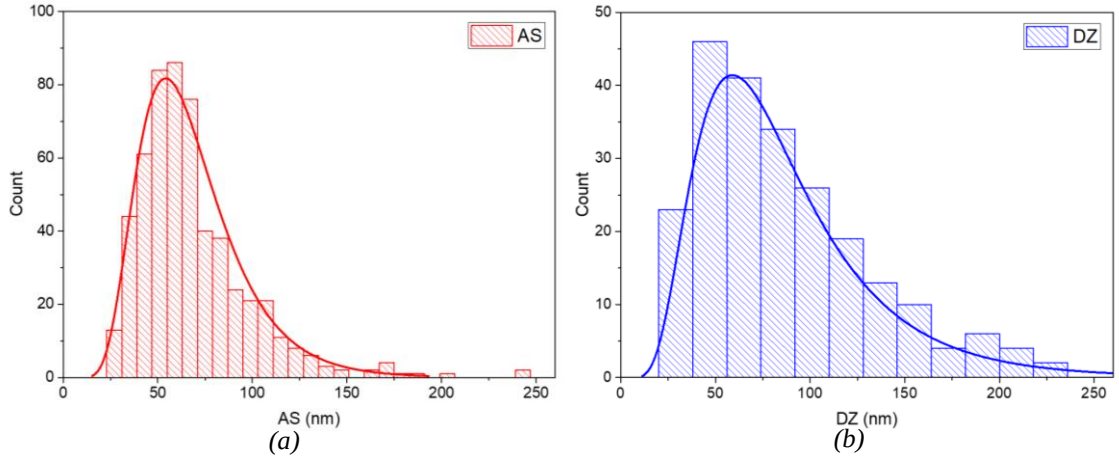

(a) *(b)*

Figure 3.28: *Trend of the dimensions of exosomes derived from the SEM acquisitions: (a) SKNAS cell line shows a peak of 59nm and an average of 68nm; (b) SKNDZ cell line shows a peak of 62nm and an average of 86nm.*

The extracted exosomes are stained with CMTMR dye, a fluorescent marker, to make them visible in the fluorescent acquisitions (with the RFP Cube). These vesicles can be diluted in the culture media in order to obtain a solution to be inserted in the syringe.
The HEK-293 cells are seeded in the µBR, with three different concentrations, to observe which one is more suitable for the experiment. The concentrations of cells seeded in the central chamber are approximately 500, 900 and 1800cell/mm^2. After two days in the incubator, it can be observed that the highest concentration is the most suitable since an adequate quantity of cells is present.
After cell seeding, the procedure followed during these experiments is the same of the biological experiments described above with the two fluorescent cells' stains. The difference consists in the contents of the infuse syringes: one is filled with the exosomes solution, and the other one with culture media. Moreover, attention must be taken in avoiding the exposition of exosomes to light, since they can be damaged.
The objective of this experiment is the observation of the internalization of exosomes by the HEK-293 cells, to understand if they are absorbed by cells, and if a difference in the exosomes concentration determines a variation in the number of exosomes internalized. To obtain these results, since the concentration gradient is not created in the central chamber, two platforms are used with different exosomes' concentrations. In particular, starting from 75µL of exosomes, with a concentration of 10^7 vesicles/µL, two solutions are created, which characteristics are reported in Table 3.8. Considering the planned duration of the experiment of 16 hours and a flowrate of 4µL/min, at least 3840µL of solution in the infuse syringes is needed. However, an excess is required to account for its loss during the preparation of the syringes and during the starting procedure of the pump. Therefore, 5000µL of solution are prepared.

Table 3.8: *Solutions employed in the biological experiment with exosomes: volume of exosomes added and final concentration of the two solutions.*

Solution	Volume of exosomes [µL]	Volume of media [µL]	Concentration of exosomes [exosomes/ µL]
1	50	4950	10^4
2	25	4975	$5 \cdot 10^3$

The solutions are loaded in the syringes, and the experiment can be started. The infuse and withdraw flow rates are set at 4µL/min, and the microbioreactors are left in the incubator overnight. The day after, the pump is stopped and the microtubes are removed from the µBRs. At this moment, it is possible to make some acquisitions with the fluorescence microscope, to observe the cells and highlight the presence of exosomes. The cells appear different with respect to the previous day. In fact, they tend to agglomerate and form some clusters. Figure 3.29 shows the difference between the cells before the starting of the exosomes' flux and after the 16 hours of experiment.

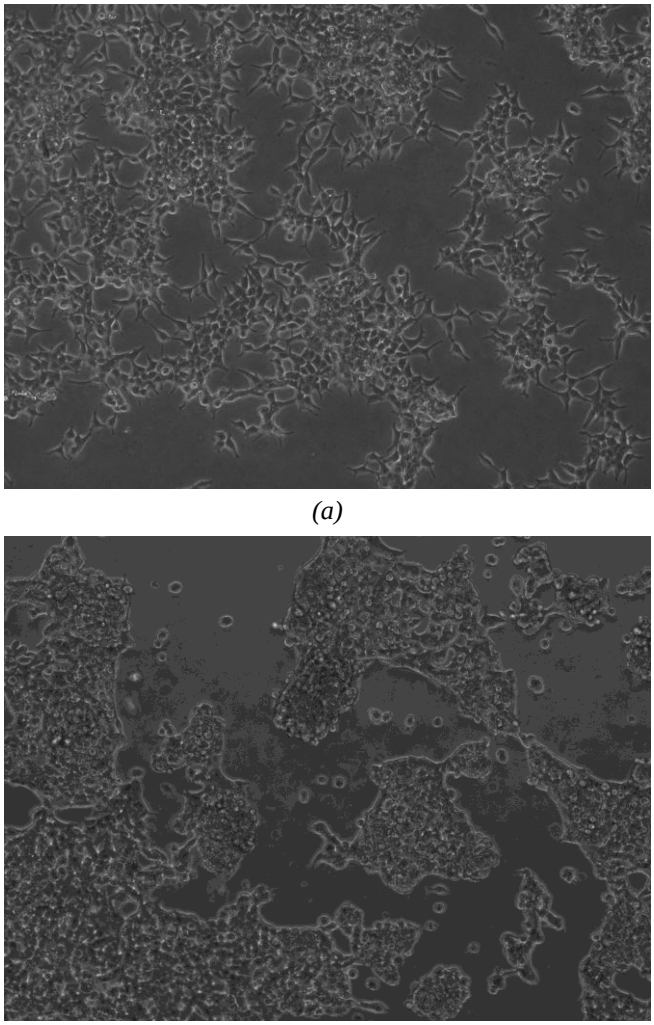

(a)

(b)

Figure 3.29: *Cells in the second microfluidic platform before (a) and after (b) the biological experiment with exosomes. The clustering of cells can be observed in the second image.*

The formation of clusters can be easily noticed. The reason of this behavior is surely a reaction of cells to the shear stress determined by the flux.

As concern the results of the experiment, the two µBRs are observed with the fluorescence microscope, to highlight the presence of red spots, i.e. exosomes. Figure 3.30 shows some cells that internalized exosomes in the µBR fluxed with the solution 1.

Only the results of the first platform are shown because, even if subjected to two different concentrations of exosomes, no relevant difference can be highlighted between the two devices. On the side fluxed with the exosomes' solution, in both the platforms, some cells absorbed the vesicles.

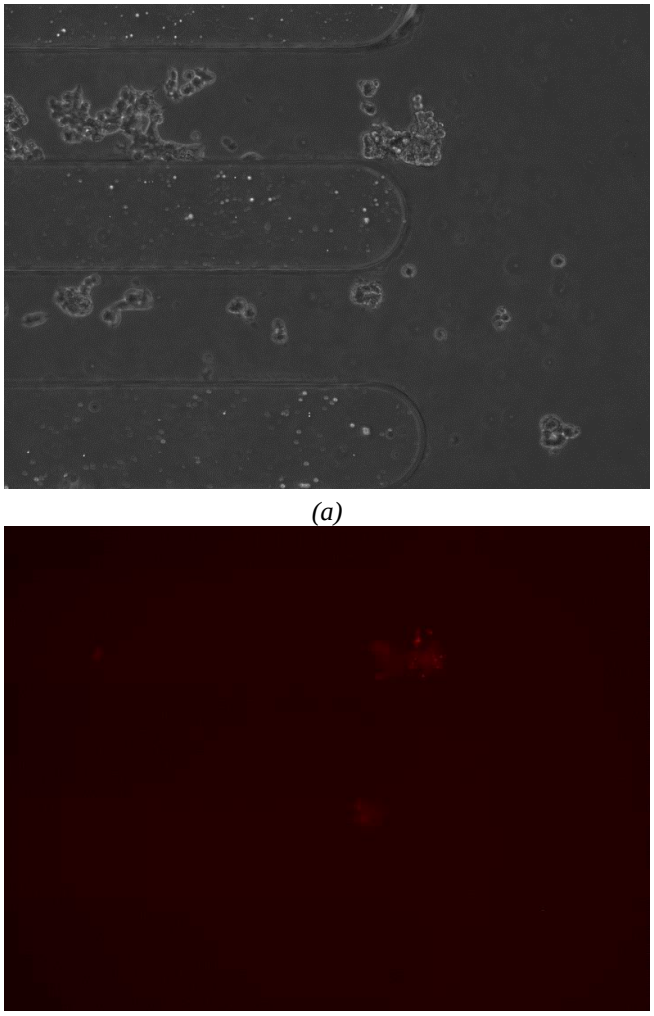

(a)

(b)

Figure 3.30: *Results of the biological experiment with exosomes in the second microfluidic platform. Some cells that internalized exosomes are highlighted with the RFP acquisition in (b).*

So, a first preliminary result of the internalization of exosomes by the HEK-293 cells has been found. However, no relevant difference can be observed between the two µBRs, thus not allowing obtaining quantitative results. Probably, this is caused by the presence of a significant shear stress in the central chamber that induced cells to clusters and hindered the exosomes' internalization.

At this point, we conducted another test to verify the ability of FN to functionalize the µBR's surface and understand if it has an effect on the cells attachment. Thus, we conducted an experiment analogous to the one described, but loading both the infuse syringes with pure culture media and treating only one device with fibronectin. This experiment showed that the attachment of cells after seeding was the same in the two cases, but less cells were present in the µBR not treated with FN after the fluxing of culture media.

To conclude, it can be stated that the following experiment must be done on the platform

modified with the suggestions in paragraph §3.2.2.3, to obtain a continuous concentration gradient in the chamber, and a lower stress on the cells.

3.3 Biological protocols

3.3.1 Growth rate estimation of HEK-293

The growth rate of the HEK-293 is estimated with the procedure described in paragraph §2.3.4, using a 6-well culture plate. On day one, $5 \cdot 10^5$ cells are inoculated in each well. Afterwards, on each following day one well is used: the cells are detached from the surface using Trypsin, and then the procedure of cellular counting reported in paragraph §2.3.3 is followed. Figure 3.31 shows the trend of cellular growth for 6 days (144h), starting from the inoculum of $5 \cdot 10^5$ cells. During the first four days cells grow fast, reaching a number higher than $2.5 \cdot 10^6$ on day 4. Afterwards, they tend to grow at lower rates, due to the overcrowding of the well.

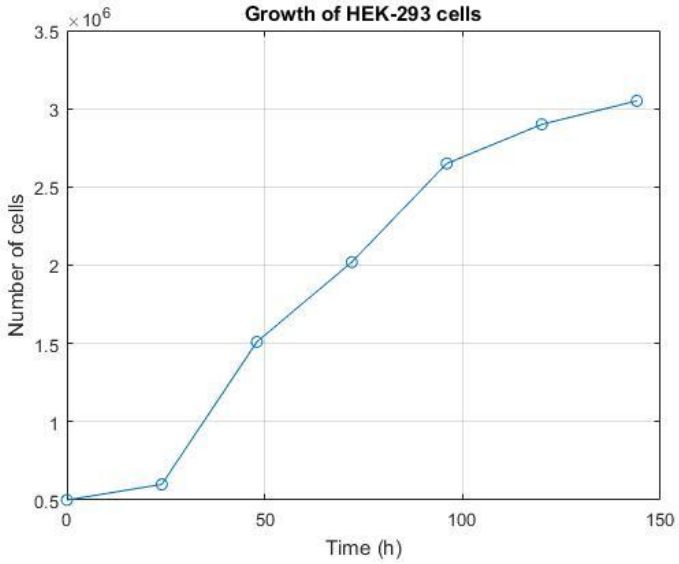

Figure 3.31*: Growth of HEK-293 in a 6-well culture plate on 6 consecutive days.*

Knowing the number of cells on each day, the percentage growth rate can be calculated with the formula in equation 2.6, finding the results in Table 3.9.

Table 3.9*: Number of cells and calculation of the percentage growth rate of HEK-293 in a 6-well culture plate.*

Day	Number of cells	Percentage growth rate [%]
0	$5 \cdot 10^5$	-
1	$6 \cdot 10^5$	20
2	$1.51 \cdot 10^6$	202.25
3	$2.02 \cdot 10^6$	304
4	$2.65 \cdot 10^6$	430
5	$2.9 \cdot 10^6$	480
6	$3.05 \cdot 10^6$	510

The growth rate can be exploited to quantify the cellular splitting procedure. In fact, knowing the initial inoculum of cells, the number of cells on each day can be found as:

$$N_{tot} = N_0 \left(1 + \frac{GR\%}{100} \right) \tag{3.1}$$

If the maximum number of cells that can be present in the flask is known, the day on which the cellular splitting procedure must be done can be easily estimated.

Conclusions

The objective of this thesis was the study and development of two microfluidic platforms for biomedical applications, produced thanks to a procedure of replica molding, employing PDMS as the production material.

The first platform's master was already produced and based on an existing design. The performances of the device were simulated with COMSOL Multiphysics® software, and used to perform a validation of the experimental data. The platform can be arranged in an irreversible configuration, thanks to the use of plasma treatment, or in a reversible configuration, thanks to a clamping unit. The performances of the device have been validated comparing the data of concentration exported from the simulation with the semi-quantitative results of the validation experiments with fluorescent tracers. The biological experiments were not carried out, since an element of the clamping unit, the clamping plate, showed signs of wear and failed to provide the same pressure on the whole platform, thus not assuring proper sealing of the microchannels. However, the procedure of cells seeding on the microbioreactor was optimized.

The second platform's master was designed and produced with a micromiller. The initial design was modified to solve the structural problems highlighted during the plasma treatment. The simulation and the fluid dynamic simulations have demonstrated that the design is not suitable to obtain a continuous concentration gradient, however, some suggestions have been presented to produce a new master. The new platform will be able to obtain the overcoming of the diffusive flux on the convective one inside the microchannels. The device was used for some biological experiments, first with tracers to further validate the performance of the platform, and then with exosomes, to observe their internalization in HEK-293 cells. The first experiments showed that the device is suitable for the cells viability, and the second one showed an internalization of exosomes by cells, even if cells slightly detached from the surface because of the continuous shear determined by the flux, and this caused the inability of obtaining quantitative results.

To conclude, the two microfluidic platforms are suitable to obtain discrete, in the first case, and continuous, in the second case, concentration gradients. However, in the future studies, some modifications are needed to ensure their performances. The clamping plate of the first device must be manufactured again, possibly using the micromiller to obtain a thicker layer of Aluminum that will not distort. The master of the second device must be modified, with the suggestions presented, to obtain a continuous concentration gradient.

Nomenclature

c	=	concentration [mol/m^3]
Ca	=	capillary number [dimensionless]
D	=	diameter [m]
D_{eq}	=	equivalent diameter [m]
D_i	=	diffusion coefficient of the species i [m^2/s]
f	=	friction factor [dimensionless]
h	=	height of the channel [m]
J_i	=	diffusive flux of the species i [mol/s]
k_B	=	Boltzmann constant [J/K]
L	=	length of the channel [m]
L_{eq}	=	Equivalent length in the equivalent diameter method [m]
N	=	number of cells per mL [cells/mL]
N_0	=	initial number of cells
$n_{i,eq}$	=	coefficient of the equivalent diameter method [dimensionless]
N_{mean}	=	mean number of cells [cells/square]
N_{tot}	=	total number of cells
P	=	semiperimeter [m]
Pe	=	Péclet number [dimensionless]
r	=	radius [m]
Re	=	Reynolds number [dimensionless]
S	=	section of the channel [m^2]
T	=	temperature [K]
V	=	average velocity [m/s]
v	=	velocity [m/s]
w	=	width of the channel [m]
ΔP	=	pressure drops [Pa]

Greek symbols

μBR	=	microbioreactor
DMEM	=	Dulbecco's Modified Eagle Medium
DMSO	=	Dimethyl sulfoxide
FBS	=	Fetal Bovine Serum
GR%	=	percentage growth rate
PBS	=	Phosphate Buffered Saline
PC	=	Polycarbonate
PDMS	=	Polydimethylsiloxane

Acronyms

μ	=	viscosity [Pa·s]
γ	=	surface tension [N]
η	=	mobility of the particle [kg/s]
ρ	=	density [kg/m^3]

Appendix

A.1 Additional data of COMSOL® Multiphysics simulation of the first platform.

The following figures show the results of the Laminar Flow in the COMSOL® Multiphysics simulation of the first microfluidic platform, for the cases 2 and 3 in Table 3.1.

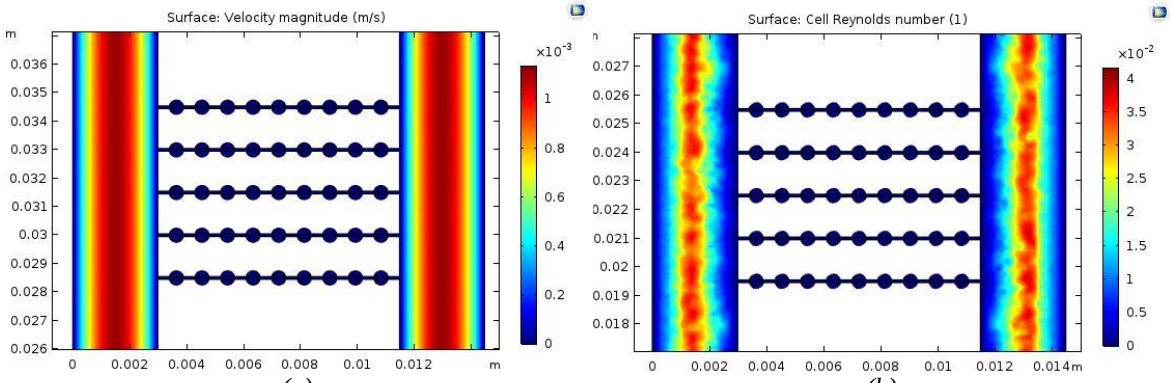

(a) *(b)*

Figure A.1: *Results of the COMSOL simulation of the first microfluidic platform for case 2: (a) velocity magnitude and (b) cell Reynolds number.*

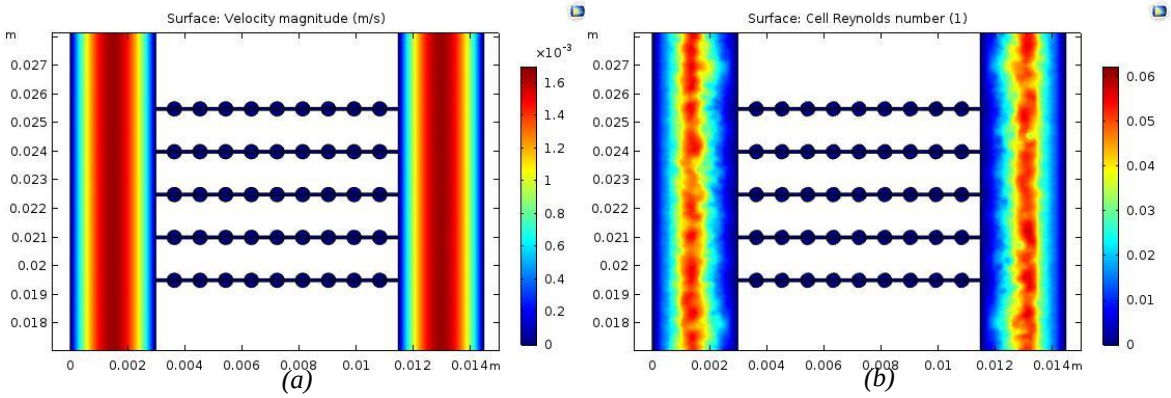

(a) *(b)*

Figure A.2: *Results of the COMSOL simulation of the first microfluidic platform for case 3: (a) velocity magnitude and (b) cell Reynolds number.*

A.2 Additional data of COMSOL® Multiphysics simulation of the second platform.

The following figures show the results of the Laminar Flow in the COMSOL® Multiphysics simulation of the second microfluidic platform, for the cases 2 and 3 in Table 3.5.

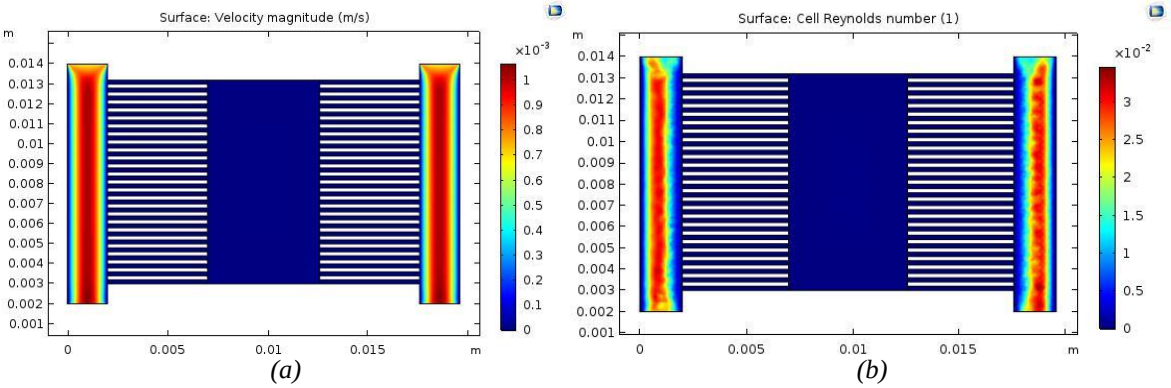

Figure A.3: *Results of the COMSOL simulation of the second microfluidic platform for case 2: (a) velocity magnitude and (b) cell Reynolds number.*

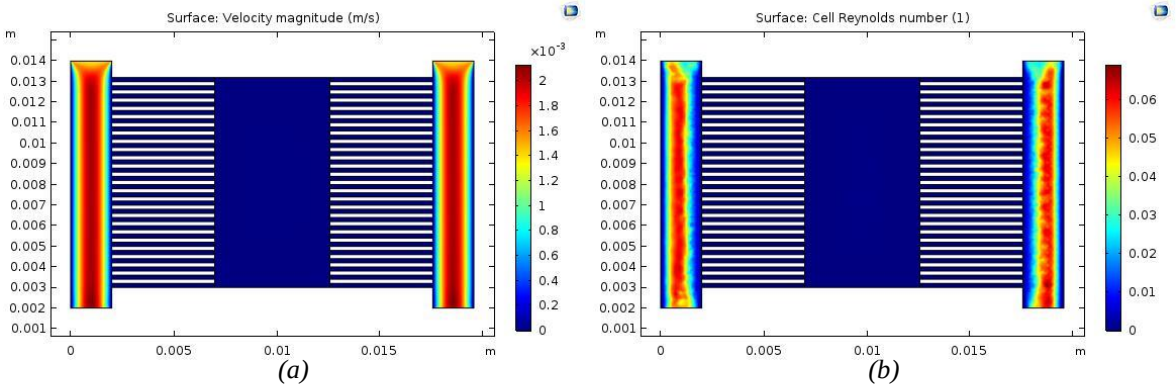

Figure A.4: *Results of the COMSOL simulation of the second microfluidic platform for case 3: (a) velocity magnitude and (b) cell Reynolds number.*

The following figures show the results of the Transport of Diluted Species in the COMSOL® Multiphysics simulation of the second microfluidic platform, for the three isothiocyanate dextrans.

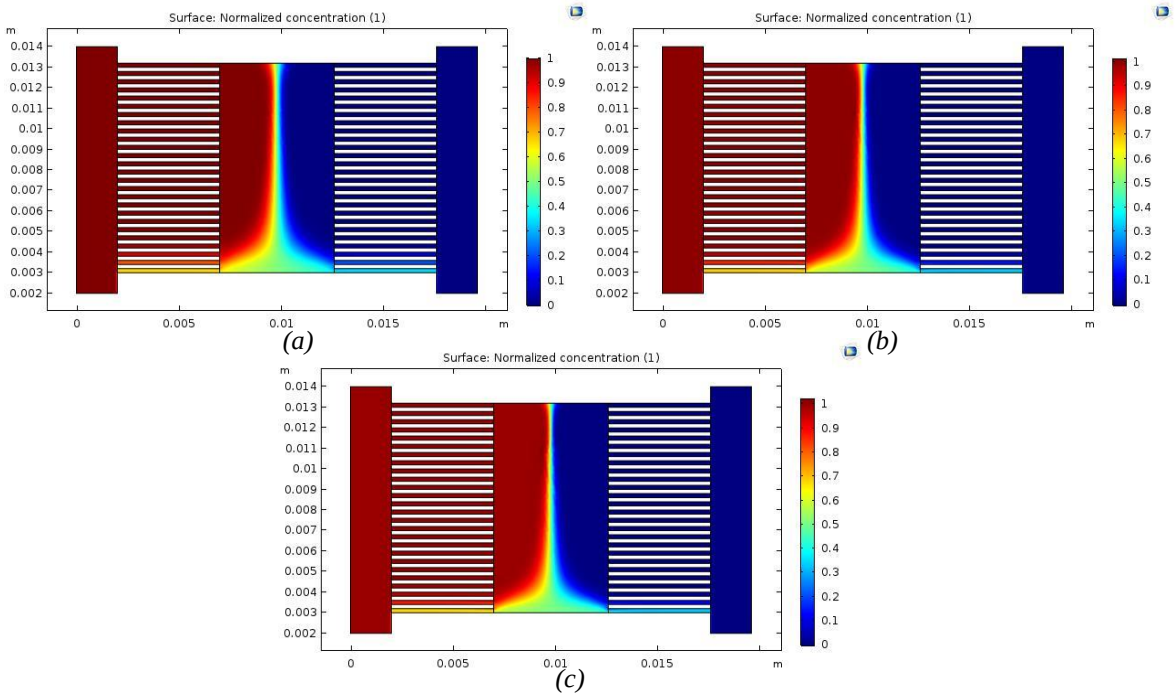

Figure A.5*: Trend of the concentration of the low MW dextran in the second microfluidic platform, at three different velocities: (a) case 1, (b) case 2, (c) case 3.*

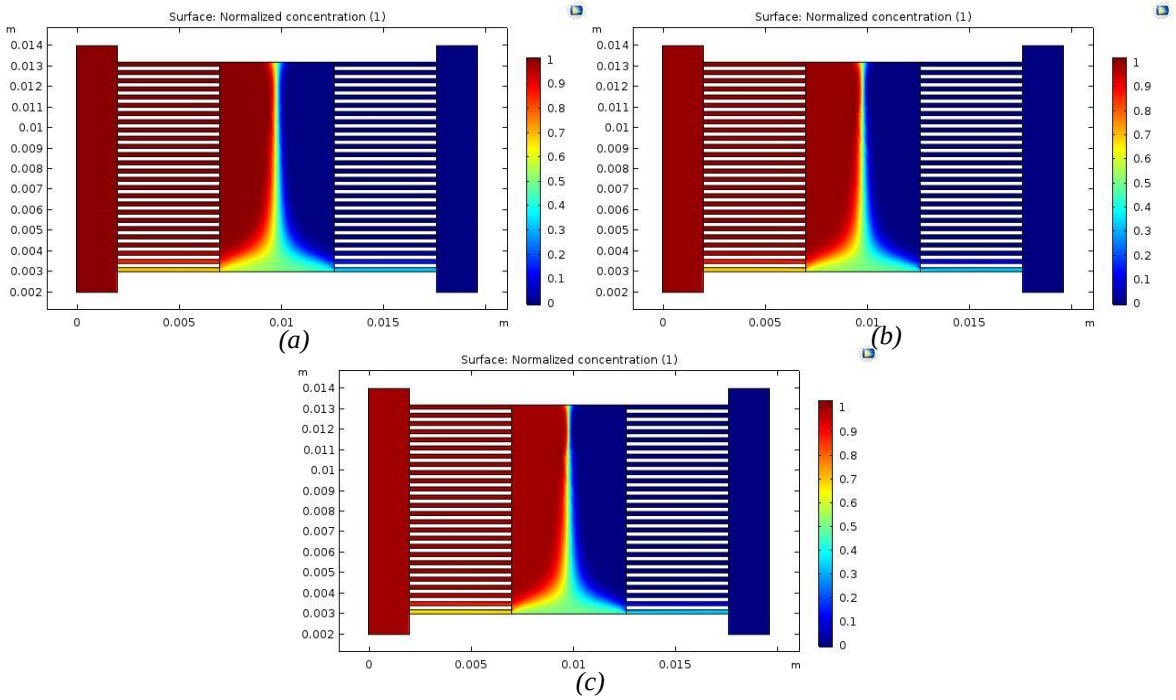

Figure A.6: Trend of the concentration of the medium MW dextran in the second microfluidic platform, at three different velocities: (a) case 1, (b) case 2, (c) case 3.

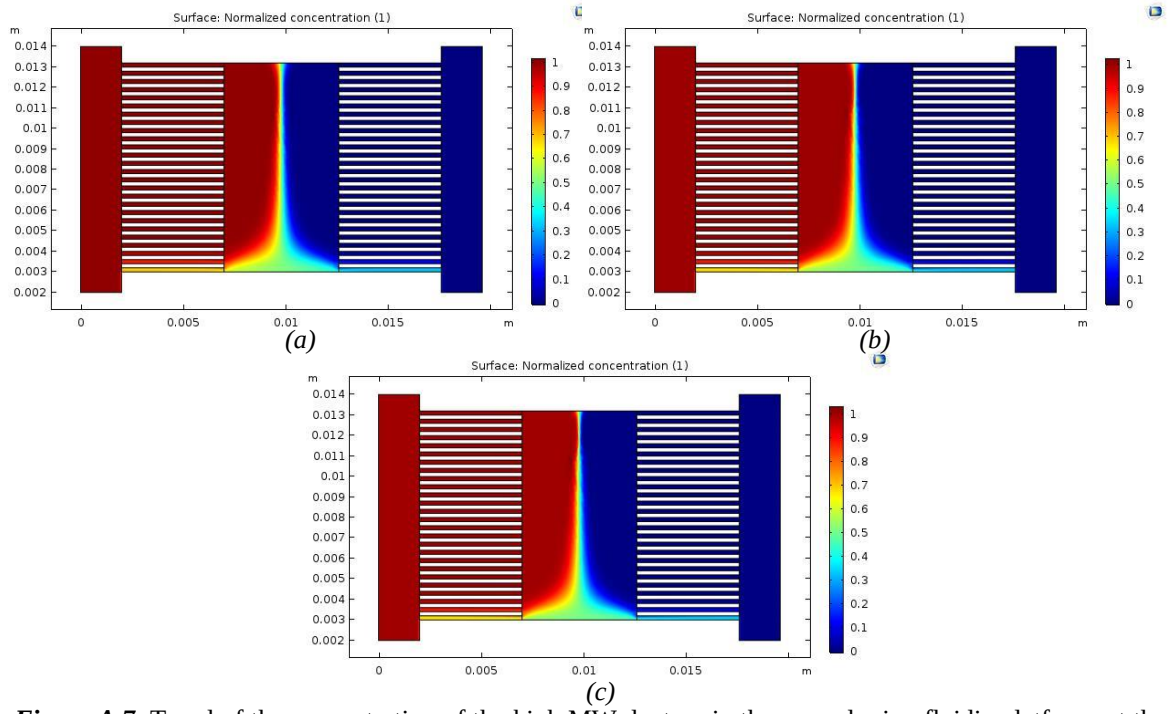

Figure A.7: Trend of the concentration of the high MW dextran in the second microfluidic platform, at three different velocities: (a) case 1, (b) case 2, (c) case 3.

A.3 Equivalent diameters method

The procedure used to calculate the equivalent length of the microchannels using the method of the equivalent diameters is here explained.

We want to add two angles of 45° at the inlet and outlet of the microchannels, and three 90° elbows along the channels, as qualitatively shown in Figure A.8. Considering that the overall dimensions of the platform must be maintained, the distance between the lateral channel and the central chamber is maintained of 5000µm. Therefore, the length of the microchannel increases and is calculated using trigonometric relations, finding a total length of 5871.14µm.

Figure A.8: Qualitative representation of the shape of the microchannels when two 45° and three 90° elbows are added.

These elbows represent concentrated pressure drops that can be considered as an additional length, considering the equivalent diameters method, where the equivalent length is calculated as:

$$L_{eq} = D_{eq} \sum n_{i,eq} \,, \tag{A.1}$$

where L_{eq} is the equivalent length [µm], D_{eq} is the equivalent diameter [µm] and $n_{i,eq}$ is a coefficient that depends on the type of elbow (15 for the 45° elbow, 35 for the 90° elbow). Therefore, adding two 45° elbows and three 90° elbows, we find:

$$n_{i,eqTOT} = 2 \cdot 15 + 3 \cdot 35 = 135 \tag{A.2}$$

$$L_{eq} = 2531.25 \mu m \tag{A.3}$$

Therefore, the total length of the microchannel can be calculated as:

$$L_{TOT} = L + L_{eq} = 8402.39 \mu m \tag{A.4}$$

This value is used in the Fanning equation to calculate the velocity as:

$$v = \frac{D_{eq}^2 \cdot \Delta P}{32 \cdot \mu \cdot L_{TOT}} \tag{A.5}$$

References

1. George M. Whitesides. The origins and the future of microfluidics. **Nature,** 368–373 (2006).
2. Squires, T. M. & Quake, S. R. Microfluidics: Fluid physics at the nanoliter scale. *Rev. Mod. Phys.* **77,** 977–1026 (2005).
3. Beebe, D. J., Mensing, G. A. & Walker, G. M. Physics and Applications of Microfluidics in Biology. *Annu. Rev. Biomed. Eng.* **4,** 261–286 (2002).
4. Green, D. W. & Perry, R. H. *Perry's Chemical Engineers' Handbook*.
5. Sackmann, E. K., Fulton, A. L. & Beebe, D. J. The present and the future role of microfluidics in biomedical reseach. (2014).
6. Breslauer, D. N., Lee, P. J. & Lee, L. P. Microfluidics-based systems biology. *Mol. Biosyst.* **2,** 97 (2006).
7. Cimetta, E. *et al.* Microfluidic bioreactor for dynamic regulation of early mesodermal commitment in human pluripotent stem cells. *Lab Chip* **13,** 355–364 (2013).
8. Mehling, M. & Tay, S. Microfluidic cell culture. (2013).
9. Duncombe, T. A., Augusto M. Tentori & Herr, A. E. Microfluidics: reframing biological enquiry. (2015).
10. Halldorsson, S., Lucumi, E., Gomez-Sjoberg, R. & Fleming, R. M. T. Advantages and challenges of microfluidic cell culture in polydimethylsiloxane devices. **Biosensors and Bioelectronics,** 218–231 (2015).
11. Introduction about soft lithography and polymer molding for microfluidics. Available at: https://www.elveflow.com/microfluidic-tutorials/soft-lithography-reviews-and-tutorials/introduction-in-soft-lithography/introduction-about-soft-lithography-and-polymer-molding-for-microfluidic/.
12. PDMS and Microfluidics. Available at: https://www.elveflow.com/microfluidic-tutorials/microfluidic-reviews-and-tutorials/the-poly-di-methyl-siloxane-pdms-and-microfluidics/.
13. Bhattacharjee, N., Urrios, A., Kang, S. & Folch, A. The upcoming 3D-printing revolution in microfluidics. *Lab. Chip* **16,** 1720–1742 (2016).
14. Johnston, I. D., McCluskey, D. K., Tan, C. K. L. & Tracey, M. C. Mechanical characterization of bulk Sylgard 184 for microfluidics and microengineering. *J. Micromechanics Microengineering* **24,** 035017 (2014).
15. PDMS datasheet.
16. Plasma: overview. Available at: http://harrickplasma.com/plasma/overview.
17. The physics of plasma. Available at: http://harrickplasma.com/plasma/physics.

18.PDMS and soft lithography. Plasma cleaner. Available at: https://www.elveflow.com /microfluidic-tutorials/soft-lithography-reviews-and-tutorials/how-to-choose-your-soft-lithography-instruments/pdms-soft-lithography-plasma-cleaner/.
19.Davidoff, A. M. Neuroblastoma. *Semin. Pediatr. Surg.* **21,** 2–14 (2012).
20.Li, W. *et al.* Role of exosomal proteins in cancer diagnosis. *Mol. Cancer* **16,** (2017).
21.Thind, A. & Wilson, C. Exosomal miRNAs as cancer biomarkers and therapeutic targets. *J. Extracell. Vesicles* **5,** 31292 (2016).
22.COMSOL Multiphysics User's Guide.
23.Fluorescein isothiocyanate dextran. Available at: https://www.sigmaaldrich.com/ technical-documents/protocols/biology/fluorescein-isothiocyanate-dextran.html.
24.MICROMASTER® 3/5X. Available at: https://www.kugler-precision.com/index.php? MICROMASTER--3-5X-EN.
25.S neox. Non-contact 3D Surface Profiler. Available at: https://www.sensofar. com/metrology/sneox/.
26.Plasma Treatment of PDMS for Microfluidics. Available at: https://plasmatreatment.co. uk/henniker-plasma-technology/plasma-treatments/plasma-surface-activation-to-improve-adhesion/plasma-treatment-of-pdms/.

Websites:

https://plasmatreatment.co.uk/ (Accessed: 15th July 2018)

https://www.sensofar.com/ (Accessed: 30th July 2018)

https://www.sigmaaldrich.com/ (Accessed: 3rd August 2018)

http://harrickplasma.com/ (Accessed: 15th July 2018)

https://www.elveflow.com/ (Accessed: 14th July 2018)